

A Thesis Submitted for the Degree of PhD at the University of Warwick

Permanent WRAP URL:

<http://wrap.warwick.ac.uk/89875>

Copyright and reuse:

This thesis is made available online and is protected by original copyright.

Please scroll down to view the document itself.

Please refer to the repository record for this item for information to help you to cite it.

Our policy information is available from the repository home page.

For more information, please contact the WRAP Team at: wrap@warwick.ac.uk



DETECTION OF POTATO STORAGE DISEASE BY GAS ANALYSIS

Massimo Rutolo

This thesis is submitted to the University of Warwick
in partial fulfilment of the requirements of the degree of

Doctor of Philosophy

School of Engineering

October 2016

This page is intentionally left blank.

ABSTRACT

The United Nations FAO (Food and Agriculture Organization) reports that a large quantity of global food production for human consumption is wasted every year (1.3 billion tons) with losses estimated between 40 and 50 % for all root and tuber crops, fruits and vegetables (FAO Global Initiative on Food Loss and Waste Reduction). Potatoes tubers are one the worldwide staple foods with an annual total production of circa 368 million tons. A major contributor to this loss is potato infection whilst in storage (in the UK circa 5% of the entire UK crop), with the main culprit being a disease of bacterial origin known as ‘soft rot’. This project attempts to address this post-harvest waste of potato tubers in storage through early detection and monitoring of the disease.

The proposed approach for this research was to use gas phase biomarkers for the early detection of soft rot (in other words ‘smelling’ the disease). The first part of the project addressed past research on volatile detection and background on other sensing technologies not previously (or marginally) investigated in these studies. The section on past studies includes all the research carried out from the 1970s by Varns and Glyn to date. Most of the studies focused on Gas Chromatography or Gas Chromatography Mass Spectroscopy. The background section that follows addresses other technologies that could also be employed for volatile monitoring, namely Field Asymmetric Ion mobility Spectrometry, Photoionization Detection, Metal Oxide, Electrochemical, and Nondispersive Infrared gas sensors.

Initial work focused on evaluating these gas sensing technologies for both symptomatic and pre-symptomatic progression of potato soft rot, under laboratory conditions. After preliminary investigation, the experimental method chosen consisted

in assessing the sensors results at two time points, both for symptomatic and pre-symptomatic disease detection. A total of 80 potato samples (40 for each time point) were tested with 25 different gas sensors. To process the data the following techniques were employed: cumulative sensor responses, unsupervised PCA and k-means and machine learning models (LDA, MARS, SVM, random forest and the C5.0 algorithm). Results show that all these techniques yielded a very high discrimination rate between healthy control and diseased tubers (with 80 to 100% accuracy) for a number of sensors. PID, 3 metal oxide and 3 electrochemical, gas sensors were shortlisted for possible later work.

The final part of the project focussed on deploying sensors identified in laboratory conditions in a real store. To this end, a bespoke instrument was developed solely for the monitoring of store environments. The instrument comprised the sensors tested in the previous part of this work that could be readily embedded into a research tool for in-situ experimentation (with the addition of few others for completeness). Three electrochemical, six metal oxide, one nondispersive infrared and the PID sensors were included in the unit. The experimental method employed was based on time course varying from few days to two weeks. Two types of experiments were carried out, namely laboratory work and store room monitoring. Time series results for four types of sample types (unwounded controls, wounded controls and two infected sets) show that some of the sensors (ethanol, ammonia, hydrocarbons, overall volatiles and carbon monoxide) deployed on the instrument could discriminate between the various sample batches and detect soft rot from a very early stage and throughout the experimental work.

The bespoke instrument was then deployed in a research store setting for testing (at the AHDB Sutton Bridge Crop Storage Research Centre, UK). Four 1 ton wooden crates controls were placed inside a (56 m³) store room (at 95% RH and 15 ± 1 °C) followed after the fourth day by a batch of infected tubers (with a proportion of infected tubers to controls of 1%). Results over a period of circa three weeks show that some of the sensors (ethanol, ammonia and hydrocarbons) could detect soft rot from a very early stage and throughout the experimental work.

In conclusion, the research reported here shows that gas analysis technology could be successfully applied for pre-symptomatic detection and monitoring of soft rot in a storage facility with readily available commercial sensors.

ACKNOWLEDGMENTS

First and foremost I would like to thank my supervisor Dr James Covington for his support and guidance in the project and during the compilation of this thesis.

Second, the author wishes to thank Dr John Clackson and Dr Daciana Iliescu for their roles and support in the supervision process.

Many thanks are also due to members of technical staff that provided assistance throughout this complex interdisciplinary project. In particular, a special acknowledgment is dedicated to Mr Francis Courtney (School of Engineering) Claire Handy and Alison Jackson (School of Life Sciences).

Last, but not least, I wish to sincerely thank my companion, my parents, friends and colleagues for their support during this step of my life.

TABLE OF CONTENTS

ABSTRACT.....	i
ACKNOWLEDGMENTS	iv
TABLE OF CONTENTS.....	v
LIST OF FIGURES	ix
LIST OF TABLES	xxi
GLOSSARY.....	xxii
1 Introduction.....	1
1.1 Context and motivation	1
1.2 Aim and Objectives	2
1.3 Thesis Layout	3
1.4 References	6
2 Background.....	7
2.1 Introduction	7
2.2 Literature Review	9
2.3 Gas Sensing Technologies.....	23
2.3.1 Ion mobility spectrometry and FAIMS	23
2.3.2 Photoionization detection.....	26
2.3.3 Metal oxide gas sensors and electronic noses	28
2.3.4 Electrochemical gas sensors.....	31
2.3.5 Infrared gas sensors.....	33
2.4 Discussion	34
2.5 Conclusion.....	37
2.6 References	38
3 Early Identification of Potato Storage Disease by Gas Analysis: a Pilot Study .45	
3.1 Introduction	45

3.2	Material and methods	46
3.2.1	Experimental sample preparation.....	46
3.2.2	Experimental sampling protocol	48
3.2.3	Data Analysis	51
3.3	Results	53
3.3.1	FAIMS response for all time points	53
3.3.2	Detection of potato quarantine pathogens at FERA.....	58
3.3.3	Effect of temperature variation on soft rot disease detection.....	60
3.3.4	PID response for ‘detection’ and ‘early detection’ time points	63
3.4	Discussion	68
3.5	Conclusion.....	73
3.6	References	74
4	Early Identification of Potato Storage Disease using Metal-Oxide, Electrochemical and NDIR Gas Sensors.....	76
4.1	Introduction	76
4.2	Material and methods	78
4.2.1	Experimental sample preparation.....	78
4.2.2	Experimental sampling protocol	78
4.2.3	Data analysis	81
4.3	Results	87
4.3.1	Metal oxide gas sensors response to ‘detection’ time point.....	87
4.3.2	Metal oxide gas sensors response to ‘early detection’ time point.....	92
4.3.3	Electrochemical/NDIR gas sensors response to ‘detection’ time point	96
4.3.4	Electrochemical/NDIR gas sensors response to ‘early detection’ time point.....	101
4.4	Discussion	105
4.5	Conclusion.....	109

4.6	References	110
5	Data Logger for Environmental Analysis of Soft Rot VOCs	112
5.1	Introduction	112
5.2	List of requirements.....	113
5.3	System architecture	116
5.4	System components	117
5.4.1	Power supply	117
5.4.2	Sensors and data acquisition	119
5.4.3	Air flow delivery	128
5.4.4	Main board and user interface.....	134
5.4.5	Firmware	137
5.5	Assembled systems.....	140
5.6	Discussion	142
5.7	Conclusion.....	143
5.8	References	144
6	Experimental work with VOC data logger	148
6.1	Introduction	148
6.2	Materials and methods.....	149
6.2.1	Experimental laboratory work at Warwick	149
6.2.2	Experimental storage facility work at SBCSR.....	151
6.3	Results	154
6.3.1	Laboratory work with completed time course	154
6.3.2	Laboratory work to evaluate early time course.....	162
6.3.3	Experimental work at the SBCSR potato store facility.....	166
6.4	Discussion	171
6.5	Conclusion.....	174
6.6	References	175

7	Conclusions and Future Work	177
7.1	Conclusions	178
7.2	Future Work	184

LIST OF FIGURES

Fig. 2.1. Potato soft rot (affecting the tuber) and blackleg (stem rot), (Bacterial Rots of Potato Tubers, 2009; Peters et al., 2012).	8
Fig. 2.2. Soft rot/blackleg disease cycle (De Boer, 2004).....	8
Fig. 2.3. Basic working principle of ion mobility spectrometer (Borsdorf and Eiceman, 2006b).	24
Fig. 2.4. Basic working principle of FAIMS.	25
Fig. 2.5. Basic working principle of PID (RAE Systems - Honeywell Inc, 2005).	27
Fig. 2.6. Ionization Potentials for common chemicals (RAE Systems - Honeywell Inc, 2005).	27
Fig. 2.7. Basic metal oxide gas sensor structure (Figaro Engineering Inc, 2015).	29
Fig. 2.8. Basic operational principle of the n-type metal oxide gas sensor. Sensor with no exposure to gas (A) causes high potential barrier to electron flow (eV in graph). When sensor is exposed to reducing gas, potential barrier is substantially reduced and electron can flow freely (Figaro Engineering Inc, 2016).	30
Fig. 2.9. Basic working principle of the electronic nose (Turner and Magan, 2004).	31
Fig. 2.10. Structure of an electrochemical gas sensor (A) and working principle (B), (Chou, 1999; Membraphor AG, 2016).....	32
Fig. 2.11. Structure and basic operating principle of infrared gas sensor (Hodgkinson et al., 2013).....	34

Fig. 3.1. Control (a, c, e, and g) and tuber infected with soft rot (b, d, f, h). (a) and (b) are positive ion matrices in A.U. (arbitrary units) while (c) and (d) show ion currents at 45% DF. (e) is the logarithmic representation on the ion current axis of (a), for control and (f) for the infected tuber in (b). Photographic analysis for control (g) and infected potato (h).54

Fig. 3.2. PCA score and k-means clustering (A) for two groups of potato tubers with controls (cyan triangles) and infected (red circles) that have been grouped with 95% confidence ellipses around the centroid identified by the k-means algorithm) for 5DPI (5 days post inoculation). Loadings for the two main principal components in (B) and (C).55

Fig. 3.3. PCA score and k-means clustering (A) for two groups of potato tubers with controls (cyan triangles) and infected (red circles) that have been grouped with 95% confidence ellipses around the centroid identified by the k-means algorithm) for 2DPI (2 days post inoculation). Loadings for the two main principal components in (B) and (C).56

Fig. 3.4. PCA score and k-means clustering (A) for two groups of potato tubers with controls (cyan triangles) and infected (red circles) that have been grouped with 95% confidence ellipses around the centroid identified by the k-means algorithm) for 1DPI (1 day post inoculation). Loadings for the two main principal components in (B) and (C).57

Fig. 3.5. Characteristics early symptoms of brown rot (A) and ring rot (B) (DEFRA 2005a; DEFRA 2005b).58

Fig. 3.6. Lonestar FAIMS PCA results obtained at FERA (Food and Environment Research Agency) for control (20 samples), brown rot (50 samples) and ring rot (15 samples).....	59
Fig. 3.7. FAIMS data for all potato tuber samples: Ion Current (ordinate, units in AU, arbitrary units) versus Compensation Voltage (abscissa, units in V) at Dispersion Field of 50% for control tubers (A), tubers infected with brown rot (B) and ring rot (C).....	60
Fig. 3.8. Logarithmic representation of the DF matrix for the same tuber infected with soft rot stored at 25 °C (A) for four days and 10 °C (B) for 24 hours after inoculation and prior to sampling.	61
Fig. 3.9. PCA score and k-means clustering for two groups of potato tubers with controls (cyan triangles) and infected (red circles) that have been grouped with 95% confidence ellipses around the centroid identified by the k-means algorithm). Each of the tubers was first stored at 25 °C for 4 days post inoculation and then for 24h at 15 °C.....	62
Fig. 3.10. PCA score and k-means clustering for two groups of potato tubers with controls (cyan triangles) and infected (red circles) that have been grouped with 95% confidence ellipses around the centroid identified by the k-means algorithm). Each of the tubers was first stored at 25 °C for 4 days post inoculation and then for 24h at 10 °C.....	62
Fig. 3.11. Data results for the Tiger VOC analyzer for ‘detection’ time point, i.e. 5 DPI (days post inoculation). “CO” refers to control, “DP” to infected tuber and “B” to background reading before sampling. The legend for 60, 30, 5 and 1m indicates	

the time period of storage of tuber in the PTFE jar prior to sampling. Units are in ppm (parts per million).....63

Fig. 3.12. Data results for the Tiger VOC analyzer for ‘early detection’ time point, i.e. 2 DPI (days post inoculation). “CO”, “DP” and “B” are as indicated in Fig 4.11. The legend for 60, 30, 5 and 1m indicates the time period of storage of tuber in the PTFE jar prior to sampling. Units are in ppm (parts per million).....65

Fig. 3.13. Data results for the Tiger VOC analyzer for ‘detection’ time point, i.e. 5 DPI (days post inoculation. “CO” refers to control, “DP” to infected tuber, “B_” to background reading before sampling, “_d1” and “_d2” to the first and second day of sampling. 5m was the period of storage of tuber in the PTFE jar before sampling. The abscissa indicate potato tuber sample number while the ordinate instrument values in ppm (parts per million).66

Fig. 3.14. Data results for the Tiger VOC analyzer for ‘early detection’ time point, i.e. 2 DPI (days post inoculation. “CO” refers to control, “DP” to infected tuber, “B_” to background reading before sampling, “_d1” and “_d2” to the first and second day of sampling. 5m was the period of storage of tuber in the PTFE jar before sampling. The abscissa indicate potato tuber sample number while the ordinate instrument values in ppm (parts per million).67

Fig. 4.1. Representation of most common feature extraction approaches for electronic nose data. ‘Maximum’ and ‘Minimum’ indicate the maximum value and minimum value respectively, while ‘Base’ refers to baseline. A detailed description of the techniques is listed in Table 4.3.82

Fig. 4.2. Representation for the W3db feature extraction method. The sensor response (ordinate), versus time (abscissa), reaches its apex at the point labelled ‘maximum’ (exposure to odorant) before returning to the baseline resistance. W3db is the measurement between the value at 70% (3 dB) of the exposure to odorant and the same value for the recovery part of the curve (absence of odorant) (Mitrovics 2009).	83
Fig. 4.3. Representation for the AreaMax feature extraction method. The sensor response (ordinate), versus time (abscissa), reaches its apex at the point labelled ‘maximum’ (exposure to odorant) before returning to the baseline resistance. AreaMax is the measurement of the area for the response time (exposure to odorant) above the baseline from the first point to the point of maximum response (Mitrovics 2009).	84
Fig. 4.4. Data analysis process: basic statistical analysis, unsupervised and supervised approaches.	86
Fig. 4.5. Bar plot of raw data indicating differences in responses for all sensors at two time points (‘tp’). ‘CO’ indicates healthy controls and ‘DP’ to diseased potato tubers. The error bars represent standard errors of the mean values. The sensors nomenclature refers to Alphamos FOX 200-4000 Manual Release 4.0.1.	87
Fig. 4.6. PCA score and k-means plot with 95% confidence intervals based on CMOS technology measurements for all sensors at time point ‘detection’. Data points indicate healthy controls (cyan, triangles) and diseased potato tubers (red, circles).	88

Fig. 4.7. Biplot for all sensors at time point ‘detection’. Data points indicate healthy controls (grey, triangles) and diseased potato tubers (red, circles).	89
Fig. 4.8. Biplot for selected sensors (SY.W, T30.1, SY.gcT) at time point ‘detection’. Data points are as indicated in Fig. 4.7.	89
Fig. 4.9. Class probability histograms of different models for all sensors at ‘detection’ time point for healthy controls (‘CO’) and diseased potato tubers (‘DP’). The following models are represented: RBFSVM (Radial Basis Function Support Vector Machine), RF (Random Forest), MARS (Multivariate Adaptive Regression Splines), LDA (Linear Discriminant Analysis), C5 (C5.0 tree algorithm).	91
Fig. 4.10. Class probability histograms for selected sensors (SY.W, T30.1, and SY.gcT) at time point ‘detection’. Legend and notation are as indicated in Fig. 4.9.	91
Fig. 4.11. PCA score and k-means plot with 95% confidence intervals based on CMOS technology measurements for all sensors at time point ‘early detection’. Data points indicate healthy controls (cyan, triangles) and diseased potato tubers (red, circles).	92
Fig. 4.12. Biplot for all sensors at time point ‘early detection’. Data points indicate healthy controls (grey, triangles) and diseased potato tubers (red, circles).	93
Fig. 4.13. Biplot for selected sensors (SY.W, T30.1, SY.gcT) at time point ‘early detection’. Data points are as indicated in Fig. 4.12.	93
Fig. 4.14. Class probability histograms of different models for all sensors at ‘early detection’ time point for healthy controls (‘CO’) and diseased potato tubers (‘DP’). The following models are represented: RBFSVM (Radial Basis Function Support	

Vector Machine), RF (Random Forest), MARS (Multivariate Adaptive Regression Splines), LDA (Linear Discriminant Analysis), C5 (C5.0 tree algorithm).....	95
Fig. 4.15. Class probability histograms for selected sensors at time point ‘early detection’. Legend and notation are as indicated in Fig. 4.14.....	95
Fig. 4.16. Bar plot of raw data indicating differences in responses for all sensors at two time points (‘tp’). ‘CO’ indicates healthy controls and ‘DP’ to diseased potato tubers. The error bars represent standard errors of the mean values. The sensors nomenclature refers to the chemical compounds to which sensors are responsive. ..	96
Fig. 4.17. PCA score and k-means plot with 95% confidence intervals based on electrochemical gas sensors technology measurements for all sensors at time point ‘detection’. Data points indicate healthy controls (cyan, triangles) and diseased potato tubers (red, circles).....	97
Fig. 4.18. Biplot for all sensors at time point ‘detection’. Data points indicate healthy controls (grey, triangles) and diseased potato tubers (red, circles).	98
Fig. 4.19. Biplot for selected sensors (CO, ETO, NO) at time point ‘detection’. Data points are as indicated in Fig. 4.18.....	98
Fig. 4.20. Class probability histograms of different models for all sensors at ‘detection’ time point for healthy controls (‘CO’) and diseased potato tubers (‘DP’). The following models are represented: RBFSVM (Radial Basis Function Support Vector Machine), RF (Random Forest), MARS (Multivariate Adaptive Regression Splines), LDA (Linear Discriminant Analysis), C5 (C5.0 tree algorithm).....	100

Fig. 4.21. Class probability histograms for selected sensors (CO, ETO, and NO) at time point ‘detection’. Legend and notation are as indicated in Fig. 4.20.....	100
Fig. 4.22. PCA score and k-means plot with 95% confidence intervals based on electrochemical gas sensors technology measurements for all sensors at time point ‘early detection’. Data points indicate healthy controls (cyan, triangles) and diseased potato tubers (red, circles).....	101
Fig. 4.23. Biplot for all sensors at time point ‘early detection’. Data points indicate healthy controls (grey, triangles) and diseased potato tubers (red, circles).	102
Fig. 4.24. Biplot for selected sensors (CO, ETO, NO) at time point ‘early detection’. Data points are as indicated in Fig. 4.23.	102
Fig. 4.25. Class probability histograms of different models for all sensors at ‘early detection’ time point for healthy controls (‘CO’) and diseased potato tubers (‘DP’). The following models are represented: RBFSVM (Radial Basis Function Support Vector Machine), RF (Random Forest), MARS (Multivariate Adaptive Regression Splines), LDA (Linear Discriminant Analysis), C5 (C5.0 tree algorithm).....	103
Fig. 4.26. Class Probability histograms for selected sensors at time point ‘early detection’. Legend and notation are as indicated in Fig. 4.25.....	104
Fig. 5.1. Block diagram of system architecture. In red the power bus and in cyan the data bus respectively.	116
Fig. 5.2. Power supply unit PCB layout.....	118
Fig. 5.3. LM317 support circuitry for desired voltage output, achieved by varying the 10 k potentiometer R3 (Texas Instruments Inc, 2014).....	118

Fig. 5.4. From left to right in (A): uncapped sensing element for Figaro TGS2611 hydrocarbons (centre) and methane (the longer metal cap contains a filter material meant to be selective for the gas of interest), (Figaro Engineering Inc, 2013a). In (B), the temperature and relative humidity sensors SHT15 (Sensirion AG, 2011)..... 122

Fig. 5.5. Basic measuring circuit for a MOX sensor (A): V_c and V_H indicate the voltage applied to sensor element (R_s) and heater (R_H) respectively; R_L and V_{RL} indicate load resistance and voltage. Variation of output voltage for various values the load resistance (B), (Figaro Engineering Inc, 2005b). 123

Fig. 5.6. Metal oxide gas sensors PCB and acrylic chamber (9 x 5 x 3 cm)..... 124

Fig. 5.7. NO, CO, ETO, PID sensors and AFE board (Alphasense Ltd). Sensors (A), rear of AFE (B) and chamber (C). 125

Fig. 5.8. Block diagram of AFE for electrochemical gas detectors with potentiostat circuit. C, R and S indicate counter, reference and sensing/working electrodes respectively (SGX Sensortech Ltd, 2015). 125

The CO₂ sensor Cirius 2 and comes equipped with an infrared transmitter board (Fig. 5.9). Cirius 2 is capable of a sensing range of up to 5000 ppm and is based on nondispersive infrared technology. The component contains a source of infrared radiation, an infrared detector and an optical waveguide for gas diffusion (Clairair Ltd, 2010). The transmitter board contains a microprocessor and display for setting sensor parameters and a communications circuit. For signal output, the board uses either a RS232 interface protocol or a current source of 4-20mA output and for ease, the latter has been implemented. The voltage output for the microcontroller (by Ohm's law) via a (250 Ohm) load resistor (Clairair Ltd, 2015). 125

Fig. 5.9. NDIR CO ₂ Cirius gas sensor (A), sensor in acrylic chamber (B) and Cirius X OEM 4-20mA Transmitter (C), (Clairair Ltd, 2015, 2010).	126
Fig. 5.10. Increase in resolution from 10-bit (A) to 16-bit (B) in experimental results.	127
Fig. 5.11. Block diagram of air flow path.	130
Fig. 5.12. Valves (A), manifold (B), pump unit (C), manual valve to change air flow (D) and flowmeter (E).	132
Fig. 5.13. Control PCB unit for data logging unit for 5 valves and pump pair unit.	133
Fig. 5.14. Valves/pumps control and protection circuit components.	134
Fig. 5.15. System control PCB.	136
Fig. 5.16. Front of user interface display front (A) and rear (B), (4D Systems Pty Ltd, 2016).	136
Fig. 5.17. Basic flowchart for firmware.	139
Fig. 5.18. Data logger for laboratory experiments (A). Side view: fan, power supply connector and slot for USB port in (B). Side view: fan discharge, air exhaust and air inlets in (C).	140
Fig. 5.19. Inside of data logger for laboratory experiments.	141
Fig. 5.20. Close-up of data logger deployed in stores at AHDB Sutton Bridge Crop Storage Research Centre.	141

Fig. 6.1. Laboratory setup. In (A) the data logging unit connected to the 4 containers via PTFE tubing. In (B) the inside of each container with acrylic mesh for suspension of samples over the water bath for humidification.	151
Fig. 6.2. Potato storage rooms (A) at Sutton Bridge Crop Storage Research Centre. In (B) the storage room employed for experiments with four 1 t potato crates.	152
Fig. 6.3. Inside the test room as shown in Fig. 6.2. Air circulation system (A); infected tubers on the left-hand side, four 1t potato crates on the right-hand side in (B), (D) and data logger in (C).	153
Fig. 6.4. Electrochemical gas sensor response for NO (nitric oxide).	156
Fig. 6.5. Electrochemical gas sensor response for ETO (ethylene oxide).	156
Fig. 6.6. Electrochemical gas sensor response for carbon monoxide.	157
Fig. 6.7. PID gas sensor.	157
Fig. 6.8. MOX VOC (volatile organic compounds) sensor results.	158
Fig. 6.9. MOX VOC sensor results.	158
Fig. 6.10. Metal oxide gas sensor response for alcohols.	160
Fig. 6.11. MOX sensor response for ammonia.	160
Fig. 6.12. MOX sensor response for methane.	161
Fig. 6.13. MOX sensor response for hydrocarbons.	161
Fig. 6.14. Response for NDIR CO ₂ sensor.	162

Fig. 6.15. Carbon monoxide sensor response.	164
Fig. 6.16. PID sensor response.....	164
Fig. 6.17. Metal oxide VOC sensor response.....	165
Fig. 6.18. Metal oxide alchools sensor response.....	165
Fig. 6.19. Metal oxide ammonia sensor response.	166
Fig. 6.20. The two infected tubers employed for this work. The first associated to V4 while the second to V5 (with large quantities of carbon monoxide).	166
Fig. 6.21. Electrochemical gas sensors: NO, ETO.....	168
Fig. 6.22. Electrochemical gas sensor: carbon monoxide. The orange line indicates when infected tubers were placed into the storage facility.	168
Fig. 6.23. Photoionization detection and metal oxide VOCs sensors.	169
Fig. 6.24. Metal oxide gas sensor for alcohols. The orange line indicates when infected tubers were placed into the storage facility.	169
Fig. 6.25. MOX sensors for methane, hydrocarbons and ammonia.....	170
Fig. 6.26. Tubers infected with soft rot after 21 days inside the storage room (A); control tubers with visible signs of sprouting after 28 days since the start of the experiment (B).	170

LIST OF TABLES

Table 3.1. Experiments carried out and number of samples (total of 156).....	50
Table 4.1. Description of FOX3000 sensors as indicated in the FOX2000-4000 Manual (Release 4.01) by Alpha MOS Ltd.	80
Table 4.2. Description of WOLF 4.1 sensors employed for experimental work as indicated by Alphasense Ltd and Clair Air Ltd.	81
Table 4.3. Short description of common electronic noses techniques (Mitrovics 2009).	82
Table 4.4. Confusion matrices metrics for the selected time point ‘detection’	90
Table 4.5. Confusion matrices metrics for the selected time point ‘early detection’.	94
Table 4.6. Confusion matrices metrics for the selected time point ‘detection’	99
Table 4.7. Confusion matrices metrics for the selected time point ‘early detection’.	103
Table 5.1. List of sensors in alphabetical order by sensed variable. MOX refers to metal oxide, EC to electrochemical and PID to Photoionization Detection.	121

GLOSSARY

ADC	Analogue Digital Conversion
AFE	Analogue Front End
AHDB	Agriculture and Horticulture Development Board
C5	C5.0 tree algorithm
CO	Carbon Monoxide
DC	Direct Current
DC/DC	Direct Current/ Direct Current
EC	Electrochemical
ETO	Ethylene Oxide
eV	Electron Volt
FAIMS	Field Asymmetric Ion Mobility Spectrometry
FAT16	File Allocation Table 16
FAT32	File Allocation Table 32
GC	Gas Chromatography
GC-MS	Gas Chromatography Mass Spectrometry
I ² C	Inter-integrated Circuit Bus
IC	Integrated Circuit
ID	Internal Diameter

IMS	Ion Mobility Spectrometry
IP	Ionization Potential
JFET	Junction Gate Field-Effect Transistor
LDA	Linear Discriminant Analysis
LP	Liquefied Petroleum
MARS	Multivariate Adaptive Regression Splines
MicroSD	Micro Secure Digital
MOSFET	Metal Oxide Semiconductor Field Effect Transistor
MOX	Metal Oxide
NDIR	Nondispersive Infrared
NO	Nitric Oxide
OD	Outer Diameter
PC	Personal Computer
PCB	Printed Circuit Board
PID	Photoionization Detection
PSU	Power Supply Unit
PTFE	Polytetrafluoroethylene
PWM	Pulse Width Modulation
qPCR	Quantitative Polymerase Chain Reaction

RBFSVM	Radial Basis Function Support Vector Machine
RF	Random Forest
RH	Relative Humidity
RS232	RS232 Standard
RTC	Real Time Clock
SD	Secure Digital
SDHC	Secure Digital High Capacity
SPI	Serial Peripheral Interface Bus
TFT	Thin Film Transistor
TTL	Transistor Logic
UART	Universal Asynchronous Receiver Transmitter
UV	Ultra Violet
VOC	Volatile Organic Compound

INTRODUCTION

This page is intentionally left blank.

1 Introduction

1.1 Context and motivation

The United Nations FAO (Food and Agriculture Organization) estimates that between 40 to 50 % of root and tuber crops, fruits and vegetables produce is wasted each year to a range of causes (FAO (Food and Agriculture Organization of the United Nations), 2016, 2015). In the United Kingdom one staple crop that is particularly susceptible is potato tubers. Most of the loss is caused by a disease of bacterial origin known as ‘soft rot’, which causes substantial post-harvest store losses to the industry (with unofficial estimates of circa 5 % of the entire crop, as indicated by staff at the UK Agriculture and Horticulture Development Board), resulting in a strong need for the detection and monitoring of this disease.

Due to the nature of consumer requirements, potato tubers are stored for longer periods of time after harvest. They are kept in such storage facilities from late September until June of the following year. On average, each of these store rooms can contain several hundred 1-ton boxes of produce. This is the most widespread practice for storing the crop in the country, although other approaches are also employed worldwide. Monitoring the disease status of potatoes in stores is difficult, due to poor access and the large volume of product. However, in an attempt to extend the storage life of these potatoes, stores are generally environmentally controlled with air forced through the tubers. Furthermore, soft rot produces a very strong odour that can easily be detected by human olfaction. Therefore, it should be possible to use artificial sensing technologies to detect the odour given off by infected tubers. Previous work on early detection of potato storage diseases has been conducted over a span of decades with results that appear, to date, to have been inconsistent or of no practical implementation.

In addition, those studies also proved to be neither cost-effective nor have a practical implementation for commercial facilities. The purpose of this study is to, in part, validate previous work to show that it is possible to detect soft rot infection by gas analysis and then deploy different sensing technologies (not previously reported) that could be more appropriate to a final, working solution. In particular, attention is given to low-cost and practical implementation of early detection and monitoring of the aforementioned potato storage disease.

1.2 Aim and Objectives

Aim of the proposed research is the pre-symptomatic evaluation and monitoring of potato soft rot under selected conditions and by means of gas analysis techniques for future deployment in commercial potato stores.

The main objectives, in which this work contributes to novel knowledge in the field of potato research, can be summarised as follows:

- 1) To research and report on previous work for detection by gas analysis of potato soft rot or other relevant studies.
- 2) To shortlist other available gas analysis technologies, not previously reported, that could be employed for monitoring of the aforementioned disease.
- 3) To evaluate such techniques for both symptomatic and pre-symptomatic progression of soft under laboratory conditions.
- 4) To shortlist a technology/sensor, or suitable set of technologies/sensors, among the ones tested with potential for ease of deployment in store and at low cost (subject to objective 3) above).

- 5) To design, manufacture and test a purpose-built research instrument comprising the aforementioned technologies (subject to objectives 3) and 4) above).
- 6) To deploy the instrument for monitoring of soft rot under laboratory and commercial store conditions (subject to objectives 3) and 4) above).

1.3 Thesis Layout

Chapter 2:

The first part of this chapter reports on previous work on soft rot infection. The literature review starts with pioneering work carried out in the 1970s and is described in chronological order. The second part introduces the reader to other available, but also well-established, mature gas sensor technologies employed in other application areas (such as security and petrochemical industries).

This chapter aims to address objectives 1) and 2) in the section ‘Aims and Objectives’ listed above.

Chapter 3:

This chapter introduces new work on the use of FAIMS (Field Asymmetric Ion Mobility Spectrometry) technology in the detection of gas phase biomarkers of soft-rot. FAIMS was used to investigate both a suitable laboratory protocol and time points in order to evaluate the technology potential for both symptomatic and pre-symptomatic soft rot diagnostics. At this stage of the project it was also possible to study and report on the results obtained with quarantine diseases brown rot and ring rot. In the subsequent sections PID (Photoionization Detection – another type of gas analysis) is studied for the selected time points, but with static headspace sampling.

This part of the thesis has also been reported in published work (Rutolo et al., 2014).

This chapter also describes in detail the experimental method for potato inoculation, sample storage and testing employed also in the next Chapter 4.

This chapter aims to address objectives 3) and 4) in the section ‘Aims and Objectives’ listed above.

Chapter 4:

This chapter investigates the use of different electronic noses technologies that could be employed for store deployment, namely MOX (metal oxide), EC (electrochemical) and NDIR (nondispersive infrared) gas sensors. Experimental work is reported on two electronic noses for detection and early detection of soft rot. The materials and methods used are as developed in the pilot study in the previous chapter. In addition, the data analysis presented here reports a basic statistic summary, an unsupervised approach to show the variance in the distribution of data and a series of machine learning models to further and strengthen the results previously obtained with a large arrays of detectors. This part of the thesis has also been reported in published work (Rutolo et al., 2016).

This chapter aims to address objectives 3) and 4) in the section ‘Aims and Objectives’ listed above.

Chapter 5:

This part details new work on the development of an instrument to be deployed within a research potato store. The instruments development was informed from the laboratory research described in previous chapters, using the best sensing strategies/sensors identified earlier. The chapter covers all of the design stages of this

instrument, from an initial list of requirements, through an overall system architecture to the final implemented solution. Finally, an overall assessment of the system is reported.

This chapter aims to address objective 5) in the section ‘Aims and Objectives’ listed above.

Chapter 6:

In this chapter material, methods and results for laboratory experiments are presented as well as research in a commercial research storage facility, using the instrument developed/described in chapter 5. Previously, symptomatic and pre-symptomatic detection were investigated at selected intervals in time. In this part of the work the method employed consists in constantly monitoring of disease spread over time. Laboratory experiments with time course were also undertaken and related to store work. A discussion on the effectiveness of the instrument for pre-symptomatic detection and monitoring of potato tuber soft rot is provided.

This chapter aims to address objective 6) in the section ‘Aims and Objectives’ listed above.

Chapter 7:

This chapter summarises and concludes the research reported in previous chapters. Suggestions for further work are given describing how best this project could be taken forward into commercial use.

This chapter aims to address all the objectives presented in the section ‘Aims and Objectives’ listed above.

1.4 References

- FAO (Food and Agriculture Organization of the United Nations), 2016. SAVE FOOD: Global Initiative on Food Loss and Waste Reduction [WWW Document]. URL <http://www.fao.org/save-food/en/> (accessed 11.8.16).
- FAO (Food and Agriculture Organization of the United Nations), 2015. Global Initiative on Food Loss and Waste Reduction. USA.
- Rutolo, M., Covington, J.A., Clarkson, J., Iliescu, D., 2014. Detection of potato storage disease via gas analysis: A pilot study using field asymmetric ion mobility spectrometry. *Sensors (Switzerland)* 14, 15939–15952.
doi:10.3390/s140915939
- Rutolo, M.F., Iliescu, D., Clarkson, J.P., Covington, J.A., 2016. Early identification of potato storage disease using an array of metal-oxide based gas sensors. *Postharvest Biol. Technol.* 116, 50–58. doi:10.1016/j.postharvbio.2015.12.028

LITERATURE REVIEW AND BACKGROUND

This page is intentionally left blank.

2 Background

2.1 Introduction

Potato tuber wastage is a major issue and every year a substantial proportion of UK potato production is lost. The main cause for post-harvest waste is estimated at circa 5% and is due to a bacterial ‘soft rot’ infection (AHDB Potatoes, 2012). The term soft rot is used for stored potatoes while blackleg is generally employed for the growing crop, since infection can be found in the field and will cause blackening of the stem in the plant, as shown in Fig. 2.1 (*Bacterial Rots of Potato Tubers*, 2009; Peters et al., 2012).

The pathogen found most frequently in the UK associated with soft rot (and blackleg) is *Pectobacterium carotovorum* ssp. *carotovorum*, but *Pectobacterium atrosepticum* is also common (*Bacterial Rots of Potato Tubers*, 2009; Czajkowski et al., 2015). Bacterial soft rot in store and blackleg can also be caused by several strains of *Dickeya* spp. (Czajkowski et al., 2011), more recently identified as *D. dianthicola*, *D. dadantii*, *D. zeae* and *D. solani* (Czajkowski et al., 2015; Peters et al., 2012; Toth et al., 2011) as well as by *P. carotovorum* subsp. *brasiliensis* (Duarte et al., 2004; Leite et al., 2014) and *P. wasabiae* (Panda et al., 2012; Pitman et al., 2010). Other two infections, namely late blight and dry rot have been reported to provide a means for secondary infection of both subspecies of *Pectobacterium* (Lui et al., 2005).



Fig. 2.1. Potato soft rot (affecting the tuber) and blackleg (stem rot), (*Bacterial Rots of Potato Tubers*, 2009; Peters et al., 2012).

Potato is a crop that is grown via vegetative propagation. This means that the plant is not grown via the true seed but from asexually produced propagules (this ‘seed’ consists of cut parts of the original tubers), since this allows a highly regulated crop that responds to the needs of industry. Potato tubers are underground storage organs of the plant to which they are attached by stolons. Once the tubers are harvested, the two main uses are consumption and processing or are ‘seed’. Bacteria and associated soft rot/blackleg symptoms can be present at various stages of the crop life cycle, as shown in Fig. 2.2 (De Boer, 2004).

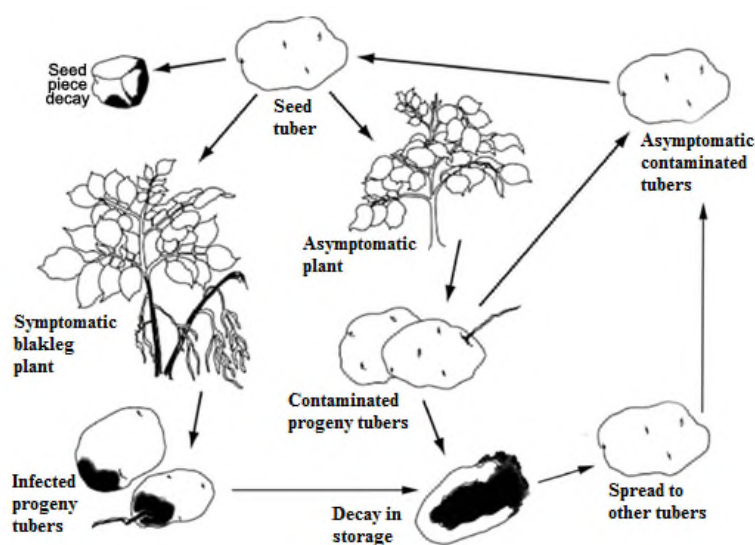


Fig. 2.2. Soft rot/blackleg disease cycle (De Boer, 2004).

Previously *P. carotovorum* ssp. *carotovorum* was known as *Erwinia carotovora* ssp. *carotovora* (ECC) and *P. atrosepticum*, as *Erwinia carotovora* ssp. *atroseptica* (ECA). For clarity and consistency, in the literature review that follows, the term *Erwinia carotovora* will be kept while, in subsequent chapters, the newer terminology will be adopted.

Soft rot (or other diseases) of potato tubers and, in general in plants, has been reported throughout the literature by means of what is referred as ‘volatile metabolites’. The terms volatile metabolites, volatiles, metabolites or more simply VOCs (volatile organic compounds) have been used interchangeably in those works and also throughout this study. According to EU Directive 1999/13/EC, Volatile Organic Compounds are defined as organic compounds having at 293.15 K a vapor pressure of at least 0.01 kPa, or having a corresponding volatility under particular conditions of use (EU law and other public EU documents, 1999). VOCs can also be more broadly defined as organic chemical compounds that under normal conditions are gaseous or can vaporize and enter the atmosphere (European Environment Agency, 2016).

2.2 Literature Review

In 1979 Varns and Glynn conducted a feasibility study on the early detection of VOCs associated with potato storage diseases, both in the laboratory and in a commercial storage facility (Varns and Glynn, 1979). In the manuscript, the authors claim that, via GC-MS (Gas Chromatography Mass Spectrometry), they identified abnormal quantities of substances to be associated with the *E. carotovora* (ssp. *carotovora*) bacterium, namely acetone, acetoin, ethanol and 2-butanone. In their laboratory set-up, inoculated potatoes (variety Chieftan) were placed into sealed Teflon bags.

Volatiles were collected by means of cryogenic air sample liquefaction (Ramussen, 1972) into 1 L stainless steel high pressure cylinders at 24 h intervals. After each sample collection, the Teflon bags were flushed with replacement purified air. Volatiles were collected on Tenax GC adsorbent and later thermally desorbed into vials for GC-MS analysis. After 96 hours, collection of volatiles from the infected potatoes showed a substantial surge in the presence of the substances previously mentioned (in particular with regard to acetone and ethanol), although other compounds were also detected in smaller quantities: acetaldehyde, methyl acetate, ethyl acetate, propanethiol, hydrogen sulphide, methyl sulphide, methyl disulphide, n-propanol, and isobutyl alcohol.

The next experimental phase was meant to determine whether acetone, acetoin, ethanol and 2-butanone could be detected in commercial stores infected with bacterial soft rot. After 6-7 months of storage, two sites were located that contained diseased and healthy bins of two potatoes varieties, Kennebec and Russet Burbank. Acetone, ethanol and 2-butanone (but not acetoin) were collected from the diseased bins of both cultivars in much larger quantities than from the healthy tubers containers, with the greater difference observed for the site with the Kennebec cultivar (and in both cases with very high concentrations of 2-butanone). The authors also suggested that the marked differences in 2-butanone concentrations for diseased tubers at both locations could be employed as a possible warning indicator of early disease development.

After this first study, further research was described in two manuscripts both dating back to 1984 and regarding overall volatile emissions. In their first work Waterer and Pritchard addressed only soft rot development (Waterer and Pritchard, 1984a) where potatoes (Russet Burbank) were either inoculated with *E. carotovora* (ssp. *carotovora*)

or left as wounded or unwounded controls. 1 kg lots for each of the three categories of tubers were placed into 3.2 L polyethylene bags (at room temperature) and filtered air was pumped through to allow a headspace volume of 2.5 L. After 24 h and at this constant time interval for 5 days, air was sampled from each bag into absorbent traps (Chromosorb 105) and then later thermally desorbed for chromatographic analysis. Fresh clean air was flushed through the bags after sample collection. 9 replicates for diseased tubers and 3 for controls were utilized and the experiment was repeated twice. In total 14 compounds were detected, with a number of them not reported earlier by Varns and Glyn (methanol, propanol, 1-butanol, 2-butanol) and no disease-specific markers could be identified. Results indicated that total volatiles concentration from the inoculated tubers increased substantially with development of infection. By contrast, the concentration of volatiles for the uninoculated samples remained low and constant for both wounded and unwounded control. The impact of temperature (4, 10, 21 °C) on the concentration of volatile metabolites was also studied. After 5 days, total reported metabolite production at 21 °C was 3 times greater than at 10 °C and 7 times greater than at 4 °C, although the temperature appeared not to affect the overall spectrum of volatiles.

In a subsequent study, volatile profiles were investigated for both another common potato tuber disease, ring rot (caused by the bacterium *Corynebacterium sepedonicum*), and soft rot (caused by *E. carotovora*) in controlled conditions, in order to assess if VOC profiling could differentiate between the two infections (Waterer and Pritchard, 1984b). Materials and methods were as employed in their previous experiments with soft rot. Disease development occurred at considerably different rates in the *E. carotovora* and *C. sepedonicum* inoculated tubers. The first visible signs

of decay were identified in the former after 3 days and in the latter after 7 days, with substantial tissue damage after 5 days for soft rot and 9 days for ring rot. The chromatograms for the two different treatments were markedly different but this was attributed to the different rates of disease development. However, in both cases, the total volatile outputs increased dramatically as disease progressed. After 5 days of infection, volatile production (as a daily average) for soft rot decay was more than 200 times greater than for ring rot, with the readings from potatoes inoculated with *C. sepedonicum* being no different to the controls. The authors reported that 9 days were required before the tubers were completely disrupted by *C. sepedonicum* while only 5 for *E. carotovora*. The total quantity of VOC produced over the entire incubation period (of 9 and 5 days respectively) was found to be very similar for both diseases. As in the previous research (Waterer and Pritchard, 1984a), the range of volatiles found in the head space of controls was also detected in the treatments infected with various pathogens. Few unidentified compounds were also found to be unique to either disease. Some metabolites peaks common to both diseases (ethanol, methanol, and 1-butanol) were also found to be more abundant in soft rot.

After these early attempts to identify potato storage disease volatiles, further research by Ouellette *et al.* (Ouellette et al., 1990) benchmarked their work against both the study by Varns and Glynn and Waterer and Pritchard using the Atlantic tuber variety. The set-up of the experiment, the materials, instrumentation, procedures and analysis employed were very different from the previous studies. The simulation utilized a dynamic headspace analysis set-up to replicate ventilated potato storage bins. Clean laboratory-grade air was first continuously passed through a molecular sieve (to further improve purification), then through a layer of water in a container (to create a

saturated atmosphere), and finally pushed through ten 7.7 L acrylic cylinders (manifold arrangement) containing control potatoes and tubers inoculated with either the soft rot bacterium *E. carotovora* or the fungus *Fusarium roseum* (ssp. *sambucinum*) which causes dry rot. At the containers outlets the volatiles were concentrated on Chromosorb 105 polymeric absorbents (replaced every 4 days) and later thermally desorbed and analysed with GC and GC-MS instrumentation. Air flow rate was set to limit CO₂ accumulation in the acrylic cylinder's headspace and a constant monitoring was set in place for this purpose. The experiment lasted 16 days and was repeated twice. Three compounds were identified as possible disease indicators, namely dimethyl disulphide and pentane, plus an unidentified compound in the case of tubers affected by spread of *F. roseum*. Dimethyl disulphide, an odoriferous substance, was found to be present in large quantities in the case of tubers infected with the bacterium *E. carotovora* (and in trace amounts for the other disease), while pentane was consistently found for both diseases. The authors believed that the presence of dimethyl disulphide was associated with potato tuber decomposition as a result of either pathogen. They dismissed chromatographic retention times by Varns and Glynn as markers for specific compounds, i.e. acetone, ethanol and 2-buthanol. The authors claimed that these chemicals could be associated with background potato volatiles rather than being disease-specific, since they were all identified in the headspace across all samples. However, the researchers pointed out that carbon dioxide levels were also well correlated with tuber decay induced by both *E. carotovora* and *F. roseum*, and as such was a possible indicator of disease development. CO₂ increase was considered to be associated with storage stress, due to an increase in respiration rate, and anaerobic microorganisms consuming oxygen. However, they also suggested that CO₂ might be indicative of maturing and bruising

as found by other researchers (Rastovski and Es, 1989; Schaper and Varns, 1978; Smith and Campbell, 1969).

Ratti also carried out research with potatoes inoculated with *E. carotovora* and subsequent dynamic headspace analysis (Ratti et al., 1995). Healthy and infected tubers were stored in containers at 12 °C. Purified air was passed through the containers until it reached absorbent traps, in a similar fashion to the protocol adopted by Ouellette (Ouellette et al., 1990). Traps were collected for analysis every 24 h and thermally desorbed for GC and GC-MS analysis. Results indicated that total amount of volatiles increased over time in the case of the diseased treatment. However, the authors claimed that three compounds were disease-specific: furan ester, styrene and phorone.

Further research was conducted in 2001 by Lyew *et al.* in which the aim was to ascertain if meaningful qualitative and quantitative changes in overall volatile profiles was suggestive of soft rot spread (Lyew et al., 2001). This focussed on avoiding the difficulties associated with obtaining consistent and reproducible results, unreliability due to storage conditions, potato cultivars, possible unrelated pathogens (that may alter overall VOCs profiling), amount of potatoes, ventilation, design and methodology of experimentation, degree of infection. The study was done in a laboratory setting with 1 kg batches of potatoes stored at room temperature and suspended over a layer of water within metal containers. The containers were fitted with volatile traps containing Chromosorb 105 and analysis of volatiles was carried out with gas chromatography. The volatiles emanating from tubers inoculated with *E. carotovora* ssp. *carotovora* and uninoculated control tubers were monitored by

periodically taking air samples of the head space. Two types of experiments were performed; the first with two sets of healthy control potatoes and another set of potatoes which were all each inoculated with *E. carotovora* (sampled every 24 h), and the second, with an additional treatment in which only one tuber from a batch of potatoes was infected (samples taken every 12 h). Comparison of the volatile profiles arranged in chronological order showed a progression over time, in the types and amounts of volatiles produced for the diseased potatoes. In the second experiment (of 144 h duration), a wider range of volatiles and larger chromatographic peaks showed that the single inoculated potatoes could be easily identified as diseased. Differences between the volatile profiles of healthy and inoculated potatoes were observed as early as 24 h into the experiment while the total quantity of volatiles produced was initially low and increased exponentially as the infection became well established. The authors reported a model of total peak area per unit weight of potatoes and per unit volume of air sample taken (as a function of time) that showed an exponential increase in volatile emissions over time.

The work by Lyew *et al.* (Lyew *et al.*, 2001) also complemented previous research by the same authors (Lyew *et al.*, 1999) where the main objective was to determine if volatiles from diseased potato tubers could be sampled and detected in a commercial storage facility. The authors acknowledged earlier achievements by other researchers in the field, but also pointed out that their study was not based on what type of volatiles, and in what measure, could be of practical use to identify soft rot. Instead, their effort was aimed at gauging the feasibility of implementing an air sampling unit in commercial storage facilities. This apparatus consisted of a sampling unit with two pump heads and a pair of volatile traps each attached to the two sides of the unit. The

traps (Chromosorb 105) were then removed and transported to laboratory for chromatographic analysis. The potatoes were kept either in a refrigerated or ventilated storage at the same facility, both rooms equipped with humidifiers. Results showed that volatiles were present in high abundance in the refrigerated storeroom containing uncleaned, unpackaged potatoes, but concentrations diminished after the potatoes had been removed. Similarly, elevated amounts of volatiles were observed in the ventilated room which also contained uncleaned, unpackaged potatoes.

De Lacy Costello further investigated volatiles from potato tubers with GC-MS infected with *E. carotovora* (de Lacy Costello et al., 1999). Tubers of the Maris Piper variety were placed after inoculation in a 2 L jar for a total weight of ca 1 kg. The containers were placed into an incubator for 12 h at 25 °C and subsequently transferred to a waterbath at 10 °C inside a purpose-built apparatus in order to simulate the environmental conditions (temperature and humidity) of commercial stores. The apparatus consisted of two temperature-controlled water baths in series, the first containing humidifying chambers and the other sample jars. Air was kept at 95% RH and temperature at 10 °C. VOCs were sampled after 4 weeks by flushing air through the potato jars for two hours with absorbent traps on the other end (and later thermally desorbed). The authors used 4 groups consisting of wounded control tubers, and tubers inoculated with *E. carotovora* ssp. *carotovora*, *Bacillus polymyxa* and *Arthrobacter* sp. The last two pathogens were included due to their potential association with soft rot symptoms. Results showed identification of twenty-two volatile compounds specific to *E. carotovora* with three specific to *B. polymyxa* and only one specific to *Arthrobacter* sp., although no quantitative details were reported. However, the authors also stated that no specific compound could be considered as disease-specific but

rather than overall increase in volatile metabolites was related to soft rot detection. They also reported that with a modified GC-MS method, sulphides and amines could also be detected and further suggested the need of sensors targeting a wide range of chemical groups. A similar approach with the same type of conclusions followed in later work investigating potato late blight and dry rot (de Lacy Costello et al., 2001).

Based on their GC-MS work the scholars also attempted to develop a sensor system for detection of soft rot (de Lacy Costello et al., 2000). An in-house test rig was employed for sensor selection, with sensing materials exposed to low concentrations (1-100 parts per million) of ethanol, acetone, butanol and 2-butanone (previously associated with soft rot) with the main feature of the unit being a high sensitivity of sensors. After this initial test, a custom-made version of metal oxides was chosen for broad volatiles detection. The sensors were then assembled into 3 and 2-sensor units interfaced to a computer for further data processing. The 3-sensor unit was first employed to examine treatments where one tuber was inoculated with *E. carotovora* ssp. *carotovora* and incubated for 7 days at 20 °C with sound tubers in a 25 kg paper sack. There was good volatile identification of the inoculated treatment whilst sampling at the sides of crates but far greater discrimination was obtained when analysis was conducted over the crates headspace. A later experiment with one inoculated tuber in a 100 kg storage crate of sound tubers was conducted with an improved system incorporating a smaller sensor chamber (to reduce dead volume) and the unit was again able to discriminate between healthy controls and diseased tubers. 128 tests were carried out with a reported substantial success rate for all sensors. The 2-sensor unit was designed to differentiate between 10 kg of uninoculated control tubers and 10 kg of tubers containing a single inoculated potato after incubation for 5

days at 4 °C. Although good discrimination was achieved, problems were encountered with sensitivity when the temperature was lowered to 4 °C. However, a series of problems encountered in the research were noted, in particular that the prototype sensors were sensitive to variations in ambient atmosphere and non-reproducibility of the sampling procedure.

Kushalappa and Zulfiqar, attempted to analyse the effects of two variables, namely humidity and temperature, as the most significant factors affecting *E. carotovora* ssp. *carotovora* disease development (Kushalappa and Zulfiqar, 2001). To address the effect of these two variables, Kushalappa and Zulfiqar conducted two core experiments, concerning infection and subsequent lesion expansion (each repeated twice). Sets of 5 inoculated tubers enclosed in nylon bags with samples removed at random, at each storage period, in order to assess disease severity. The purpose of this approach was to determine if mathematical models could be developed to predict disease development based on prevailing environmental conditions in commercial stores. Their modelling approach was based on the most significant factors thus removing the need to develop models for each variable. In the study, infection was quantified for at 10, 15, 20, 25 °C with incubation times of 3, 6, 12, 24, 48 hours while lesion expansion was quantified at 4, 8, 12, 16 °C and storage times of 15, 30, 45, 60, 90 days. From this a cubic regression model was created that explained 95% of the variation for infection potential, in the first case, and a quadratic one able to account for 96% of data obtained for the latter. Moreover, the researchers also reported that damaged tubers did not result in soft rot if suitable air circulation was available thus implying that anaerobic conditions were required for development of soft rot. Hence the research addressed and quantified experimentally and mathematically the effect of

temperature and humidity on the progression of soft rot caused by *E. carotovora*, albeit in laboratory conditions.

A different study by the same authors (Kushalappa et al., 2002) involved placing single inoculated and uninoculated potato tubers (Russet Burbank) on a steel support in 1 L jars (each holding 100 ml of water to create a saturated atmosphere) with cap fitted with a particular VOC trap and solid phase micro extraction (SPME) fibre, for GC processing. Uninoculated control treatments consisted of tubers injected with sterile distilled water while inoculated tubers were injected with a range of potato pathogens comprising *E. carotovora* subsp. *carotovora*, *E. carotovora* subsp. *atroseptica*, *Pythium ultimum* (pathogen causing leak), *Phytophthora infestans* (cause of late blight), or *F. sambucinum* (for dry rot). The experiment was repeated 8 times over six months for a total of 144 fingerprints. Samples were stored at 20 °C and every 24 h, after the volatiles were sampled (at day 3, 4 and 5), water was removed, bottles resealed and flushed with pure dry air. Rather than attempting to identify disease-specific compounds or changes in volatile profiles using GC/GC-MS, analysis of data was performed by implementing a particular set of algorithms known as neural networks. The input to the neural network consisted of sixteen volatiles as detected by the GC and six outputs corresponding to the different diseases considered in the experiment (plus one control). The neural network yielded clear-cut quantitative results such as, for example, the ability to discriminate *P. ultimum* from either strain of *E. carotovora*. However, in the case of another disease-inducing oomycete, *P. infestans*, the pathogen could be distinguished from all other samples but not the controls. The authors acknowledged these limitations and others for which they suggested further research, with particular regard to the avoidance of tuber

sterilization, mixing diseases (in the experiment each disease in turn was considered), and variation of environmental variables. The authors also highlighted that their approach and techniques yielded only discriminative results that were not necessarily disease-specific.

Another research group investigated disease-specific volatile markers as a means of discriminating diseases when more than one was present (Lui et al., 2005). Tubers (variety Russet Burbank) were used for five treatments consisting of unwounded / wounded non-inoculated controls and potatoes inoculated with *E. carotovora* ssp. *carotovora*, *E. carotovora* ssp. *atroseptica*, or *F. sambucinum*. Each tuber was stored at 20 °C in a 1 L bottle with water at the bottom for humidification. VOCs were sampled 3 and 6 days post-inoculation and the experiment was repeated 10 times. Metabolites were sampled and analysed by means of a portable GC/GC-MS system (HAPSITE-10122) and later compared to the USA NIST (National Institute of Standards and Technology) database of chemical compounds. A total of 81 metabolites were consistently detected and present at high levels. Of these, thirteen metabolites in significant quantities, were identified as discriminating the two subspecies of *E. carotovora* from *F. sambucinum* and the control treatments, with one unique chemical compound (acetic acid ethenyl ester) specific to *E. carotovora* ssp. *atroseptica*. Three compounds (cyclohexene, diazene and methoxy (1, 1-dimethyl-2-dihydroxy-ethyl)-amine) were also specific to *E. carotovora* ssp. *carotovora*. Moreover, the authors also reported the presence of alcohols, esters and ketones only in the tubers inoculated with the strains of *E. carotovora* with ethanol, acetone, and 2-butanone specific to both pathogens. However, there was a high level of variability within the results obtained across the set of 10 experiments. It was also suggested that

the volatiles interact with each other thus generating new compounds, or that the volatiles could potentially be reabsorbed by the same tubers that generated them in the first place. They also noted that high levels of humidity (on bottle and tuber surface) affected the quantity and types of volatiles sampled, as also demonstrated in another study (Toivonen, 1997). Nevertheless, Lui and his team proposed that VOC detection was a possible methodology for commercial stores and recommended dynamic headspace sampling and collection of tubers (on a regular basis) for laboratory testing. Last, but not least, they also suggested further work with regard to addressing the variability of results both with different cultivars and with cross-contamination among the pathogens investigated.

More recently, Biondi *et al.* completed a study using a commercial electronic nose to detect the quarantine potato tuber diseases brown rot and ring rot caused by *Ralstonia solanacearum* and *C. michiganensis* subsp. *sepedonicus* respectively (Biondi et al., 2014). Seed potatoes of the varieties Spunta and Kennebec were inoculated with each of the bacteria and harvested after 4 months in the field. The authors carried out 3 types of experiments: laboratory, intermediate and commercial scale and two types of data collection were employed: passive and active sampling. In the laboratory, circa 250 and 400 g of potatoes were placed into 0.5 and 1 L jars for active and passive sampling (qualitative analysis) respectively and stored at room temperature for 7 days. At the intermediate stage, net bags of 100 potatoes were prepared for both healthy controls and for different percentages (50%, 75% and 100%) of tubers affected by ring rot and subsequently stored at 4 °C for 7 days. In the commercial experiment, healthy control potatoes (analysed by the local Phytosanitary Service) were kept at 4 °C in 1.25 ton polypropylene bags. The electronic nose used was coupled with a commercial

desorption unit (EDU3, Airsense Analytics GmbH, Germany) and tested with different adsorbent materials (Tenax TA, Carbotrap, Tenax GR, and Carboxen 569). For passive sampling, a Radiello Carbograph cartridge was coupled to containers for 7 days, thermally desorbed into a purpose-built apparatus and then fed into the electronic nose for analysis. The instrument employed was a commercially available electronic nose (PEN3, Airsense Analytics GmbH, Germany) with a sensor array containing 10 metal oxide semiconductor sensors (aromatics, aliphatics, sulfur- and chloro-organic compounds, methane and aliphatics, alcohols, hydrogen). The passive sampling resulted in a high degree of discrimination for ring rot in laboratory and intermediate scale work. Volatile profiles reported by the authors were claimed to be in line with findings of previous works with GC-MS (Blasioli et al., 2014; Stinson et al., 2006), i.e. abundance of VOCs, alcohols and aliphatic substances. In the commercial tests, the scientists verified that data collected from the healthy tubers could be classified accurately as controls. The active sample approach yielded a success rate of only 57.4% discrimination and was not further investigated for intermediate and commercial scale work. Despite the fact that the research relied on an impractical analytical approach, it showed potential of electronic nose for potato disease monitoring.

As a concluding remark, it should also be mentioned that other academic work was done over the course of the years with regard to soft rot. However, all these other approaches relied on biological means for detection and identification of *Pectobacterium* and *Dickeya* as causing pathogens for the aforementioned disease. These techniques are summarised in a recent paper by Czajkowski (Czajkowski et al., 2015). The past work with GC/GC-MS and the novel contribution to knowledge

reported throughout this manuscript aims to address soft rot detection by means of instrumentation for volatile metabolites profiling.

2.3 Gas Sensing Technologies

In the past studies on detection of volatile metabolites associated to potato disease spread, the technology of choice was the GC (Gas Chromatography) or GC-MS (Gas Chromatography Mass Spectrometry). The purpose of the short excursus that follows is the elucidation on working principles of other technologies that could be employed for symptomatic and pre-symptomatic soft rot disease detection. This piece of work does not aim to be a detailed technical explanation but rather its purpose is to draw attention to the fact that other possibilities exist and that they have been available for some time. No information is available on their use for soft rot identification and, more in general for potato disease detection. All these approaches have advantages and disadvantages with regard to parameters such as sensitivity, selectivity, response time, operating life, cross –sensitivity and poisoning.

2.3.1 Ion mobility spectrometry and FAIMS

Ion mobility spectrometry, or IMS, has been developed as a technique for detecting and identifying volatile organic compounds. This method is based on mobilities in electric fields of gas-phase ions from constituents in samples under analysis. The first studies with regard to mobility of gas-phase ions in electric fields date to the early part of the past century when also mobility theory was well developed. However, the first modern ion mobility spectrometers were available commercially only in 1970s (Borsdorf and Eiceman, 2006a). The basic working principle of an IMS is shown in

Fig. 2.3. The instrument is composed of three main parts, an ionization and reaction chamber, a drift region and a detection sensor. An electric field, with decreasing voltage potential (towards the detection unit), is employed to characterise gas-phase ions.

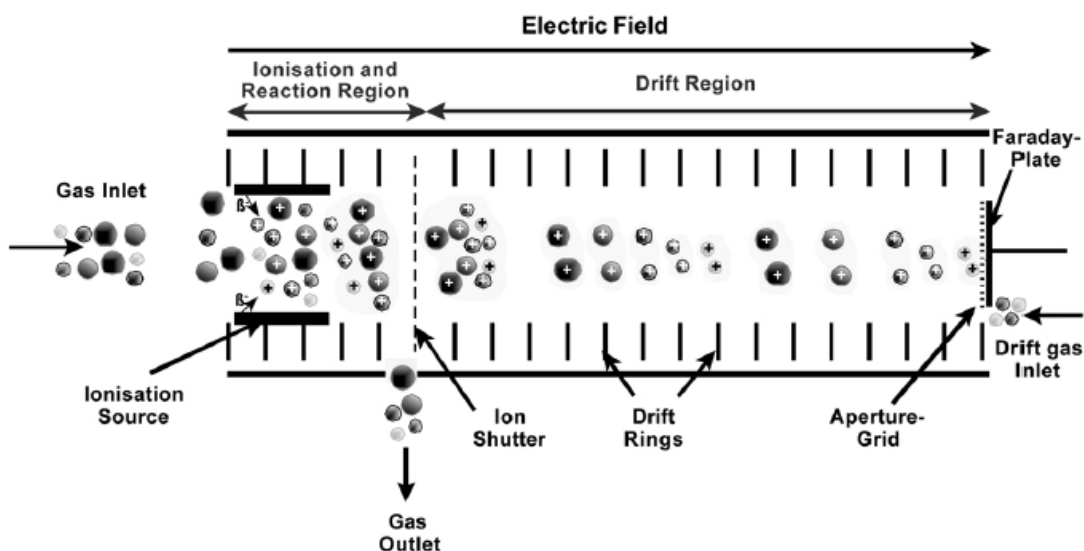


Fig. 2.3. Basic working principle of ion mobility spectrometer (Borsdorf and Eiceman, 2006b).

The sample to be analysed is fed by means of a carrier gas, into the ionisation chamber, where the molecules of the substance to be analysed are ionised. The specific technology used in the chamber depends on application and is also commonly found with mass spectroscopy. Once ionized, the decreasing gradient of the applied electric field (usually from 1 to 10 kV DC) forces the ions out of the ionisation and reaction chamber into the drift region (by means of the electronic ion shutter, which is opened periodically) towards the detection region. Once in the drift region the motion of the ions is countered by what is known as drift-gas (or buffer gas) with opposing flow direction, starting from the drift gas inlet to the outlet and, depending on the ions' mobility, which is a function of mass, charge, size and shape, the time to migrate

through the drift region to the detector becomes a characterizing feature of the different types of ions. The area of an ion that the drift-gas molecules collide with is defined as cross-section and, the greater the section, the more area is exposed to the possibility of collision with the drift-gas (consequently delaying the ions drift), which will then require a longer time for the ions to migrate to the detector region. Ions are then separated according to their mobility on their arrival at the detector with different drift times (t_d), thus generating an electrical signal characteristic of the molecules of the measured sample. The resulting plot of detector response (ordinate) versus drift time (t_d , abscissa) is known as ion mobility spectrum.

FAIMS is the most recent incarnation in further development of the IMS. FAIMS, in Fig. 2.4, has a similar structure to the IMS.

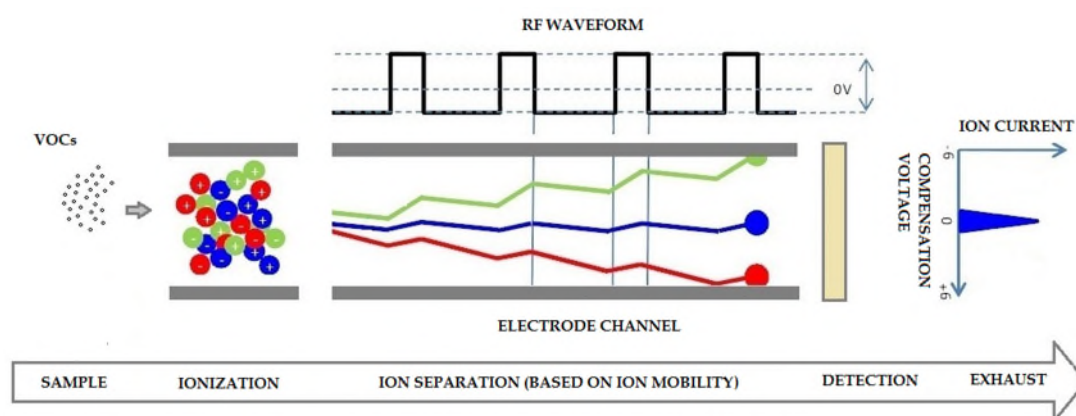


Fig. 2.4. Basic working principle of FAIMS.

It features an ionization chamber, an electrode channel and a detector plate. However, its peculiar working principle resides on an asymmetric (radio frequency) field applied to the two electrodes through which the ions flow (the field is orthogonal to the motion of the ions). This generates a saw-like trajectory migration of the gas-phase ions from the ionization chamber towards the detector plate. Because of the different mobility characteristic of each ion type, only a very restricted set of ions are then able to reach the

sensing unit. Hence, ions with the incorrect mobility lose their charges, via a saw-like trajectory, against the electrodes while those with the right one (i.e. with a less pronounced saw-like path) collide with the sensor plate, thus generating an electrical signal. To allow ions with different mobilities to reach the detector, a compensation voltage (CV is scanned between top and bottom electrodes and a CV spectrum is produced (ion current for the ordinate and compensation voltage for the abscissa). The compensation voltage is applied to different sets of the asymmetric waveforms, since variation of this radio frequency field will also affect ion's mobility. The amount of ions, positive or negative, reaching the detector is defined as the ion current. Thus, a mobility spectrum is generated for all the chemical compounds under analysis. The spectrum for IMS is bi-dimensional while the FAIMS spectrum is based on a three dimensional graph in which one component is the CV sweep, another is the electric field variation (or Dispersion Field) and the last the abundance of the analyte.

2.3.2 Photoionization detection

Photoionization detection, or PID, has been employed as a technique for detection of VOCs and is based on a numerical response indicative of cumulative presence of the overall spectrum of volatiles present in the gas sample under analysis. The technology, as indicated in Fig. 2.5 (RAE Systems - Honeywell Inc, 2005), is based on two main components, an ultraviolet (UV) lamp and a sensing unit. The principle of the photoionization detector utilizes UV light to ionize the gas molecules of the chemical under analysis. The gas then becomes electrically charged and the ions produce an electric current by contact with the sensing electrode, thus producing the signal output. UV levels are usually measured in eV, electron Volts. Each VOC has an ionization potential, or IP also measured in eV. All volatiles with ionization

potential below the eV levels of the lamp employed will be ionised. Fig. 2.6 (RAE Systems - Honeywell Inc, 2005) shows IP for common chemicals and lamps. Typical manufactured lamps are for 9.8, 10.6, 11.7 eV. This technology offers detection for a wide range of chemicals and also for a broad range of concentrations, ranging from 1 parts per billion (ppb) to 20,000 parts per million (ppm) with a few seconds for both response time and clearing down (Chou, 1999; Ion Science Ltd, n.d.).

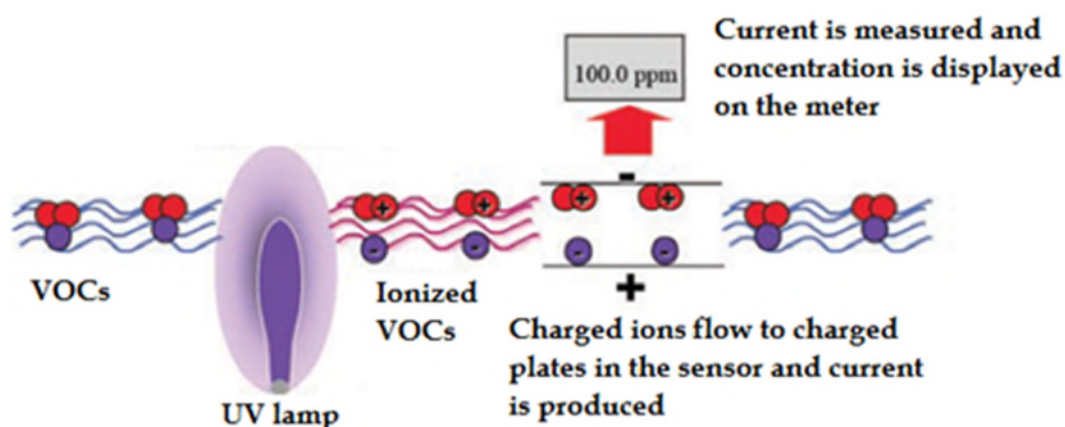


Fig. 2.5. Basic working principle of PID (RAE Systems - Honeywell Inc, 2005).

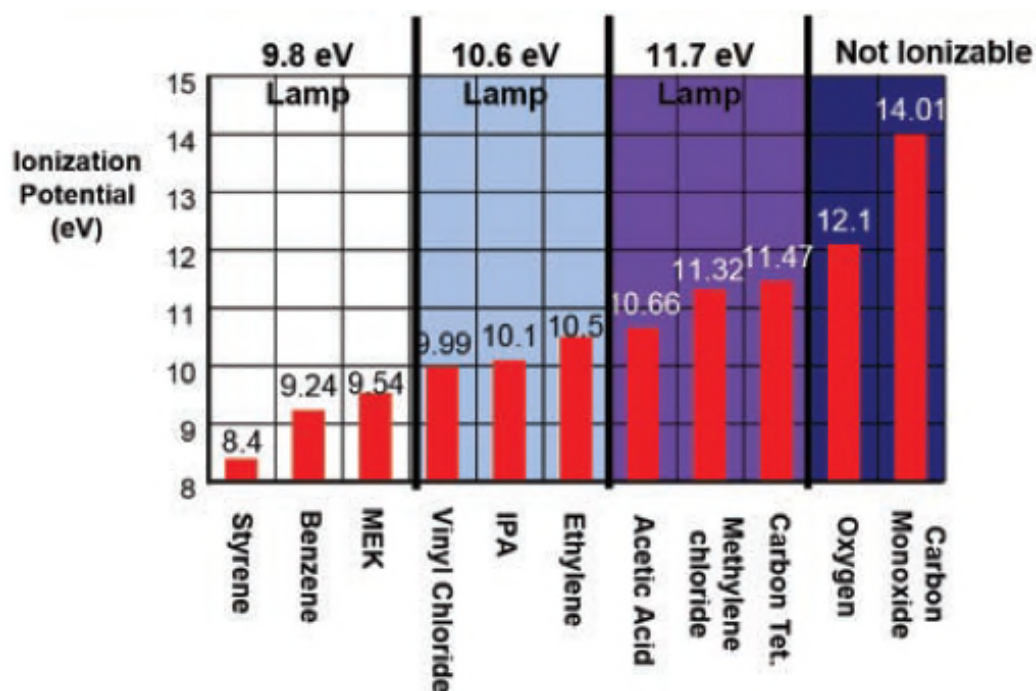


Fig. 2.6. Ionization Potentials for common chemicals (RAE Systems - Honeywell Inc, 2005).

2.3.3 Metal oxide gas sensors and electronic noses

The origin of the solid state gas sensors can be dated back to the early studies on semiconductor p-n junctions from the 1950s onwards. Scientists discovered that these junctions were sensitive to environmental background gases and this represented a problem. However, in 1968 Taguchi exploited such a feature of the p-n junction and marketed a simple solid-state sensor with the aim to provide a more reliable alternative to the catalytic bead sensors for combustible gas detection. The disadvantage of catalytic bead sensors is that they burn the gas being detected and by doing so deplete the sensor material in the process. The sensor will have reduction in sensitivity and life expectancy with time, or if exposed to higher gas concentrations. With semiconductors, instead, the gas is absorbed onto the sensor surface, altering its electrical resistance, but not wasting any material. When the sensor is no longer exposed to the gas, it returns to its original state. Solid-state gas sensors spread considerably in the 1980s, when Japan issued legislation requiring gas monitors in residential premises where gas bottles were in use (Chou, 1999).

These sensors consist of a ceramic substrate heated by wire and coated with a metal oxide semiconducting film, as shown in Fig. 2.7 (Figaro Engineering Inc, 2015). Under normal environmental conditions, oxygen is adsorbed on the metal oxide surface. Adsorbed oxygen then attracts electrons inside the metal oxide, forming a potential barrier that prevents the flow of electrons inside the semiconductor, thus causing high sensor resistance as shown in Fig. 2.8 (Figaro Engineering Inc, 2016). If the gas sensor is exposed to reducing gas, the density of adsorbed oxygen on metal oxide surface decreases, and the potential barrier is reduced. In this case, electrons can flow through the semiconductor, reducing electrical resistance (Figaro Engineering Inc, 2016). The working principle illustrated previously refers to n-type materials.

However, the oxide coating may be either an n-type or p-type. The n-type semiconductor (such as SnO_2) responds to oxidising chemical compounds with an increase in electrical resistance (or decrease if in the presence of reducing gases). Conversely, the p-type material responds to reducing compounds with an increase in sensor resistance (Fine et al., 2010).

Gas concentration in air can then be detected by measuring the resistance change by means of electrodes embedded into the metal oxide. The changes in the conductivity from the interaction of the sensor with the gas are measured as an electrical signal. The chemical reaction of gases on metal oxide surface varies depending on the reactivity of sensing material and sensor working temperature. The heater has the function to heat the metal oxide material to a temperature (typically 250-450 °C) that is optimal for the gas to be detected (Figaro Engineering Inc, 2016). The main advantage of the metal-oxide gas sensors resides in their long life expectancy (typically of at least 10 years). This is a major advantage compared to other sensor types, such as catalytic bead or electrochemical sensors that last no longer than a couple of years. However, solid-state can also be susceptible to interference gases more than the other types of sensors (Chou, 1999).

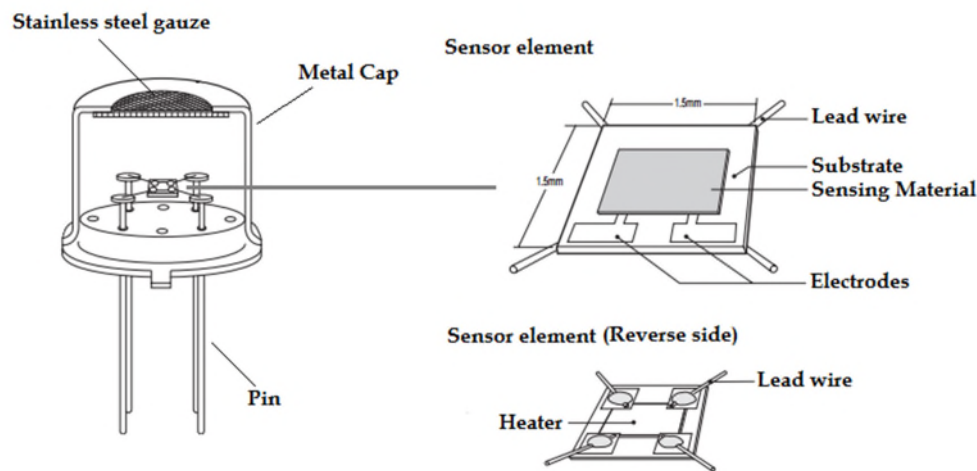


Fig. 2.7. Basic metal oxide gas sensor structure (Figaro Engineering Inc, 2015).

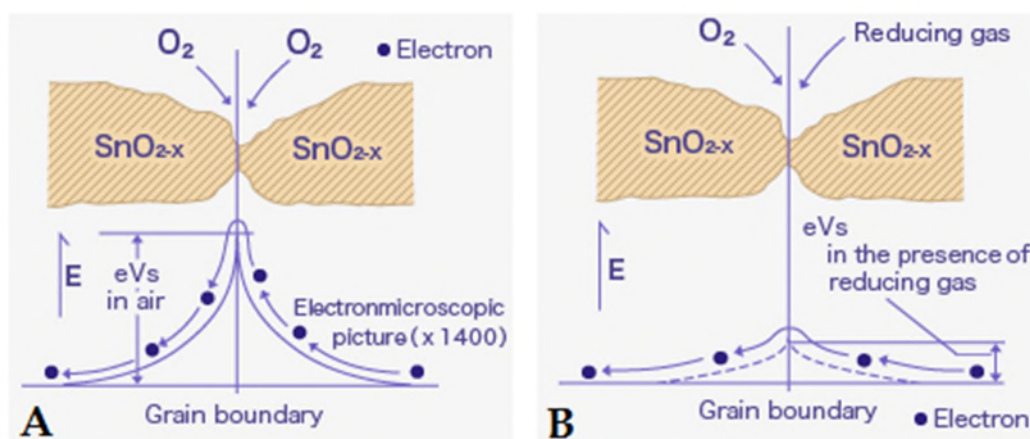


Fig. 2.8. Basic operational principle of the n-type metal oxide gas sensor. Sensor with no exposure to gas (A) causes high potential barrier to electron flow (eV in graph). When sensor is exposed to reducing gas, potential barrier is substantially reduced and electron can flow freely (Figaro Engineering Inc, 2016).

Although the first gas sensor were used for more reliable gas monitoring, they were also employed in arrays, as in electronic noses. The first modern electronic nose was reported in the literature in 1982 in a study by Persaud and Dodd, although previous work had been carried out since 1953 (Pearce, 1997). In the electronic nose the molecules of the sample under analysis are transported by a carrier gas until they reach an array of sensors, mostly metal oxides and typically numbering between 6 and 18. In the array each sensor is composed of a material, which in turn reacts differently to the sample molecules. The change of the sensor is transduced into an electrical signal and is then processed by a pattern recognition system. The final output is a characteristic 'odour' specific to each sample, odour which can be learned by the instrument by means of machine learning techniques. If a similar chemical pattern is analysed, the electronic nose will then recognise the specific odour under analysis.

The basic working principle of a modern electronic nose is presented in Fig. 2.9 (Turner and Magan, 2004).

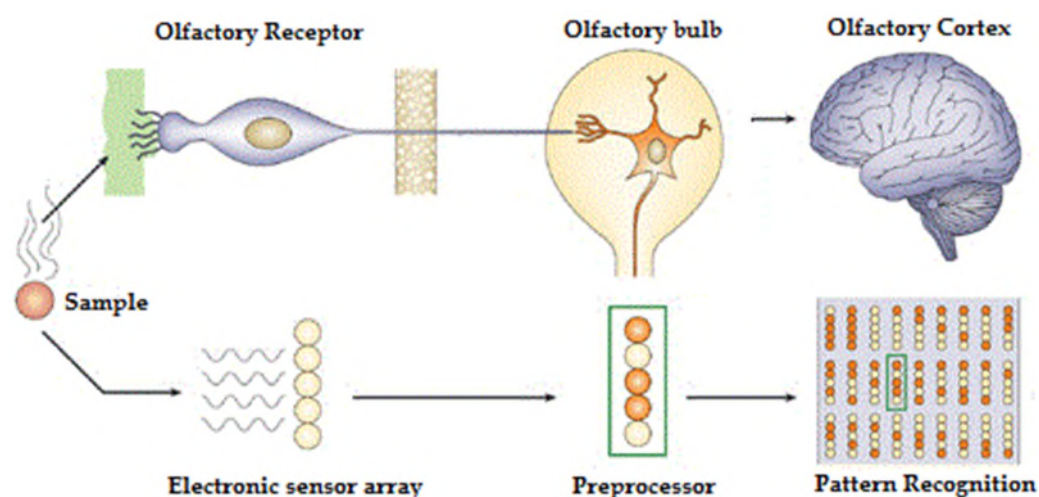


Fig. 2.9. Basic working principle of the electronic nose (Turner and Magan, 2004).

2.3.4 Electrochemical gas sensors

The first electrochemical sensor was developed in the 50s by Leland C. Clark who proposed a membrane-covered oxygen sensor. Later, as legislation was passed requiring the monitoring of toxic and combustible gases, new and better electrochemical sensors were developed. Growth was more significant in the 1980s when smaller sensors with higher sensitivity and selectivity became available for detection of a wide range of toxic gases (Chou, 1999; Nei, 2007).

Electrochemical sensors operate by reacting with the analyte and producing an electrical signal that is proportional to gas concentration. An electrochemical sensor (Fig. 2.10 - Chou, 1999; Membraphor AG, 2016) consists of a capillary and a hydrophobic membrane, a sensing electrode (also known as working electrode), a

counter electrode, an electrolyte and a reference electrode. The gas molecules of the sample first pass a small capillary opening and then diffuse through the hydrophobic barrier. The barrier allows a sufficient amount of gas to reach the working electrode but prevents the electrolyte from leaking out of the sensor. A filter may be present between the capillary and the membrane to remove interfering gases and/or to increase the lifespan of the sensor by reducing any over exposure. Proper selection of the filter may improve selectivity. The gas molecules that diffuse through the hydrophobic membrane react at the surface of the sensing electrode involving either an oxidation or reduction reaction (i.e. production or consumption of electrons), thus generating an electric signal. The counter electrode balances the reaction at the working electrode. The ionic current between these two electrodes is transported by the electrolyte, while the current path is provided through wiring with pin connectors (this operating principle is simplified in Fig. 2.10). Measurement of this current flow will provide details on gas concentration. The function of the reference electrode is to maintain the voltage at the working electrode stable (Membraphor AG, 2016).

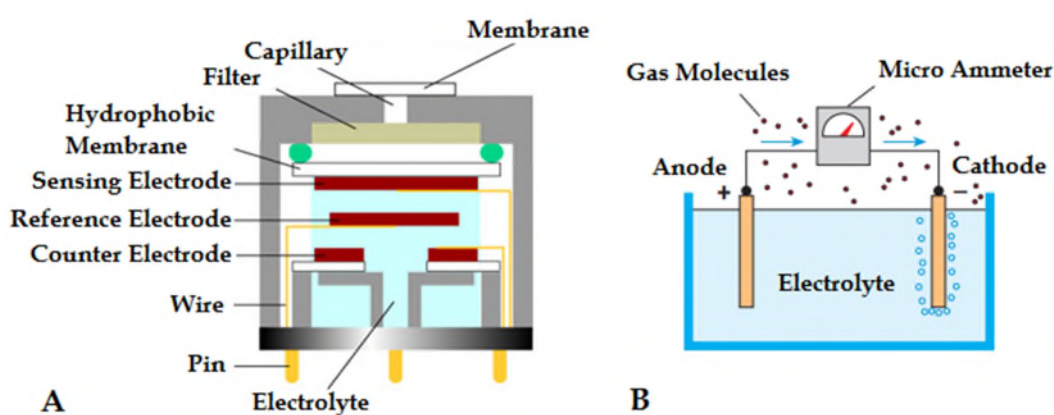


Fig. 2.10. Structure of an electrochemical gas sensor (A) and working principle (B), (Chou, 1999; Membraphor AG, 2016).

2.3.5 Infrared gas sensors

The history of infrared sensing can be dated back to 1840 to John Herschel who discovered the presence of absorption bands in the infrared part of the solar spectrum. However, the first practical device was developed by Luft over a century later. Further developments occurred in the 50s when these type of technology started being employed for gas analysis (Hodgkinson *et al.*, 2013).

A typical infrared gas sensor is composed of a source, a gas cell, a filter, an optical component and a detector, as indicated in Fig. 2.11 (Hodgkinson *et al.*, 2013). With no target chemical present, the optical signal sent from the emitter and reaching the detector is at its maximum. When the target gas is present in the cell, the radiation pattern received at the detector is reduced in intensity at specific wavelengths (or absorption bands) that are unique to each specific gas. The function of the source is to generate a signal in the infrared region of the spectrum. This region of the spectrum is employed for gas analysis since numerous VOCs show characteristic absorption with narrow and non-overlapping bands in the infrared. Detectors then convert electromagnetic radiation into electrical signals. There are various types of infrared detectors each with different characteristics (thermoelectric, thermistor bolometer, pyroelectric, photon, luft, photoacoustic). The optical component depends on the type of device employed: dispersive or nondispersive (also known as NDIR, nondispersive infrared). Almost all gas sensors available on the market are of the NDIR type and employ optical bandpass filters to filter out undesired radiation. The usefulness of this type of technology resides in the fact that the detector does not come into contact with the gases to be detected (Chou, 1999). However, they are more expensive than other sensing technologies, thus are focussed towards hard to detect gases (CO₂ and CH₄).

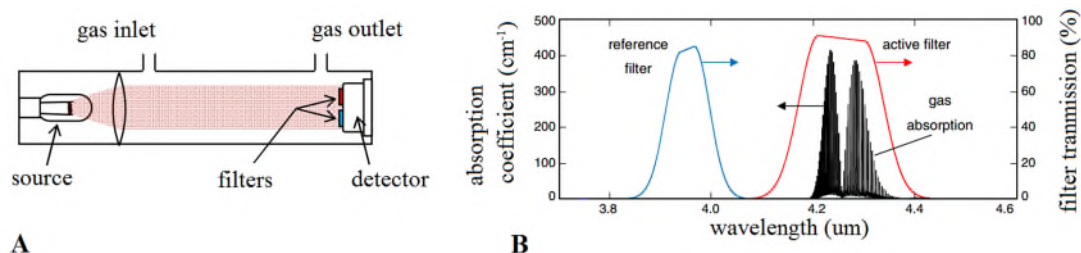


Fig. 2.11. Structure and basic operating principle of infrared gas sensor (Hodgkinson *et al.*, 2013).

2.4 Discussion

In the literature cited, the instrumentation of choice has been the gas chromatograph or the gas chromatograph mass spectrometer and no other alternatives have been applied to potato storage diseases, in particular for soft rot - the focus of this research. In some of the studies, the reported results appear to indicate potential markers of disease inception and progression, while in others the overall VOC profile was considered as a possible discriminating factor between controls and diseased tubers. Measuring the overall increase in volatile metabolites appears to be a more feasible approach rather than identifying specific chemicals, especially when engineering a practical solution to store management.

GC and GC-MS are recognized as technologies of choice for volatile metabolites analysis because of an optimal combination of high accuracy, selectivity and other related parameters. However the drawback of the instrument, aside of high costs, is that manual processing of samples and complex data sets, even by experienced staff, and this is labour intensive, time consuming and prone to errors (Jansen *et al.*, 2011). This makes it less suitable for continuous monitoring in commercial potato stores.

Under this light, a priori knowledge of chemicals involved is not necessary nor is sought after. Other technologies listed before appear to offer new possibilities in soft rot identification, or more in general, disease detection.

The advantage of FAIMS lays in increased sensitivity and selectivity: in either case, potential chemicals or chemical groups could be indicating spread of infection (that will result in a characteristic fingerprint) and could do so at an early stage, when no sensorial symptoms could be identified. In the case of the PID, this sensing technology offers the clear advantages of being portable, easy to use, robust, and not prone to saturation, as well as offering the possibility to quickly quantify the total amount of VOC under test. PID has never been reported to date for plant disease monitoring. Most recently though, FAIMS instrumentation has been used to detect citrus greening disease (Aksenov et al., 2014). This thesis is the first time that FAIMS and PID have been applied to diagnose soft rot, or any other potato disease.

However, electronic noses-based technologies could also be employed for VOC monitoring and quantification and this will also be explored in this research since it has been proven in principle to be possible with custom-made metal oxide sensors (de Lacy Costello et al., 2000) or with a commercial unit applied to brown rot and ring rot disease monitoring (Biondi et al., 2014). In the first study this was done to address sensitivity to VOC in general and no chemical families were of particular interest for the research. It may be argued, as Water and Pritchard also reported in their work, that baseline determination was of particular relevance, and consequently trend determination over time, not sensitivity, could be the key to accurate disease monitoring in potato stores. In the latter case (static headspace sampling) it is the

accumulation of metabolites over time that was investigated (Waterer and Pritchard, 1984a, 1984b). Thus a question that comes to mind is if a real-world dynamic sampling approach would yield any results at all. Last but not least, identification of chemical families could also be achieved. Hence, with regard to metal-oxide gas sensors, the aim of this work is to explore if chemical families could discriminate disease from control treatments. The use of commercially available sensors would also imply a cost-effective solution to the task at hand. No accounts are available with regard to the investigation or application of electrochemical and NDIR technologies to diagnose potato diseases, in particular to soft rot.

2.5 Conclusion

In this chapter it has been shown that detection of soft rot was attempted for over 40 years with the use of GC or GC-MS. The outcome of the studies at best provided inconclusive results. However, gas analysis technologies could be employed as diagnostics techniques for pre-symptomatic detection and monitoring of potato soft rot. The hypothesis is that these techniques could offer a practical and cost-effective engineering alternative to GC or GC-MS. These could also address two of the main suggestions for further work proposed by other researchers: overall increase of volatiles over time and identification of specific markers, both to be associated to soft rot inception and spread. Moreover, gas sensing instruments are mature technologies that have been in use over many years and thus could operate reliably in harsher environmental conditions, such as those of commercial store facilities.

2.6 References

- AHDB Potatoes, 2012. War on waste in the potato supply chain. [WWW Document]. URL <http://www.potato.org.uk/news/war-waste-potato-supply-chain>
- Aksenov, A.A., Pasamontes, A., Peirano, D.J., Zhao, W., Dandekar, A.M., Fiehn, O., Ehsani, R., Davis, C.E., 2014. Detection of Huanglongbing disease using differential mobility spectrometry. *Anal. Chem.* 86, 2481–8. doi:10.1021/ac403469y
- Bacterial Rots of Potato Tubers, 2009. FERA, The Food and Environment Research Agency, York, UK.
- Biondi, E., Blasioli, S., Galeone, A., Spinelli, F., Cellini, A., Lucchese, C., Braschi, I., 2014. Detection of potato brown rot and ring rot by electronic nose: from laboratory to real scale. *Talanta* 129, 422–30. doi:10.1016/j.talanta.2014.04.057
- Blasioli, S., Biondi, E., Samudrala, D., Spinelli, F., Cellini, A., Bertaccini, A., Cristescu, S.M., Braschi, I., 2014. Identification of volatile markers in potato brown rot and ring rot by combined GC-MS and PTR-MS techniques: study on in vitro and in vivo samples. *J. Agric. Food Chem.* 62, 337–47. doi:10.1021/jf403436t
- Borsdorf, H., Eiceman, G.A., 2006a. Ion Mobility Spectrometry: Principles and Applications. *Appl. Spectrosc. Rev.* 41, 323–375. doi:10.1080/05704920600663469
- Borsdorf, H., Eiceman, G.A., 2006b. Ion Mobility Spectrometry: Principles and Applications. *Appl. Spectrosc. Rev.* 41, 323–375. doi:10.1080/05704920600663469
- Chou, J., 1999. Hazardous Gas Monitors. McGraw-Hill and SciTech Publishing Inc,

USA.

- Czajkowski, R., Pérombelon, M., Jafra, S., Lojkowska, E., Potrykus, M., van der Wolf, J., Sledz, W., 2015. Detection, identification and differentiation of *Pectobacterium* and *Dickeya* species causing potato blackleg and tuber soft rot: a review. *Ann. Appl. Biol.* 166, 18–38. doi:10.1111/aab.12166
- Czajkowski, R., Pérombelon, M.C.M., van Veen, J.A., van der Wolf, J.M., 2011. Control of blackleg and tuber soft rot of potato caused by *Pectobacterium* and *Dickeya* species: a review. *Plant Pathol.* 60, 999–1013. doi:10.1111/j.1365-3059.2011.02470.x
- De Boer, S.H., 2004. Blackleg of potato. *Plant Heal. Instr.* doi:10.1094/PHI-I-2004-0712-01
- de Lacy Costello, B.P.J., Evans, P., Ewen, R.J., Gunson, H.E., Jones, P.R.H., Ratcliffe, N.M., Spencer-Phillips, P.T.N., 2001. Gas chromatography-mass spectrometry analyses of volatile organic compounds from potato tubers inoculated with *Phytophthora infestans* or *Fusarium coeruleum*. *Plant Pathol.* 50, 489–496. doi:10.1046/j.1365-3059.2001.00594.x
- de Lacy Costello, B.P.J., Evans, P., Ewen, R.J., Gunson, H.E., Ratcliffe, N.M., Spencer-Phillips, P.T.N., 1999. Identification of volatiles generated by potato tubers (*Solanum tuberosum* CV: Maris Piper) infected by *Erwinia carotovora*, *Bacillus polymyxa* and *Arthrobacter* sp. *Plant Pathol.* 48, 345–351. doi:10.1046/j.1365-3059.1999.00357.x
- de Lacy Costello, B.P.J., Ewen, R.J., Gunson, H.E., Ratcliffe, N.M., Spencer-Phillips, P.T.N., 2000. The development of a sensor system for the early detection of soft rot in stored potato tubers. *Meas. Sci. Technol.* 11, 1685–1691. doi:10.1088/0957-0233/11/12/305

- Duarte, V., De Boer, S.H., Ward, L.J., Oliveira, A.M.R., 2004. Characterization of atypical *Erwinia carotovora* strains causing blackleg of potato in Brazil. *J. Appl. Microbiol.* 96, 535–545. doi:10.1111/j.1365-2672.2004.02173.x
- EU law and other public EU documents, 1999. Council Directive 1999/13/EC of 11 March 1999 [WWW Document]. URL <http://eur-lex.europa.eu/legal-content/EN/TXT/?uri=CELEX%3A31999L0013> (accessed 10.9.16).
- European Environment Agency, 2016. VOC [WWW Document]. URL <http://www.eea.europa.eu/themes/air/air-quality/resources/glossary/voc> (accessed 10.9.16).
- Figaro Engineering Inc, 2016. Operating Principles of Metal Oxide Gas Sensors [WWW Document]. URL <http://www.figaro.co.jp/en/technicalinfo/principle/mos-type.html> (accessed 5.8.16).
- Figaro Engineering Inc, 2015. Technical Information for Volatile Organic Compound (VOC) Sensors.
- Fine, G.F., Cavanagh, L.M., Afonja, A., Binions, R., 2010. Metal oxide semiconductor gas sensors in environmental monitoring. *Sensors (Basel)*. 10, 5469–5502. doi:10.3390/s100605469
- Hodgkinson, J., Tatam, R.P., 2013. Optical gas sensing: a review. *Meas. Sci. Technol.* 24, 12004. doi:10.1088/0957-0233/24/1/012004
- Ion Science Ltd, n.d. Tiger VOC Detector [WWW Document]. URL <http://www.ionscience.com/products/tiger-handheld-voc-gas-detector> (accessed 5.6.16).
- Jansen, R.M.C., Wildt, J., Kappers, I.F., Bouwmeester, H.J., Hofstee, J.W., van Henten, E.J., 2011. Detection of diseased plants by analysis of volatile organic

compound emission. Annu. Rev. Phytopathol. 49, 157–74.

doi:10.1146/annurev-phyto-072910-095227

Kushalappa, A.C., Lui, L.H., Chen, C.R., Lee, B., 2002. Volatile Fingerprinting (SPME-GC-FID) to Detect and Discriminate Diseases of Potato Tubers. Plant Dis.

Kushalappa, A.C., Zulfiquar, M., 2001. Effect of wet incubation time and temperature on infection, and of storage time and temperature on soft rot lesion expansion in potatoes inoculated with *Erwinia carotovora* ssp.*carotovora*. Potato Res. 44, 233–242. doi:10.1007/BF02357901

Leite, L.N., de Haan, E.G., Krijger, M., Kastelein, P., van der Zouwen, P.S., van den Bovenkamp, G.W., Tebaldi, N.D. and van der Wolf, J.M., 2014. First report of potato blackleg caused by *Pectobacterium carotovorum* subsp. *brasiliensis* in the Netherlands. New Dis. Reports 24. doi:http://dx.doi.org/10.5197/j.2044-0588.2014.029.024

Lui, L.H., Vikram, A., Abu-Nada, Y., Kushalappa, A.C., Raghavan, G.S. V., Al-Mughrabi, K., 2005. Volatile metabolic profiling for discrimination of potato tubers inoculated with dry and soft rot pathogens. Am. J. Potato Res. 82, 1–8. doi:10.1007/BF02894914

Lyew, D., Gariépy, Y., Raghavan, G.S.V., Kushalappa, A.C., 2001. Changes in volatile production during an infection of potatoes by *Erwinia carotovora*. Food Res. Int. 34, 807–813. doi:10.1016/S0963-9969(01)00102-8

Lyew, D., Gariépy, Y., Ratti, C., Raghavan, G.S. V., Kushalappa, A.C., 1999. An apparatus to sample volatiles in a commercial storage facility. Appl. Eng. Agric. 15, 243–247.

Membraphor AG, 2016. Electrochemical Gas Sensors [WWW Document]. URL

- <http://www.membrapor.ch/electrochemical-gas-sensors/> (accessed 5.9.16).
- Nei, L., 2007. Some Milestones in the 50-year History of Electrochemical Oxygen Sensor Development, in: ECS Transactions. ECS, pp. 33–38.
doi:10.1149/1.2409016
- Ouellette, E., Raghavan, G.S.V., Reeleder, R.D., Greenhalgh, R., 1990. Volatile Monitoring Technique For Disease Detection In Stored Potatoes. J. Food Process. Preserv. 14, 279–300. doi:10.1111/j.1745-4549.1990.tb00134.x
- Panda, P., Fiers, M.A.W.J., Armstrong, K., Pitman, A.R., 2012. First report of blackleg and soft rot of potato caused by *Pectobacterium carotovorum* subsp . *brasiliensis* in New Zealand. New Dis. Reports 15.
- Pearce, T.C., 1997. Computational parallels between the biological olfactory pathway and its analogue ‘The Electronic Nose’: Part II. Sensor-based machine olfaction. Biosystems 41, 69–90. doi:10.1016/S0303-2647(96)01660-7
- Peters, J., Toth, I., Wale, S., 2012. Managing the risk of blackleg and soft rot. Sutton Bridge, Spalding, Lincs. PE12 9YD.
- Pitman, A.R., Harrow, S.A., Visnovsky, S.B., 2010. Genetic characterisation of *Pectobacterium wasabiae* causing soft rot disease of potato in New Zealand. Eur. J. Plant Pathol. 126, 423–435. doi:10.1007/s10658-009-9551-y
- R. A. Ramussen, 1972. A Quantitative Cryogenic Sampler. Am Lab 20, 19–27.
- RAE Systems - Honeywell Inc, 2005. Application Note AP-000. USA.
- Rastovski, A., Es, A. van, 1989. Storage of Potatoes. Postharvest Behaviour, Store Design, Storage Practice, Handling. PUDOC; Wageningen 1987. Second revised edition, 468 pages, with 280 figures and 67 tables, index. Hardcover Dfl. 160.00/US-Dollar 80. Starch - Stärke 41, 324–325.
doi:10.1002/star.19890410815

- Ratti, C., Gariépy, Y., Raghavan, G.S.V., 1995. Proceedings of the International Conference on Harvest and Postharvest Technologies, in: Collection and Analysis of Headspace Volatiles for Disease Detection in Stored Potatoes. pp. 255–261.
- Schaper, L.A., Varns, J.L., 1978. Carbon dioxide accumulation and flushing in potato storage bins. *Am. Potato J.* 55, 1–14. doi:10.1007/BF02852006
- Smith, O., Campbell, J.C., 1969. Potatoes, production, storing, processing. *Am. Potato J.* 46, 145–145. doi:10.1007/BF02863107
- Stinson, J.A., Persaud, K.C., Bryning, G., 2006. Generic system for the detection of statutory potato pathogens. *Sensors Actuators B Chem.* 116, 100–106. doi:10.1016/j.snb.2005.12.061
- Toivonen, P.M., 1997. Non-ethylene, non-respiratory volatiles in harvested fruits and vegetables: their occurrence, biological activity and control. *Postharvest Biol. Technol.* 12, 109–125. doi:10.1016/S0925-5214(97)00048-3
- Toth, I.K., van der Wolf, J.M., Saddler, G., Lojkowska, E., Hélias, V., Pirhonen, M., Tsrer Lahkim, L., Elphinstone, J.G., 2011. *Dickeya* species: an emerging problem for potato production in Europe. *Plant Pathol.* 60, 385–399. doi:10.1111/j.1365-3059.2011.02427.x
- Turner, A.P., Magan, N., 2004. Electronic noses and disease diagnostics. *Nat. Rev. Microbiol.* 2, 161–6. doi:10.1038/nrmicro823
- Varns, J.L., Glynn, M.T., 1979. Detection of disease in stored potatoes by volatile monitoring. *Am. Potato J.* 56, 185–197. doi:10.1007/BF02853365
- Waterer, D.R., Pritchard, M.K., 1984a. Monitoring of volatiles: A technique for detection of soft rot (*Erwinia carotovora*) in potato tubers. *Can. J. Plant Pathol.* 6, 165–171. doi:10.1080/07060668409501578

Waterer, D.R., Pritchard, M.K., 1984b. Volatile monitoring as a technique for differentiating between *E. carotovora* and *C. sepedonicum* infections in stored potatoes. Am. Potato J. 61, 345–353. doi:10.1007/BF02854536

EARLY IDENTIFICATION OF POTATO
STORAGE DISEASE BY GAS ANALYSIS: A
PILOT STUDY

This page is intentionally left blank.

3 Early Identification of Potato Storage Disease by Gas Analysis: a Pilot Study

3.1 Introduction

Monitoring the disease status of potatoes in stores is difficult, due to poor access. Current practice for detection of soft rot in store relies solely on sensorial analysis (visual or tactile inspection and smell by farmers). However, these stores are environmentally controlled, with air forced through the crop. Therefore, disease monitoring could potentially be achieved through the use of gas analysis.

Previous work on early detection of potato storage diseases through gas analysis has been conducted over many years, dating back to the early work of Varns and Glynn in 1979 (Varns & Glynn 1979) followed by the study of Waterer and Pritchard (Waterer & Pritchard 1984). Most of this research has been based on GC (Gas Chromatograph) or GC-MS (Gas Chromatograph Mass Spectrometer) in order to identify specific chemical compounds that might be characteristic markers of infected potato tubers (Ratti et al. 1995; Lyew et al. 1999; de Lacy Costello et al. 1999; Lyew et al. 2001; Lui et al. 2005; Kushalappa & Zulfiquar 2001; Kushalappa et al. 2002).

However, a large number of different volatile biomarkers have been identified in many previous studies. These studies differ in hosts, pathogens, environmental factors, methodologies of experimentation, instruments limitations and usage, different analytical and data processing techniques, but above all, the relative time frames under consideration. In fact, according to Dixon et al. and Fiehn, plants produce a very large number of volatile metabolites, both before and after harvest (Dixon et al. 2002; Fiehn 2002). Wilson and Wisniewski claim that various environmental stresses can substantially increase the amount of volatiles that plants produce (Wilson &

Wisniewski 1989). In addition, GC and GC-MS are expensive, require expert training, specialized infra-structure and therefore are unsuitable for continuous monitoring in real stores.

The work presented in this chapter reports on the experimental results to assess the potential of FAIMS (Field Asymmetric Ion Mobility Spectrometry) and PID (Photo-Ionization Detector) technologies for identification and early detection of potato tuber soft rot in a laboratory setting. These technologies allow determination of a broad range of gases/vapours or volatile metabolites without prior or needed knowledge of the substances involved in disease inception and progression, rather than identification of specific chemical compounds as was done in previous studies. In addition, FAIMS and PID are also considered to be more sensitive, reliable, cost effective and easier to use/deploy in a potato store if compared with GC-MS. This is the first time FAIMS and PID technologies have been used to detect potato disease spread and more in general applied to agriculture.

3.2 Material and methods

3.2.1 Experimental sample preparation

Sample preparation was devised in consultation and under the guidance of researchers from AHDB Potatoes at Sutton Bridge Crop Storage Research for both potato variety selection and sample preparation. The potato tuber chosen for experimental work was ‘Maris Piper’. This variety was preferred over others due to its commercial value to the industry. ‘Maris Piper’ is both the main multipurpose crop for all the requirements of food processing and storage and is also the most widespread one, with a planted

area larger than the other three most common varieties (Markies, Maris Peer, Lady Rosetta) combined (Maslowski et al. 2015).

A standard sample preparation procedure was developed for this project and consisted in inoculating 'Maris Piper' potato tubers with *P. carotovorum*, in order to cause the pathology known as soft rot. Potatoes were first soaked in water for one hour before use and dried with a paper towel. Each tuber was stabbed at the stolon end with a sterile 200 µl pipette tip. To a 48 h culture of *P. carotovorum* grown on nutrient agar at 25°C, 2 ml of sterile water was added and the colonies gently scraped (using a sterile plastic loop) to create a bacterial suspension. 20µl (high inoculum) of this bacterial suspension was then pipetted into the stab wound in each tuber. A further set of tubers (controls) were stabbed at the stolon but not inoculated. After treatment the potato tubers were placed in sealed boxes at 25±1 °C in an incubator (to allow rapid disease progression) and suspended on a mesh over water (400 ml), with the expected humidity to be above normal laboratory (neither absolute nor relative humidity levels were measured). No determination for latent *Pectobacterium* prior to infection was carried out, but controls were checked for infection throughout and at the end of the experimental procedure. The *P. carotovorum* isolate used in this study was originally isolated by Dr Glyn Harper (AHDB Potatoes, Sutton Bridge Crop Storage Research) and was isolated from an infected tuber, variety *Marfona*, and showing characteristic symptoms of bacterial soft rot. Isolated and in pure culture it caused pitting in CVP agar at 27 °C, was identified by PCR as *P. carotovorum* (*Pectobacterium* primer sets courtesy of Dr J. Elphinstone, FERA, UK) and could infect potato tubers causing the original symptoms. No strain reference has been used to date for this isolate since it is the first time a paper has been published using it. The strain has been suggested by Dr Glyn Harper to be identified as SBEU_08.

3.2.2 Experimental sampling protocol

Three types of experimental protocols are reported here. The first and second ones are associated with method development for assessing the potential of FAIMS technology. In the third case the experimental method reported is for a different technology (PID) and took into account the specific requirements of the instrument employed. In all cases all work was done with 1 L PTFE (Polytetrafluoroethylene) containers (Fisher Scientific Ltd, UK), with a gas path inlet and outlet added via 1/8" push-fits (SMC Pneumatics Ltd 2016), at both ends. PTFE containers were chosen since the polymer is inert to most chemicals and the reason why it is used in a broad variety of applications. For the first set of experiments with the FAIMS (Lonestar, Owlstone Ltd, UK), each tuber was placed into a PTFE container provided and sampling was carried out for each individual tuber by allowing clean air to flow around it, the mixture of gases and VOCs emanating from the potato were then fed for analysis to the FAIMS instrument (Lonestar, Owlstone Nanotech Ltd, Cambridge, UK) at a flow rate of 2 L/min. Other FAIMS parameters included a dispersion field (DF) from 0 to 100% in 51 scanning steps and a compensation voltage (CV) from -6 to 6 V in 512 steps in order to build a 3D data matrix characteristic of the sample under analysis. These settings are typical for normal FAIMS operation. Each potato tuber was scanned in such a manner twice. Prior to entering the sampling container the air was scrubbed clean and dried using moisture and hydrocarbon traps. PTFE containers were employed always separating usage for controls and infected tubers to avoid accidental cross contamination. The containers were also replaced, when appropriate, in order to eliminate potential by-product of potato decomposition that might have affected results. After sampling each tuber was repositioned in the containing box in the

incubator. Prior and after experimentation containers were thoroughly cleaned and sterilized with ethanol at 99% (Fisher Scientific Ltd, UK).

Four sets of experiments were performed where 3 to 4 tubers were inoculated at days 1, 2 and 5 before testing, (with corresponding controls). The sampling procedure was carried out twice (two consecutive days). For the first experiment, on day one of testing, 18 potatoes were analysed and the procedure was repeated on the second day with the same tubers, giving a total of 36 samples. This procedure was carried out for all other experiments with 36 samples for the first three experiments, while the number of samples was increased in the fourth experiment to 48 (24 tubers analysed in the first day and again in the following day for a repeat). The number of potato tubers tested was 78 for a total number of samples of 156 (with repeats). Details of the experiments are shown in Table 3.1. The first part of the protocol had the objective to verify the ability of the Lonestar FAIMS to discriminate between controls and soft rot infected tubers sampled after 5 days of storage in the incubator, when the symptoms of the disease could be identified by olfactive, tactile and visual inspection of the sample. The second part of the experimental procedure had the aim to characterize early detection and consequently to probe the possibility of the instrument to detect the disease and discriminate between control and infection, when no visible, odour or tactile symptoms of the disease were present (one and two days post inoculation). Hence the terms “standard disease detection” or “disease detection” (5 days post inoculation) and “early disease detection” (1 and 2 days post inoculation) were employed. At the end of the sampling procedure all tubers were cut in half and photographed to gather indication of the degree of infection.

Experiment	Number of Potato Tubers						Tests	
	1 Day post inoculation		2 Days post inoculation		5 Days post inoculation			
	Control	Infected	Control	Infected	Control	Infected	1 st	2 nd (repeat)
No 1	3	3	3	3	3	3	18	18
No 2	3	3	3	3	3	3	18	18
No 3	3	3	3	3	3	3	18	18
No 4	4	4	4	4	4	4	24	24
Total	13	13	13	13	13	13	78	78

Table 3.1. Experiments carried out and number of samples (total of 156).

For the second set of FAIMS experiments, potato tubers (cultivars Melody, Nectar, Agria, and Annosa) previously inoculated by staff at FERA (Food and Environment Research Agency) with the quarantine pathogens *R. solanacearum* (brown rot) and *C. michiganensis* (ring rot) were stored in a controlled environment in cardboard boxes. Samples for FAIMS testing included 30 tubers for controls, 50 for brown rot and 15 for ring rot. After initial experimentation with different laboratory set-ups, tubers for sampling were placed in PTFE containers to optimise air flow and, as before, air was purified by means of moisture and hydrocarbon traps prior to delivery to the FAIMS instrument. All sample potato tubers were washed in a water bath before sampling which was carried out 2 hours after potato tubers had been removed from the storage room.

In the third set of experiments, tubers were inoculated 5 days before sampling, as described in previous section, using 4 tubers per time point (with 4 corresponding controls). Sampling was done using FAIMS (as above at 25 °C), after which the incubator temperature was reduced to 15°C and the next day the sampling procedure was repeated. The total number of samples was 48, with 24 sampled after being stored at 25 °C and 24 after being stored (for more than 12 hours) at 15 °C. This was repeated

but with the temperature on day 2 of sampling further reduced to 10 °C, which is close to commercial store temperature.

The laboratory protocol that was developed for PID (Tiger VOC analyser, Ion Science Ltd, UK), differed from other analytical instrument in that static headspace collection was employed rather than a dynamic one (i.e. where clean air is passed over the potato, which is placed in a chamber, and then into the instrument). Tubers were moved into the 1L Fisher Scientific PTFE jar and left in the sealed containers for approximately five minutes, after which sampling was carried out at one end of the container (i.e. an internal pump within the instrument drew a small volume of air to the detector). The output of the instrument was taken in the form a single numerical value per measurement (total VOC level). After having established the specified protocol for collection of volatiles (which was based on 32 samples), a total of 80 samples were measured.

3.2.3 Data Analysis

With the FAIMS parameters used as stated previously, for a single scan and for one type of ion matrix (either positive or negative) amounts to 51 x 512 data points. For analysis, a single line of data points (one dimensional array) at 45% DF (dispersion field) was selected for each positive ions matrix thus yielding a number of variables of 512 for each sample. The 45% DF was selected since it accounts for most of the difference between controls and infected. The decision to use a single line, instead of the whole data set, was taken because more lines, both for positive and negative ions, yielded no improved outcome when undertaking data analysis methods used here. The second scan was used from each sample (two scans per sample were carried out) to

ensure the stability of the sampling setup. However the first scan could have been equally used.

For the analysis, two unsupervised techniques were employed: PCA (Principal Component Analysis) for dimensionality reduction and feature extraction and k-means for clustering. PCA is a multivariate statistics technique in which linear data dimensionality reduction is carried out for a set of observations. A set of indices (known as principal components) represents a different linear combination of all the original variables. Each of the variables contributes with a different weight (or loading) to a principal component. The linear creation of each index is such that variability in the data is unevenly distributed among all indices (first principal components cater for the most variability) in such a manner to allow for few new variables (principal components) to represent most of the variation occurring in the larger set of variables, where the amount of variability retained depends on the linear combinations of variables and the whole data set (Pearson 1901). The purpose of the k-means is to partition an N-dimensional population into k-sets and has been chosen instead of agglomerative hierarchical clustering because of its computational efficiency. After selection of the number of k groups, k initial seeds are randomly generated. After the selection of the k seeds, all samples are assigned to each seed according to the minimum Euclidean distance between the seed and each object. The whole process is iteratively repeated until optimal convergence is achieved (MacQueen 1967). Two initial (distinct) cluster centers for k have been used. A 95% confidence interval was applied to the two centroids obtained with the k-means algorithm. The analysis was performed using the statistical environment R (version 3.0.1, R Foundation for Statistical Computing, Vienna, Austria).

3.3 Results

3.3.1 FAIMS response for all time points

Fig. 3.1 shows representative positive ion matrices ((a), (b)), cross section for each ion matrix at 45% dispersion field ((c), (d)), positive ion matrices (logarithmic base 10 for ion current axis) ((e),(f)) and photographs ((g), (h)), for a control tuber and an infected one as representative of the two groups. Results for each of the four sets of experiments are shown in Fig. 3.2 to Fig. 3.4 for all three time points (5, 2, 1 days post inoculation). In all graphs PCA and k-means clustering have been used for data representation. PCA scree plots for all experiments showed that most of the variance was explained by the first two principal components. The variance explained in the first two principal components of the time point ‘detection’ is 41.1% and 35.2%, for the time point at two days post inoculation 69.6% and 14.5% while being 35.3% and 25.5% for the last. Analysis of data was carried out by assuming no prior knowledge of the data. Results are presented in only two categories, “control” and “infected”, regardless of degree of infection of inoculated potato tubers. However, some controls showed clear signs of infection while a number of inoculated tubers manifested varying degrees of mild infection. Following a first analysis with PCA and k-means for the whole data set of the experiments, an interpretation of the principal components has been attempted by employing the Lonestar DF matrices and photographic analysis of the internal part of samples cut in half after the sampling procedure. By looking at the data sets it has been noticed that the height of the Ion Current increases without any major shape difference going along the ordinate (i.e. 2nd principal component) while, instead of an intensity change, a shape change along the abscissa. Hence, the first principal component appears to be correlated with a change in total volatile metabolites of the same type while the second principal component seems to be related to a change in the type of

volatiles emitted. All samples outside the two confidences ellipses have shown intermediate characteristics between the two.

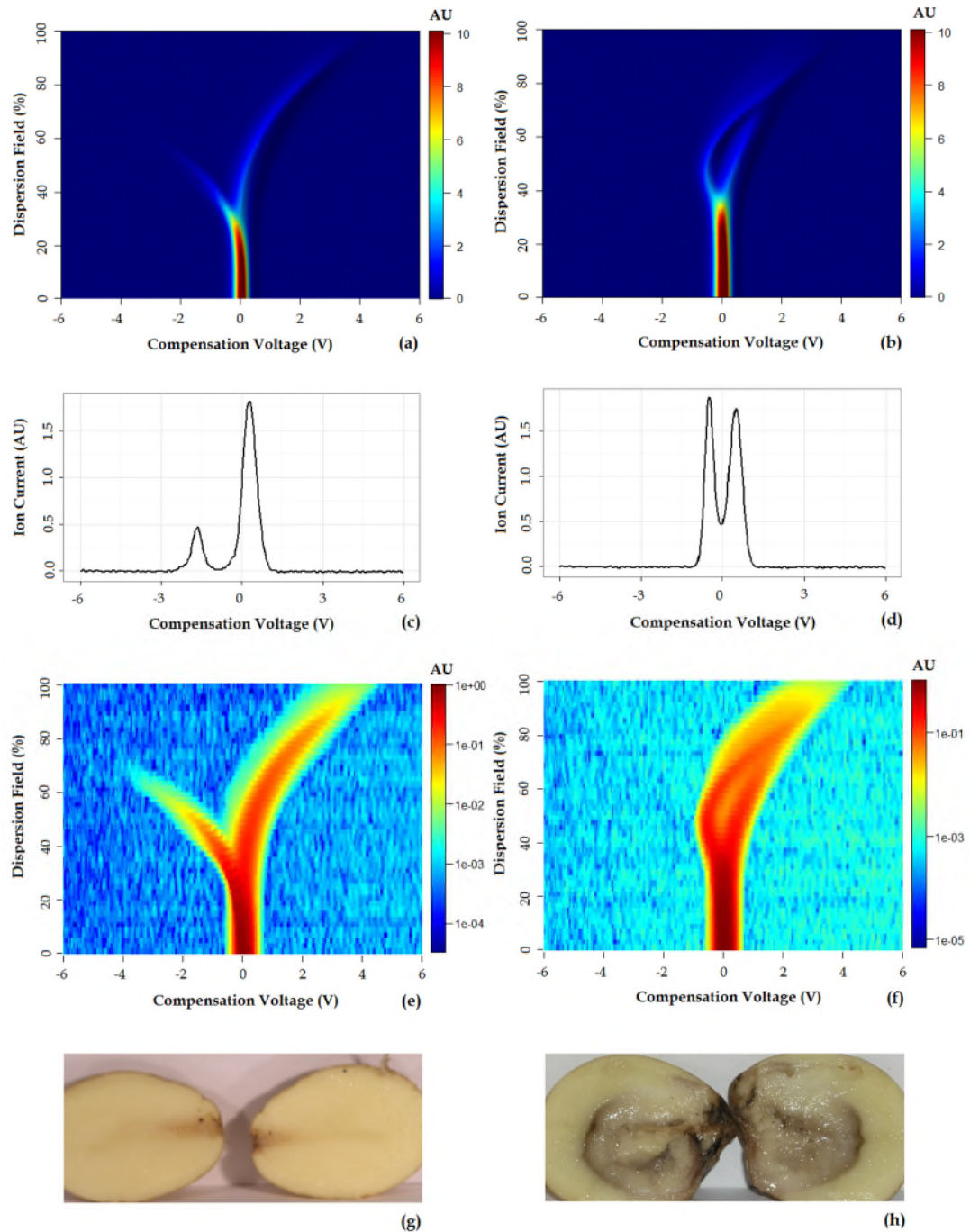


Fig. 3.1. Control (a, c, e, and g) and tuber infected with soft rot (b, d, f, h). (a) and (b) are positive ion matrices in A.U. (arbitrary units) while (c) and (d) show ion currents at 45% DF. (e) is the logarithmic representation on the ion current axis of (a), for

control and (f) for the infected tuber in (b). Photographic analysis for control (g) and infected potato (h).

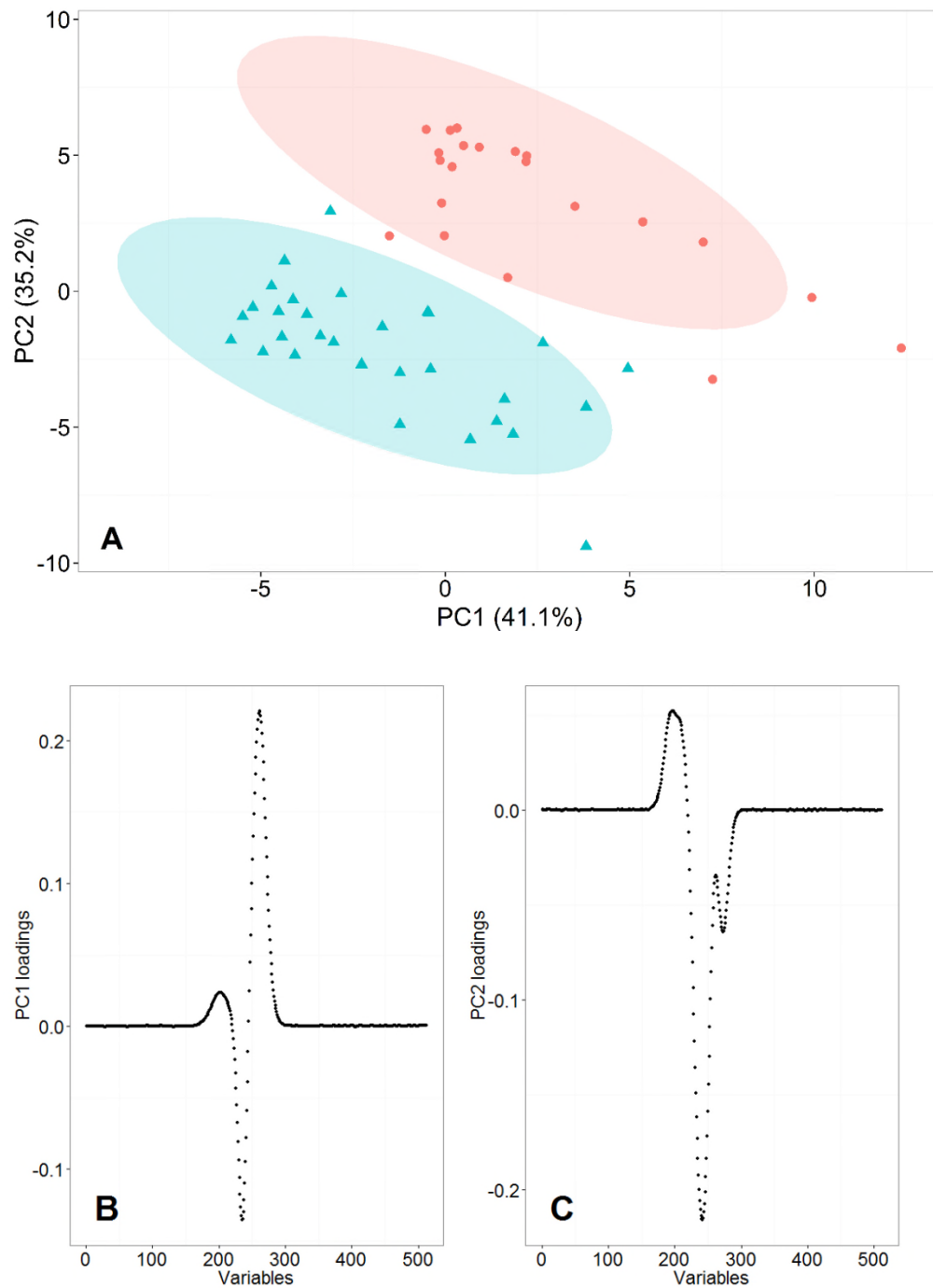


Fig. 3.2. PCA score and k-means clustering (A) for two groups of potato tubers with controls (cyan triangles) and infected (red circles) that have been grouped with 95% confidence ellipses around the centroid identified by the k-means algorithm) for 5DPI (5 days post inoculation). Loadings for the two main principal components in (B) and (C).

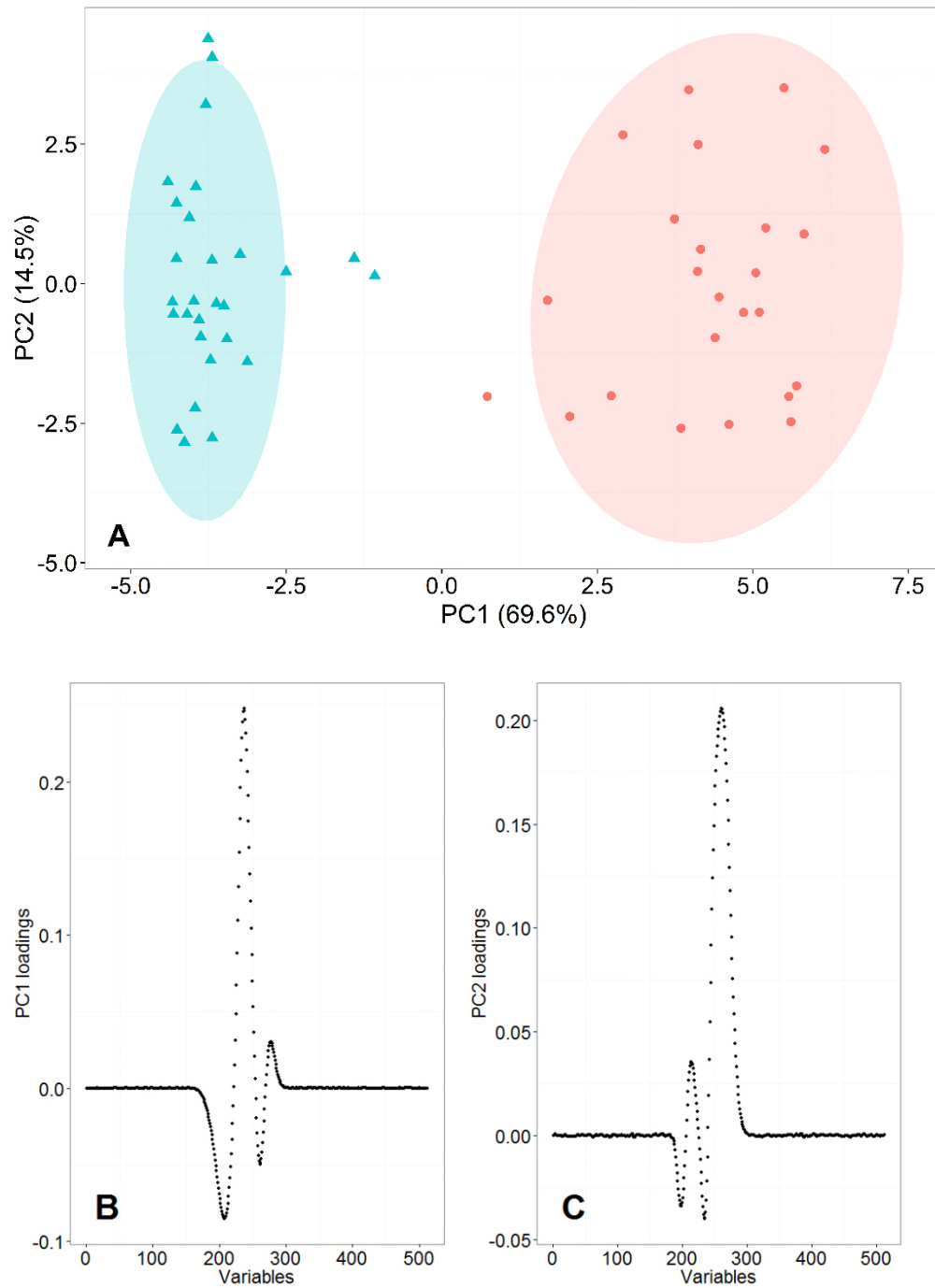


Fig. 3.3. PCA score and k-means clustering (A) for two groups of potato tubers with controls (cyan triangles) and infected (red circles) that have been grouped with 95% confidence ellipses around the centroid identified by the k-means algorithm) for 2DPI (2 days post inoculation). Loadings for the two main principal components in (B) and (C).

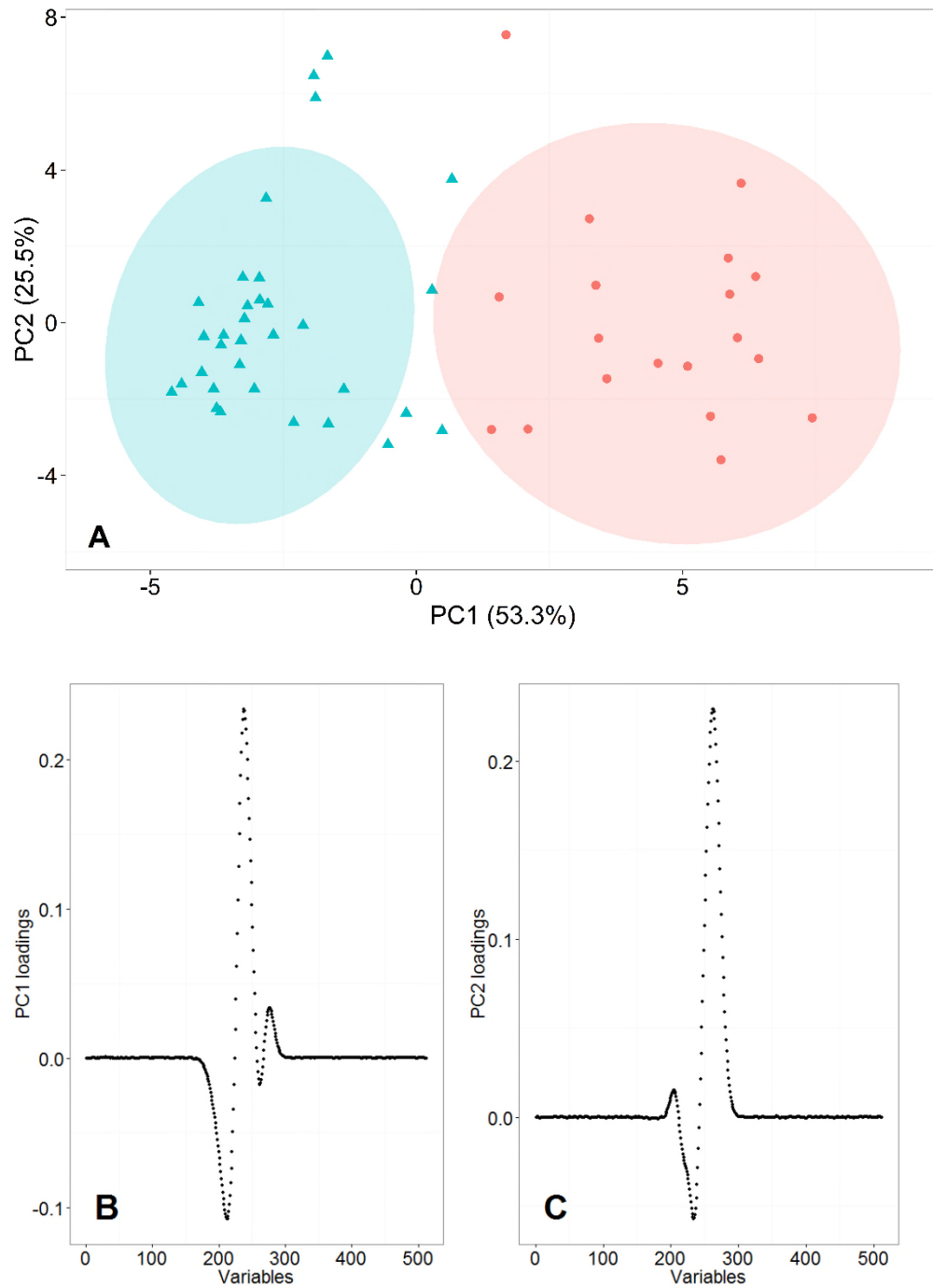


Fig. 3.4. PCA score and k-means clustering (A) for two groups of potato tubers with controls (cyan triangles) and infected (red circles) that have been grouped with 95% confidence ellipses around the centroid identified by the k-means algorithm) for 1DPI (1 day post inoculation). Loadings for the two main principal components in (B) and (C).

3.3.2 Detection of potato quarantine pathogens at FERA

Laboratory work at FERA (Food and Environment Research Agency, York, UK) was carried out with the Lonestar FAIMS (after the most appropriate set-up was devised at the University of Warwick for their environment) for two quarantine diseases, namely brown rot and ring rot. Brown rot is caused by the bacterium *R. solanacearum* while ring rot is caused by the bacterium *C. michiganensis* subsp. *sepedonicus* (DEFRA 2005a; DEFRA 2005b). Brown rot is characterized by browning and necrosis of the vascular ring and surrounding tissue which may cause secondary rotting. Symptoms of ring rot are cheese-like degradation around the vascular tissue, as it can be seen from Fig. 3.5 (DEFRA 2005a; DEFRA 2005b).

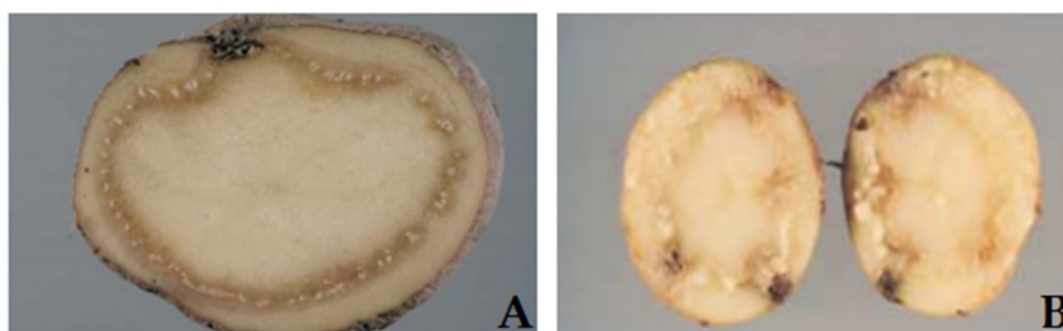


Fig. 3.5. Characteristics early symptoms of brown rot (A) and ring rot (B) (DEFRA 2005a; DEFRA 2005b).

Unlike other potato tubers diseases, brown rot cannot be easily detected because of the lack of distinctive “odour” identifiable by human olfaction. The core idea was to evaluate the potential of “artificial olfaction” with FAIMS for the detection of the selected infection, at different stages of disease development. Some results for the experiments with brown rot and ring rot, another quarantine disease selected for study, are shown in Fig. 3.6.

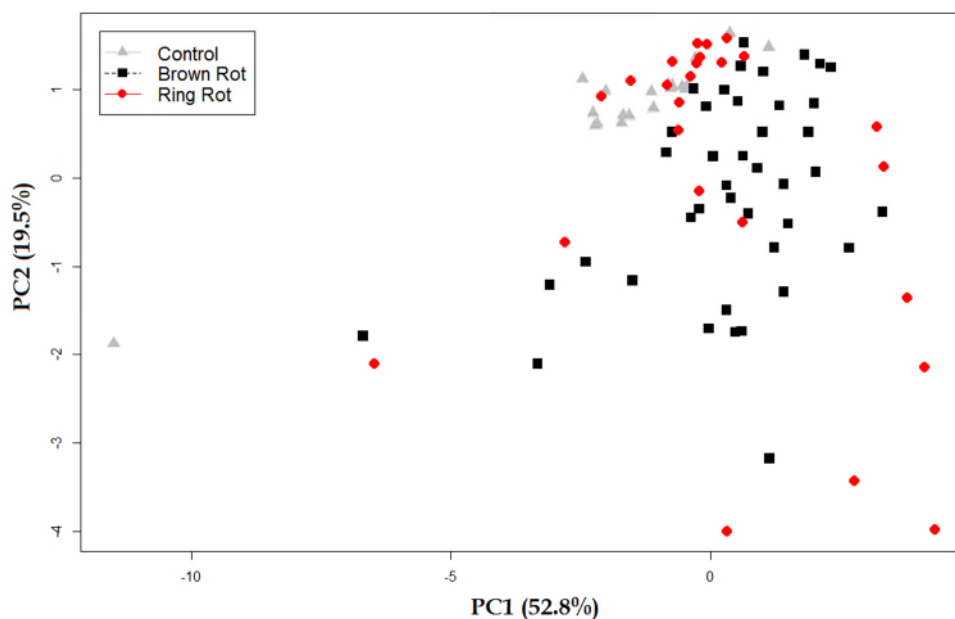


Fig. 3.6. Lonestar FAIMS PCA results obtained at FERA (Food and Environment Research Agency) for control (20 samples), brown rot (50 samples) and ring rot (15 samples).

Partial discrimination between control and brown rot was achieved while the data for ring rot yielded no results, as shown in Fig. 3.6. Because of the initial experimental conditions, the results raised the possibility that temperature could affect volatile emissions in such a manner to make gas analysis by FAIMS or any other technology unfeasible (which has led to further study on effect of temperature on volatile emissions as described later). The graph in Fig. 3.7 shows part of the DF matrix of data, the Ion Current (ordinate) versus Dispersion Field at 50% (abscissa), in short the first being the quantity of ions reaching the detector of the device while the latter the range of (direct current) voltage, which were applied to the ions, acts as a filtering system. Apart from few samples, the control and ring rot features a similar profile (hence not distinguishable) while the brown rot showed a more complex profile.

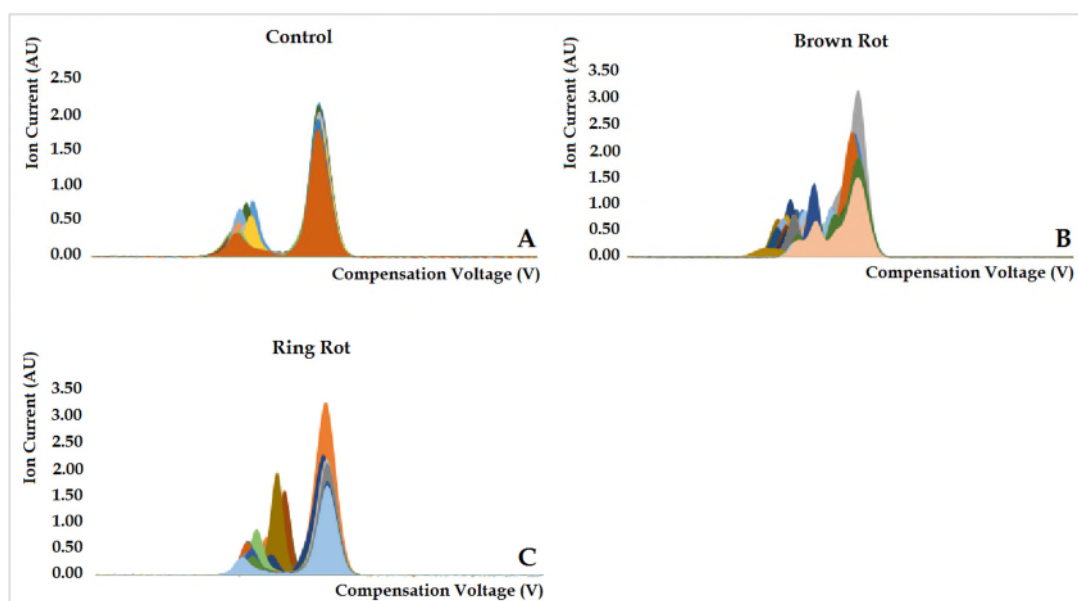


Fig. 3.7. FAIMS data for all potato tuber samples: Ion Current (ordinate, units in AU, arbitrary units) versus Compensation Voltage (abscissa, units in V) at Dispersion Field of 50% for control tubers (A), tubers infected with brown rot (B) and ring rot (C).

3.3.3 Effect of temperature variation on soft rot disease detection

This next set of experiments had the objective to ascertain if low temperatures could affect the FAIMS profile for gas/vapour/volatiles, and if so to what extent. Experiments were devised with the objective to have a first estimate for the potential of the instrument to detect signs of disease at conditions in which the tubers could be commonly stored. Fig. 3.8 shows what can be considered the characteristic outline of a ‘double plume’ for each infected tuber when sampled (after being kept at 25 °C) that appeared to be very similar in shape to the one after the same tuber was stored at 10 °C for 24h, as shown in Fig. 3.8. Results when temperature for storage was lowered from 25 °C to 15 °C (as in the first set of experiments) yielded similar outcome when conditions for storage of tubers were changed from 25 °C to 10 °C (second set of experiments). An important point to consider is that each tuber was taken from the incubator and immediately sampled. Data are shown PCA and k-means in Fig. 3.9 for

tubers at 25-15 °C and Fig. 3.10 for the ones at 25-10 °C. Data collected in each Figure represents all controls for each temperature pair (25-10 °C or vice versa 25-15 °C) against all diseased for the same temperature pair. Apart of the expected number of outliers and variation of experimental work, the data points are closely related together in a similar fashion to what was obtained in the previous section. Hence it can be concluded that gas analysis can be performed at low temperatures, which is relevant to potato storage.

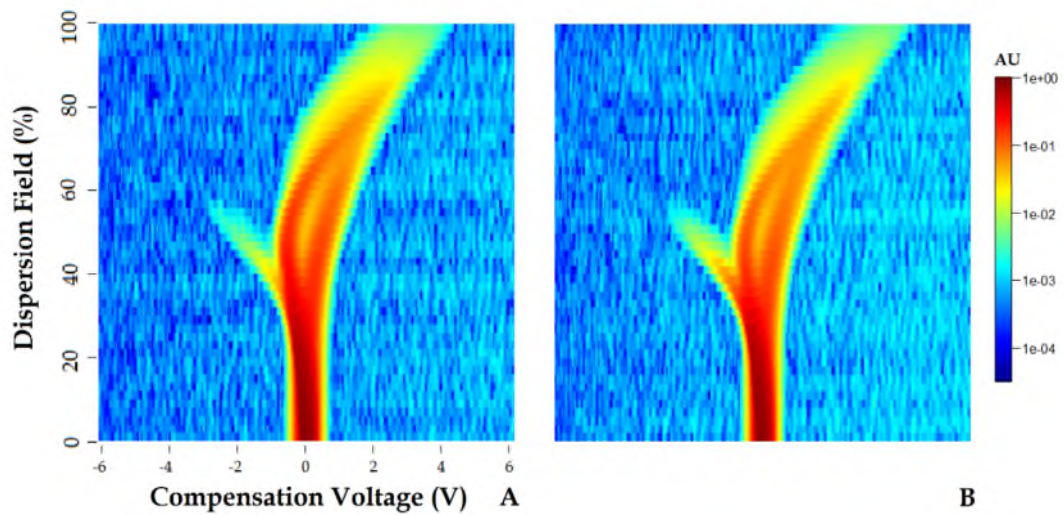


Fig. 3.8. Logarithmic representation of the DF matrix for the same tuber infected with soft rot stored at 25 °C (A) for four days and 10 °C (B) for 24 hours after inoculation and prior to sampling.

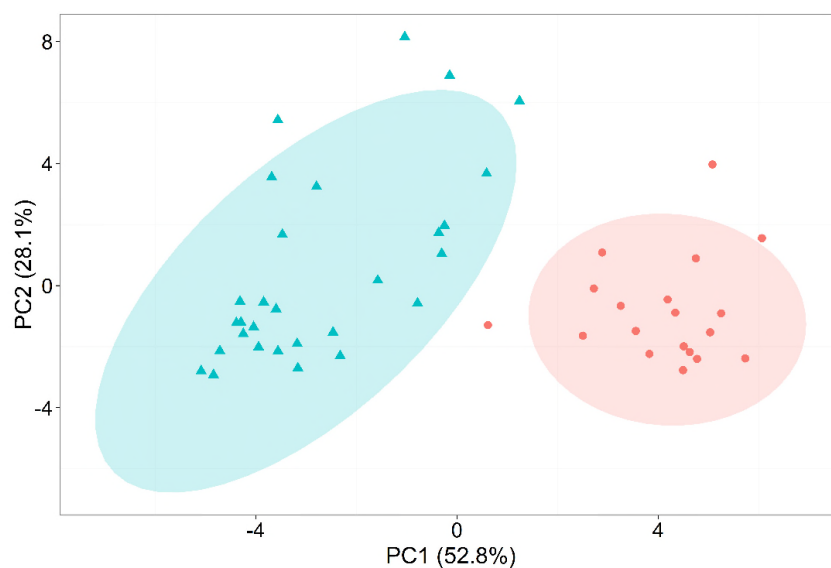


Fig. 3.9. PCA score and k-means clustering for two groups of potato tubers with controls (cyan triangles) and infected (red circles) that have been grouped with 95% confidence ellipses around the centroid identified by the k-means algorithm). Each of the tubers was first stored at 25 °C for 4 days post inoculation and then for 24h at 15 °C.

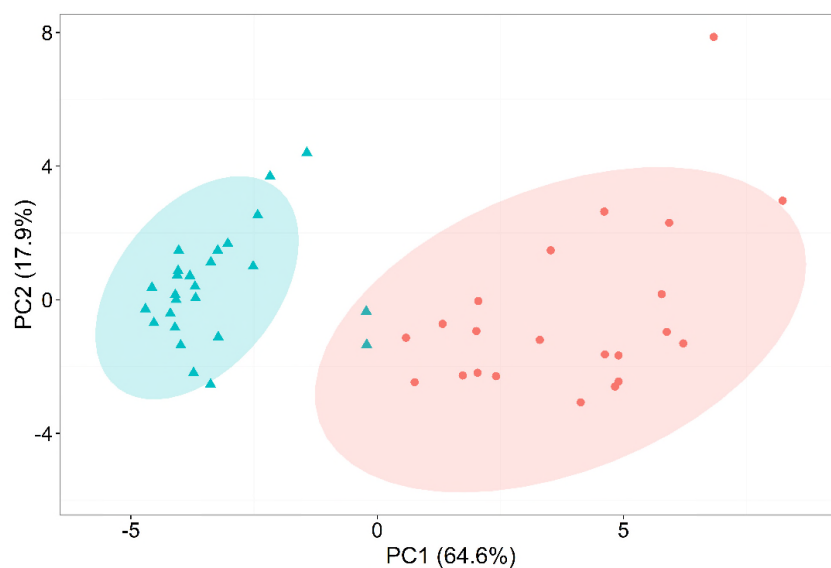


Fig. 3.10. PCA score and k-means clustering for two groups of potato tubers with controls (cyan triangles) and infected (red circles) that have been grouped with 95% confidence ellipses around the centroid identified by the k-means algorithm). Each of the tubers was first stored at 25 °C for 4 days post inoculation and then for 24h at 10 °C.

3.3.4 PID response for ‘detection’ and ‘early detection’ time points

Fig. 3.11 shows results for the first experiments with the Tiger PID analyser (Ion Science Ltd, UK). The aim of this experimental work was to determine the optimal amount of storage time for volatile collection with regard to the 5 DPI time point. 60, 30, 5 and 1m time periods were used for storing each potato tuber prior to sampling.

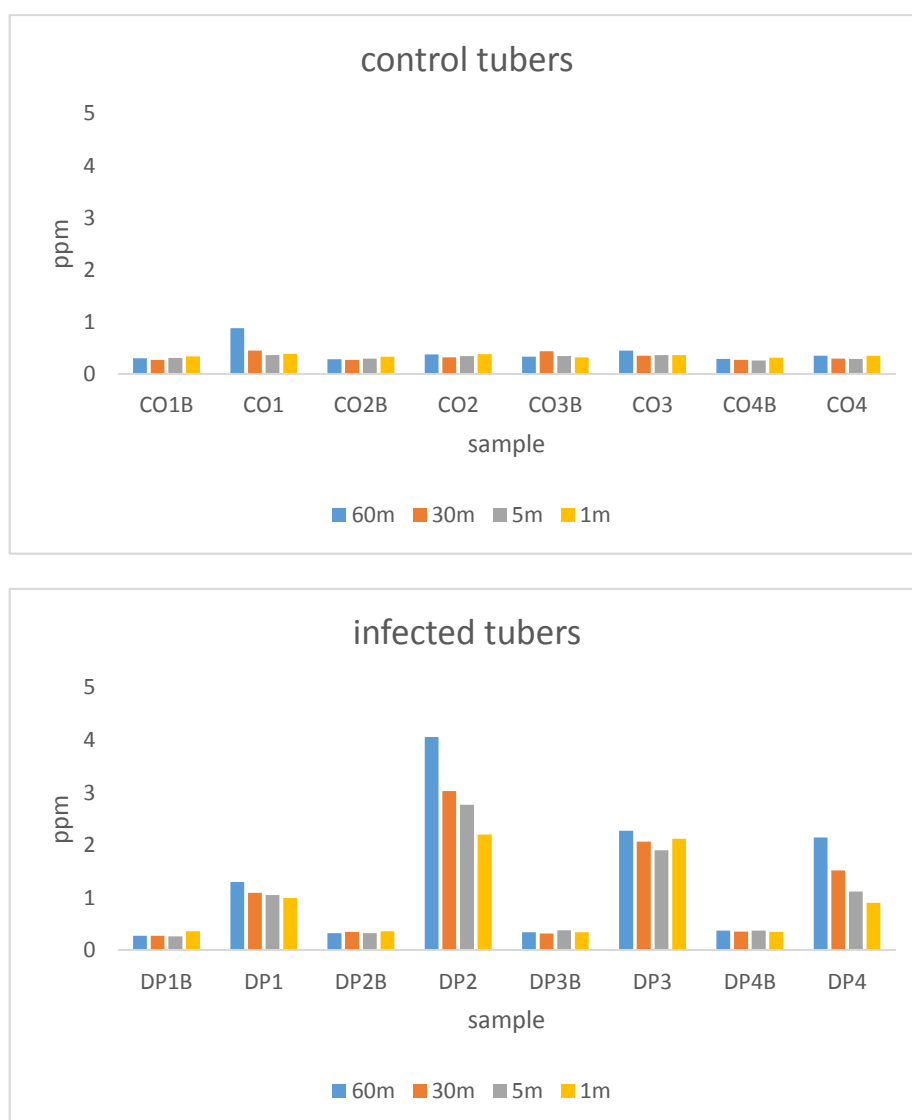


Fig. 3.11. Data results for the Tiger VOC analyzer for ‘detection’ time point, i.e. 5 DPI (days post inoculation). “CO” refers to control, “DP” to infected tuber and “B” to background reading before sampling. The legend for 60, 30, 5 and 1m indicates the time period of storage of tuber in the PTFE jar prior to sampling. Units are in ppm (parts per million).

The background value was also taken prior to tuber datum collection and no significant difference was found between background and sample reading for control tubers. However, substantial difference was identified when background and infected tubers were compared. Similar results were obtained for the other time point 'early detection' (Fig. 3.12), the only difference being the smaller amount of headspace volatiles for infected tubers. Based on this early work, a time collection period of 5 minutes was chosen in order to corroborate previous data as it best accounted for both the biological course of disease spread and practical experimental considerations. The results for these experiments are shown in Fig. 3.13 for the 'detection' time point for both controls and infected potatoes. The data further substantiate the fact that storage time did not affect the increase in VOCs for uninfected potato. The outcome for infected tubers thus showed that total VOCs from a tuber increases with the presence of disease (and this can be quantified). Furthermore, this implies that a lower cost technological approach can achieve the similar results as FAIMS. Fig. 3.14 indicates that for the second time point 'early detection' and, for both sample types, the results still hold albeit with a substantial change in VOC emission between the two time points, which could be associated with severity of disease progression. There is then a substantial difference with FAIMS outcome, since in that former case the Lonestar instrument was able to detect the same amount of an not yet identified chemical compounds (probably due to the high sensitivity of the technology) whilst in the latter case, the PID could also offer a numerical evaluation of overall VOCs trend associated with disease increase over time as it could be expected and achieved in a real storage facility.

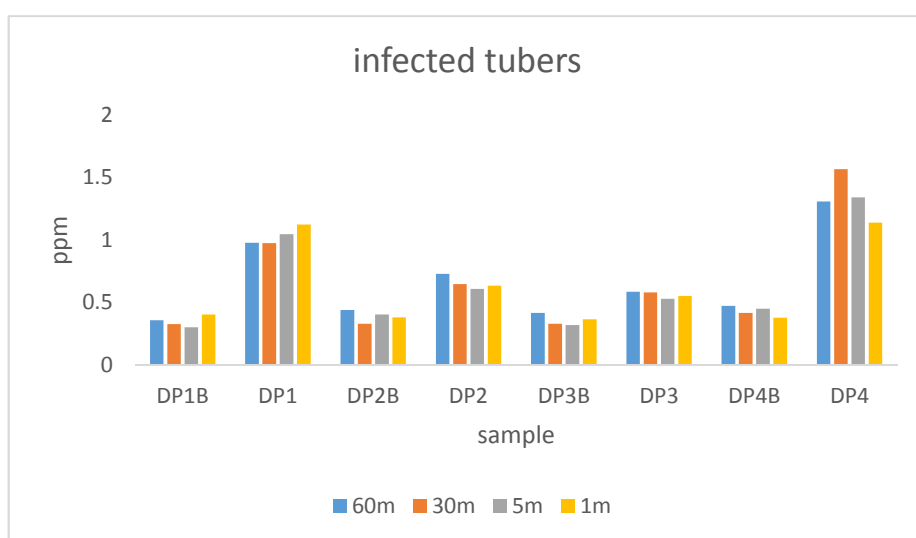
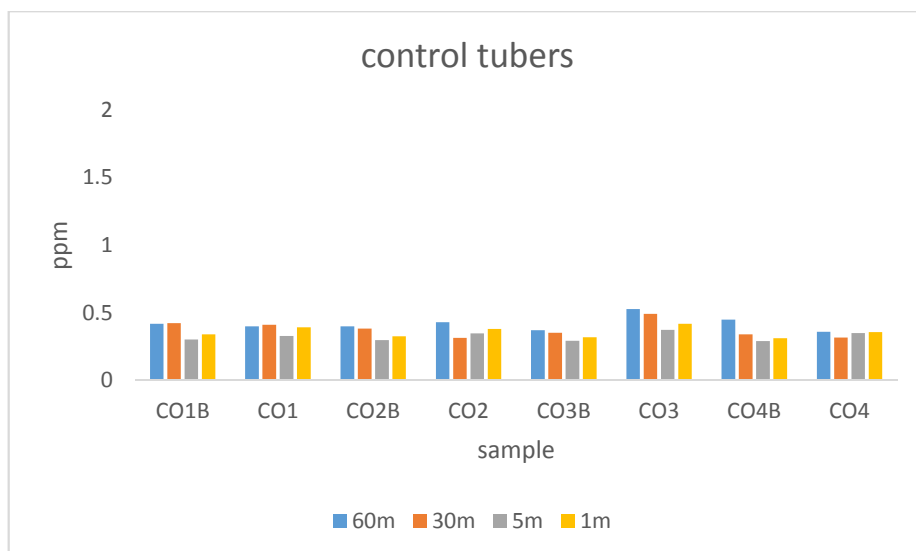


Fig. 3.12. Data results for the Tiger VOC analyzer for ‘early detection’ time point, i.e. 2 DPI (days post inoculation). “CO”, “DP” and “B” are as indicated in Fig 4.11. The legend for 60, 30, 5 and 1m indicates the time period of storage of tuber in the PTFE jar prior to sampling. Units are in ppm (parts per million).

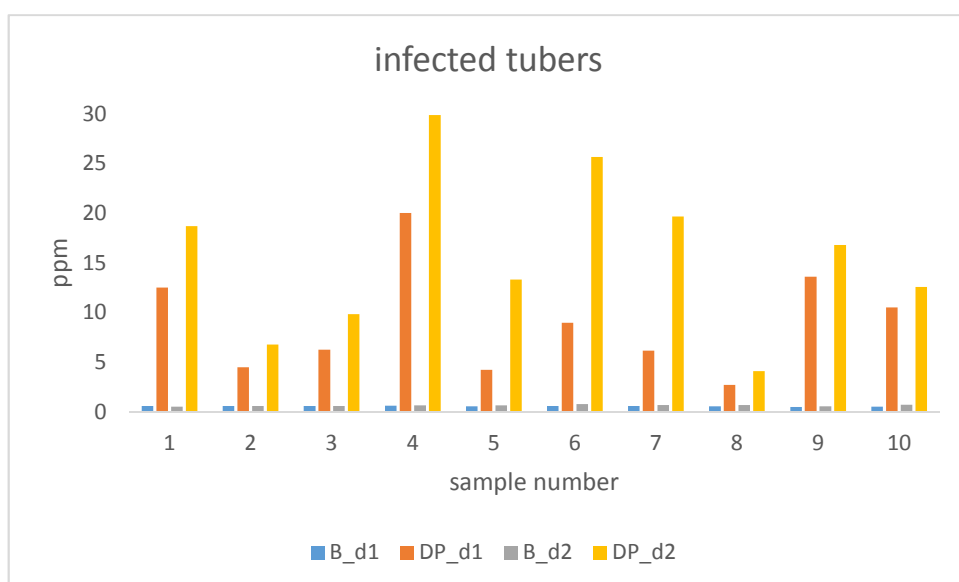
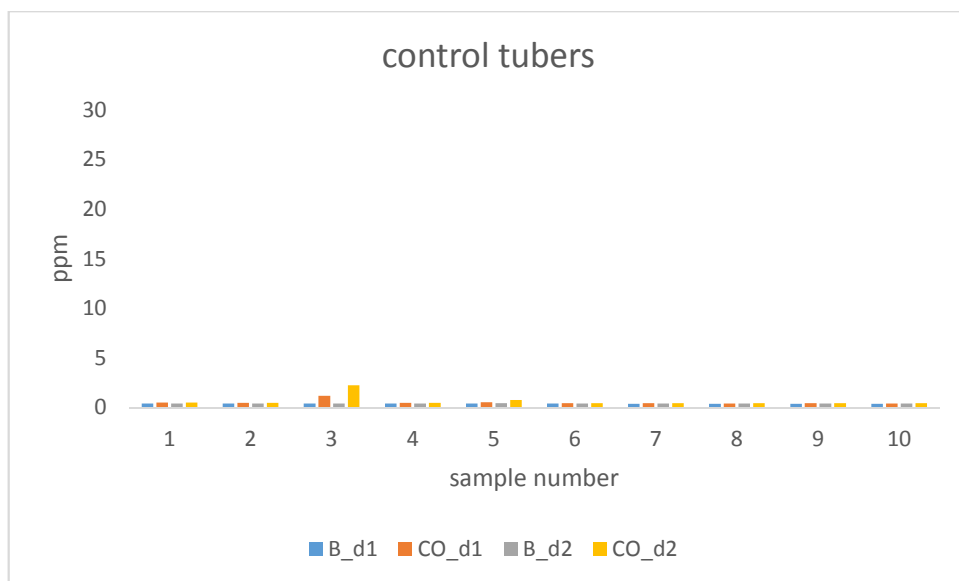


Fig. 3.13. Data results for the Tiger VOC analyzer for ‘detection’ time point, i.e. 5 DPI (days post inoculation. “CO” refers to control, “DP” to infected tuber, “B_” to background reading before sampling, “_d1” and “_d2” to the first and second day of sampling. 5m was the period of storage of tuber in the PTFE jar before sampling. The abscissa indicate potato tuber sample number while the ordinate instrument values in ppm (parts per million).

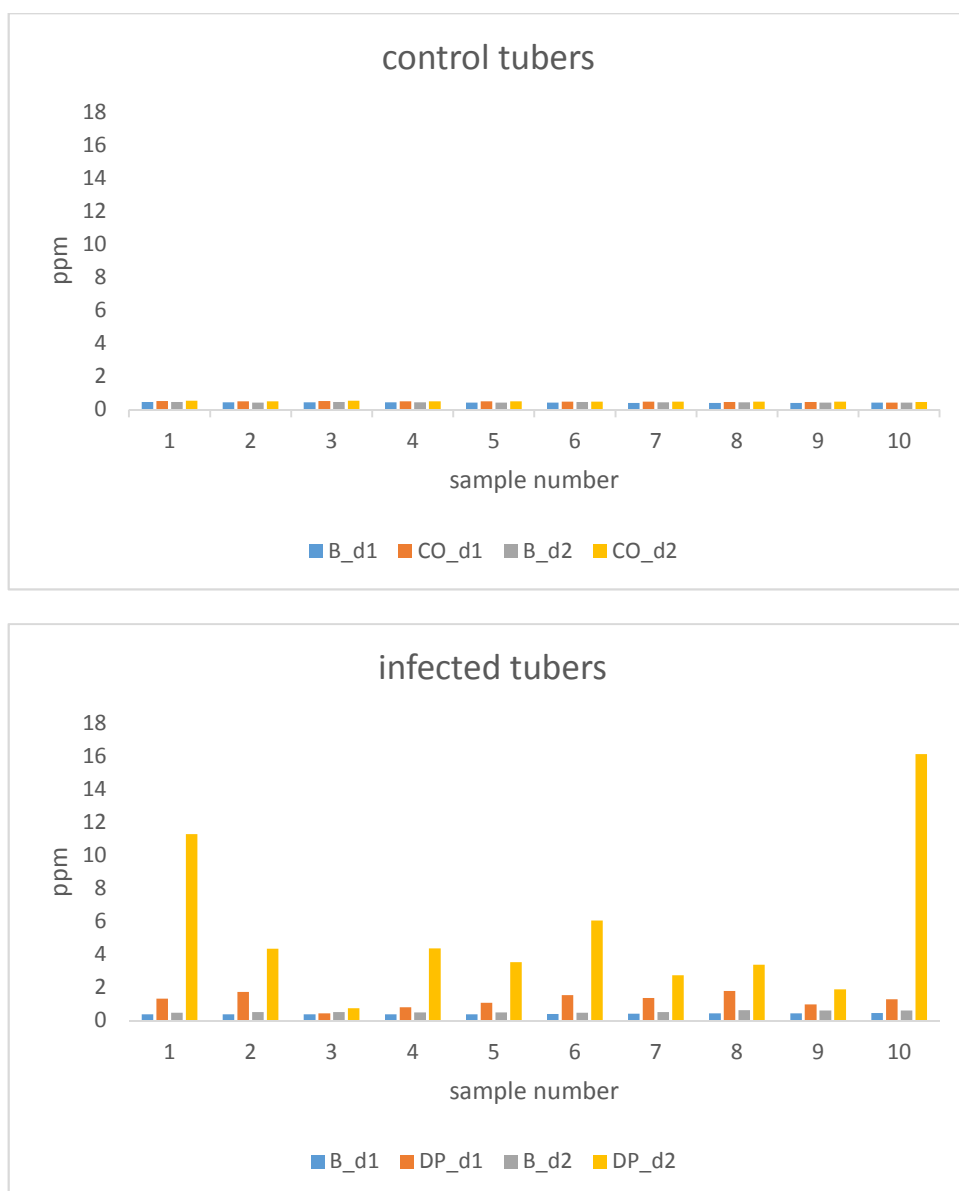


Fig. 3.14. Data results for the Tiger VOC analyzer for ‘early detection’ time point, i.e. 2 DPI (days post inoculation. “CO” refers to control, “DP” to infected tuber, “B_” to background reading before sampling, “_d1” and “_d2” to the first and second day of sampling. 5m was the period of storage of tuber in the PTFE jar before sampling. The abscissa indicate potato tuber sample number while the ordinate instrument values in ppm (parts per million).

3.4 Discussion

Results show that both FAIMS (Field Asymmetric Ion Mobility Spectrometry) and PID (Photoionization Detection) technologies can discriminate controls from tubers infected with *P. carotovorum*, the most widespread pathogen affecting potatoes both in the field and in store. Identification of soft rot infection with the Lonestar FAIMS was achieved for samples 5 days post inoculation (“disease detection”) and after allowing for rapid disease progression, by storing potato tubers at 25 °C in a humid environment. Discrimination between infected tubers and controls was also achieved for samples 48 and 24 hours post inoculation (“early disease detection”). The instrument yielded similar results in both cases, under the same experimental and data analysis conditions, thus indicating the potential of the technology not only for disease identification (at 5 days post inoculation) but also for early diagnostics (1 and 2 days post inoculation) in laboratory conditions.

It should be noted that the classification of results into two groups “detection” and “early detection” was aimed at answering two core objectives of the work. The first being if the technology could yield any result, and if so, how it could be benchmarked with current practices of identification employed by farmers (sensorial analysis). The second aim was to identify how early this identification could occur when the other approach failed. It has been shown that when no symptoms were identifiable by sensorial analysis (tactile, olfaction or visual inspection) of potato tubers, the Lonestar instrument performed well. Once established that both 48 and 24 hours were equally suitable for the time point “early detection”, the former was selected in order to facilitate soft rot determination by sensorial analysis at the termination of experimental work, as in the case of the Tiger PID instrument.

The whole data set for the Lonestar FAIMS was separated in two groups using both PCA and k-means analysis with a small numbers of samples outside the two 95% confidence intervals. The presence of these outliers can be attributed to different causes: varying biological conditions affecting each potato tuber differently, data processing, environmental conditions influencing the ionization of samples or the characteristics of the sensing unit.

With regard to biology, a number of controls appeared infected while previously inoculated samples appeared to show varying degrees of disease progression (or no disease at all). In the first case this was not unexpected as potatoes frequently carry soft rot bacterial pathogens, such as *Pectobacterium*, on their surface. When the potatoes are wounded (as was done in the control treatments) and then put in a warm, humid environment, both these factors can result in soft rot occurring. In the second case, lack of disease inception may well be attributed to low bacterial colony growth. These observations were made by sensorial analysis of the symptoms of the tubers cut in half, standard practice among experts in the field, and by the analysis of size and distribution FAIMS and PID data. No preliminary analysis on latent populations of bacteria was carried out.

For data processing, k-means is a computationally efficient algorithm, if compared to hierarchical clustering, but it is known to be sensitive to noise and outliers in the data set. In the data processing some of the outliers could be related to the k-means algorithm. In addition, the PCA scree plots of FAIMS data showed that most of the variance in the data set was accounted for in the first two principal components, thus indicating that the first two indices represent most of the variance for the whole data set. PCA loadings plots also indicated that most of the weight in the principal

components can be attributed to a restricted number of variables estimated to be circa 30% (150 variables). However, further work needs to be carried out in order to assess the effect of environmental conditions on FAIMS instrument performance. It may be argued that lack of apparent differences in results for FAIMS at different time points after inoculation may be due to the high potency of inoculum used. This would imply that the methodology described almost certainly resulted in very high populations of the bacterium, as well as high concentrations of extracellular peptic enzymes, being injected directly into susceptible tuber tissues, which would then cause rotting within 24 hours under the incubation conditions described. This is to a certain extent true, but previous preliminary experiments showed that extensive rotting in the tubers only occurred after 3-4 days under the selected experimental conditions. In addition, an increase in total VOC output over time was observed, as indicated by the PID results. An important point to remember is that a high inoculum load was used to ensure rapid and reproducible infection to test the FAIMS instrument as ‘proof of concept’ as a viable detection method. Further work may be devoted to examine the potential to detect latent populations of bacteria before any symptoms occur.

Another important consideration is the fundamental differences between the FAIMS and PID technologies. PID relies on the principle that all chemical substances in gaseous/vapour form are below the ionization potential of the UV lamp employed (available only in few set values) will be ionized and consequently detected – without any selectivity. This implies that, unlike electronic noses and FAIMS, the Tiger PID device can then be only be employed to detect overall gas/vapour (below the ionization potential of the UV lamp) increase over time, which has been shown to be indicative of soft rot spread. Furthermore, commercial PID detectors can be found with specifications for both high sensitivity (to 0.5 ppb) and wide dynamic range (in the

specific case of the Tiger instrument this ranges from 0.5 ppb to 20,000 ppm). This contrasts with the sensitivity and range of detection of the Lonestar FAIMS where excessive quantities of target chemicals may cause saturation of the sensor and consequently incorrect or unreliable readings, as occurred in earlier experimental work. In addition, FAIMS technology also suffers from a humidity intolerance, which is not as prevalent in other gas analysis technologies. On one side this implies that some compounds may not be identified because they cannot be properly ionized (and afterwards detected) and, on the other side, that humidity is an important parameter which can completely alter the results at the detector. For this reason, FAIMS requires continuous filtering of the inlet air flow. Hence the PID may be a more suitable for stores, whilst FAIMS as a very sensitive laboratory technology for soft rot disease identification.

Finally, it should be noted that all experimental results were obtained with a specific and widespread variety of potato tuber (Maris Piper). It is possible that other varieties of potatoes may produce different chemical signals as a result of the disease, which would require further investigation. For example, the FAIMS fingerprint may be associated with the volatile metabolites of generic breakdown products from the rotting tissue or by the specific metabolic activity caused by bacterial colonies inducing soft rot symptoms. More, these chemical signals may be common to this specific disease or to a wide-range of bacterial infections. This could well be possible, although other pathogens causing rots may have a similar FAIMS fingerprint or may provide no useful signal for detection. As a result, some preliminary work was carried out (as a proof of concept) at FERA (UK Food and Environment Research Agency) with two quarantine bacterial diseases of potato. In the study the sample size was small, the

inoculation and storage procedure very different from the one employed for soft rot but some differences between brown rot and controls were observed.

3.5 Conclusion

In conclusion, it has been shown that gas analysis can be employed as an effective diagnostic technique for both symptomatic and pre-symptomatic detection of potato soft rot. Furthermore, both techniques applied here offer a decisively more practical and reliable engineering solution when compared to previous past experimental work with GC or GC-MS. Finally, though FAIMS has the advantages of portability and high sensitivity, the PID has the ability to operate reliably with a wide detection range and at lower costs in harsher environmental conditions, such as those of commercial storage facilities, thus providing a more financially viable technical solution.

3.6 References

- de Lacy Costello, B.P.J., Evans, P., Ewen, R.J., Gunson, H.E., Ratcliffe, N.M., Spencer-Phillips, P.T.N., 1999. Identification of volatiles generated by potato tubers (*Solanum tuberosum* CV: Maris Piper) infected by *Erwinia carotovora*, *Bacillus polymyxa* and *Arthrobacter* sp. *Plant Pathol.* 48, 345–351.
doi:10.1046/j.1365-3059.1999.00357.x
- DEFRA, 2005a. Brown Rot of Potato.
- DEFRA, 2005b. Ring Rot of Potato.
- Dixon, R.A., Achnine, L., Kota, P., Liu, C.-J., Reddy, M.S.S., Wang, L., 2002. The phenylpropanoid pathway and plant defence-a genomics perspective. *Mol. Plant Pathol.* 3, 371–90. doi:10.1046/j.1364-3703.2002.00131.x
- Fiehn, O., 2002. Metabolomics – the link between genotypes and phenotypes. *Plant Mol. Biol.* 48, 155–171. doi:10.1023/A:1013713905833
- Kushalappa, A.C., Zulfiquar, M., 2001. Effect of wet incubation time and temperature on infection, and of storage time and temperature on soft rot lesion expansion in potatoes inoculated with *Erwinia carotovora* ssp. *carotovora*. *Potato Res.* 44, 233–242. doi:10.1007/BF02357901
- Lui, L.H., Vikram, A., Abu-Nada, Y., Kushalappa, A.C., Raghavan, G.S. V., Al-Mughrabi, K., 2005. Volatile metabolic profiling for discrimination of potato tubers inoculated with dry and soft rot pathogens. *Am. J. Potato Res.* 82, 1–8. doi:10.1007/BF02894914
- Lyew, D., Gariépy, Y., Raghavan, G.S.V., Kushalappa, A.C., 2001. Changes in volatile production during an infection of potatoes by *Erwinia carotovora*. *Food Res. Int.* 34, 807–813. doi:10.1016/S0963-9969(01)00102-8
- Lyew, D., Gariépy, Y., Ratti, C., Raghavan, G.S. V., Kushalappa, A.C., 1999. An

- apparatus to sample volatiles in a commercial storage facility. Appl. Eng. Agric. 15, 243–247.
- MacQueen, J., 1967. Some methods for classification and analysis of multivariate observations, in: Proceedings of the Fifth Berkeley Symposium on Mathematical Statistics and Probability, Volume 1: Statistics. The Regents of the University of California.
- Maslowski, S., Marshall, A., Hughes, R., 2015. GB Potatoes Market Intelligence 248.
- Pearson, K., 1901. LIII. On lines and planes of closest fit to systems of points in space. Philos. Mag. Ser. 6 2, 559–572. doi:10.1080/14786440109462720
- Ratti, C., Gariépy, Y., Raghavan, G.S.V., 1995. Proceedings of the International Conference on Harvest and Postharvest Technologies, in: Collection and Analysis of Headspace Volatiles for Disease Detection in Stored Potatoes. pp. 255–261.
- SMC Pneumatics Ltd, 2016. Industrial Automation Product Catalogue. UK.
- Varns, J.L., Glynn, M.T., 1979. Detection of disease in stored potatoes by volatile monitoring. Am. Potato J. 56, 185–197. doi:10.1007/BF02853365
- Waterer, D.R., Pritchard, M.K., 1984. Monitoring of volatiles: A technique for detection of soft rot (*Erwinia carotovora*) in potato tubers. Can. J. Plant Pathol. 6, 165–171. doi:10.1080/07060668409501578
- Wilson, C.L., Wisniewski, M.E., 1989. Biological Control of Postharvest Diseases of Fruits and Vegetables: An Emerging Technology*. Annu. Rev. Phytopathol. 27, 425–441. doi:10.1146/annurev.py.27.090189.002233

EARLY IDENTIFICATION OF POTATO
STORAGE DISEASE USING METAL-
OXIDE, ELECTROCHEMICAL AND NDIR
GAS SENSORS

This page is intentionally left blank.

4 Early Identification of Potato Storage Disease using Metal-Oxide, Electrochemical and NDIR Gas Sensors

4.1 Introduction

In the previous chapter, it was shown that two specific technologies, namely FAIMS and PID, have the potential to be employed for the detection of soft rot disease in potato tubers. Of particular interest was that not only disease detection could be achieved with very high accuracy at par with sensorial analysis, but more importantly, that determination of pre symptomatic characteristic of soft rot could be identified by means of gas/vapour analysis at a very early stage. It proved the hypothesis that infected potatoes emit VOC from an early stage of infection. In addition it provided a 'proof-of-concept' for usage of such technologies and a means for benchmarking instrument performance against other techniques.

Although the results achieved were numerically consistent in advocating deployment in a commercial storage facility, there are a substantial number of technical and financial challenges that such technologies pose. In fact, purchase, maintenance, management of a FAIMS unit may provide financially prohibitive and especially critical in an industry with such low margins. PID is a far more reliable/less problematic technology that could potentially be implemented in a store in the form of a hand-held instrument. However, even if the instrument were adopted in its current form it still would cost in the low thousands of pounds (though far less than the Lonestar FAIMS). Hence, there is a need for a more financially viable solution for early detection and monitoring of potato stores and therefore an electronic nose- based approach was explored.

Early work with electronic noses and potato tuber infection was done almost two decades ago by de Lacy Costello *et al.* (de Lacy Costello et al. 2000). Their study was based on fabrication and testing of purpose-built sensors for general VOCs monitoring associated with soft rot disease spread. More recently, Biondi *et al.* completed a study also with both GC and GC-MS coupled with a commercial electronic nose based on the quarantine potato diseases brown rot and ring rot (Biondi et al. 2014). Despite the fact that both approaches relied on an impractical final approach, they showed potential of using an electronic nose for potato disease monitoring.

Previous research in this work and related studies has led to the conclusion that development, manufacture and test deployment of a prototype gas analysis system could be feasible. The system would be composed of small-size sensor units that “in use” would be located throughout the stores to monitor the gas phase environment around it and warn of disease. By using this approach, a smart network on monitoring points would be created that could provide key information to the farmer or store manager about the state of the crop and (if a zone shows signs of infection) allows these crops to be sold immediately, producing income to the farmer and reducing cross infection.

The aim of this chapter is the identification of the most important sensor subset that could then be used in such a future product. The materials and methods employed to undertake this selection are similar those applied to the Lonestar FAIMS unit. In particular, the use of two time points. The only major difference is the analytical methods adopted that take into account the differences between various technologies.

4.2 Material and methods

4.2.1 Experimental sample preparation

The experimental procedure for sample preparation and handling in this part of the work is the one suggested by Dr Glyn Harper (AHDB Potato Council, Sutton Bridge Crop Storage Research) with the use of *P. carotovorum* isolate SBEU_08. This protocol is briefly outlined below and for further details the reader is referred to the relevant section chapter on FAIMS laboratory work at the University of Warwick (3.2.2 Experimental sampling protocol):

- Rehydrating tubers by soaking them in water prior to inoculation and storage.
- Inoculation with *P. carotovorum* isolate SBEU_0 or only wounding with a pipette tip at the stolon of the tuber for controls.
- Storage in the incubator at in sealed plastic boxes at 25 ± 1 °C in an incubator to allow rapid disease progression and suspended on a mesh over water (400 mL), to maintain high humidity.
- All tubers used were apparently healthy at the start of all experiments but control tubers were checked for symptoms of infection throughout and at the end of the experiments alongside the inoculated tubers.

4.2.2 Experimental sampling protocol

For gas sampling, each tuber was placed into a 1 L PTFE container (Fisher Scientific Ltd, UK), with a gas path inlet and outlet added (1/8" push-fit, Pneu-store, UK). Sampling was carried out for each individual tuber by passing zero-grade air around it at a flow rate of 200 mL/min and the mixture of air and emissions from the tuber fed to a commercial FOX 3000 electronic nose (AlphaMOS, Toulouse, France) for

analysis. Available sensors in the unit as indicated by the manufacturer are listed in Table 4.1. The acquisition time was 120 s, purge of 30 s, start injection of 20 s, injection time of 10 s. For the WOLF 4.1 (sensors list is listed in Table 4.2) acquisition time was of 120 s, start injection of 20 s, injection time of 10 s, and flow rate of 300 mL/min. Sampling containers were kept separate for controls and infected tubers throughout all experiments to avoid accidental cross contamination. The containers were regularly replaced with clean ones, in order to eliminate the potential of any by-products of tuber decomposition to affect the results. Containers were also thoroughly flushed with zero grade lab air for 5 to 10 minutes before starting any experimental work and after equipment cleaning in order to remove potential residual odorous emissions (originating from either laboratory practice or from the cleaning process) that could affect experimental work. After sampling, each tuber was returned to the sealed plastic boxes in the incubator at 25 °C. Prior to, and after experimentation, containers were thoroughly cleaned and sterilized. After previous preliminary work had established the optimal time points for sampling, four experiments were carried out where four tubers were inoculated 2 and 5 days before sampling. Sampling was then carried out for two consecutive days with corresponding uninoculated healthy controls. The first sampling time point (defined as ‘detection’) was used to verify the potential of the electronic nose to discriminate between healthy controls and soft rot infected tubers, sampled after 5 days of storage in the incubator at 25 °C, when the symptoms of the disease could be identified by (human) olfactive, visual and tactile inspection of the sample. The second sampling time (‘early detection’) after 2 days of tubers stored at 25 °C was used to assess the potential of the instrument to detect the disease early, by discriminating between uninoculated controls and inoculated tubers, when no obvious symptoms of the disease could be observed. At the end of the

sampling procedure, all tubers were cut in half and photographed to assess the degree of infection. In total, 40 potato tubers (20 inoculated, 20 uninoculated) were analysed for each of the two time points.

Sensor Name	Responsive to:	Type of sensor
P10.1	Hydrocarbons	P Type
P10.2	Hydrocarbons	P Type
P40	Fluorinated and chlorinated compounds, aldehydes	P Type
PA2	Polar compounds, solvents	P Type
SX00	Air quality	SX Type
SY.cG	Amine, amine compounds	SX Type
SY.G	Fluorinated and chlorinated compounds, aldehydes	SY Type
SY.gCT	Hydrocarbons	SY Type
SY.GW	Polar compounds, solvents	SY Type
SY.W	Hydrocarbons	SY Type
T30.1	Polar compounds, solvents	T Type
T70.2	Alcohol and aromatic compounds	T Type

Table 4.1. Description of FOX3000 sensors as indicated in the FOX2000-4000 Manual (Release 4.01) by Alpha MOS Ltd.

Sensor Name	Responsive to:	Type of sensor
Cirius CH4 NDIR	Methane	NDIR (Nondispersive infrared)
Cirius CO2 NDIR	Carbon Dioxide	NDIR (Nondispersive infrared)
Carbon Monoxide (CO)	Carbon Monoxide	Electrochemical
Ethylene Oxide (ETO)	Ethylene Oxide	Electrochemical
Hydrogen (H₂)	Hydrogen	Electrochemical
Hydrogen Sulphide (H₂S)	Hydrogen Sulphide	Electrochemical
Nitric Oxide (NO)	Nitric Oxide	Electrochemical
Nitrogen Dioxide (NO₂)	Nitrogen Dioxide	Electrochemical
Oxygen (O₂)	Oxygen	Electrochemical
Ozone (O₃)	Ozone	Electrochemical
Sulphur Dioxide (SO₂)	Sulphur Dioxide	Electrochemical

Table 4.2. Description of WOLF 4.1 sensors employed for experimental work as indicated by Alphasense Ltd and Clair Air Ltd.

4.2.3 Data analysis

Data processing in chapter 3 relied on a simpler format of the underlying data set (i.e. extracting one line of FAIMS values). In fact, the Lonestar FAIMS (Owlstone Ltd, UK) dispersion field data matrix (or DF) is a graphical representation associated to a specific chemical or range of chemicals (often unknown to the experimenter). Thus, a simple pattern characteristic of infection can be considered the main feature needed to explore data outcome for a number of samples under investigation. In a similar manner, the outcome for each single measured value of the Tiger photoionization detector unit (Ion Science Ltd, UK) yields itself to numerical interpretation with regard to presence of disease, despite the naturally occurring variability of disease progression of individual samples. However, unlike the other two approaches, data

processing of electronic nose data is related to both that the type of sensor response to odorant and the relationship between the different sensor curves. As a result, electronic nose data processing requires determination of a more sophisticated set of features of each sensors response, which is representative of the underlying data set. A range of different features can be extracted from an electronic nose raw sensor signal (Fig. 4.1 and Table 4.3) and these can be used either individually or in different combinations.

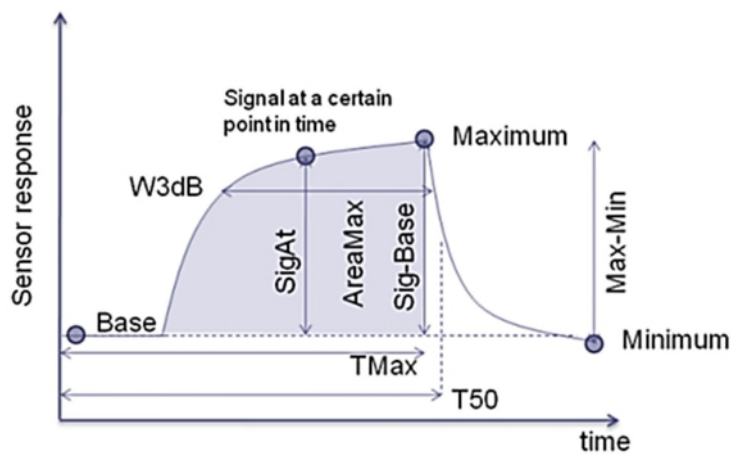


Fig. 4.1. Representation of most common feature extraction approaches for electronic nose data. ‘Maximum’ and ‘Minimum’ indicate the maximum value and minimum value respectively, while ‘Base’ refers to baseline. A detailed description of the techniques is listed in Table 4.3.

Technique	Short description
SigAt	Signal at a measurement point.
AreaMax	Area of the response curve above the baseline
Sig-Base	Signal divided by the baseline
Max-Min	Span of the response curve.
TMax	Number of the measurement point at which the maximum of the response is reached.
T50	Number of the measurement point at which the signal has returned to 50% of the maximum in the response curve after the maximum had been reached

Table 4.3. Short description of common electronic noses techniques (Mitrovics 2009).

With regard to metal oxide gas sensors, W3dB was found to be the most suitable pre-processing technique. W3db, represented in Fig. 4.2, is the measurement between the

value at 70% (3 dB) of the response time (exposure to odorant) and the same measurement for the recovery time (return to baseline resistance from the peak) of the sensor response curve (Mitrovics 2009). It relates to the rate of absorption/desorption of a molecule and this is based on a complex interaction between the gas components and the surface of the metal-oxide. W3dB was particularly useful since it took into account the rate of the response of the large number of sensors involved in the analysis. In particular, it allowed to deal with the slow return to the baseline for the recovery time part of the sensor response curve.

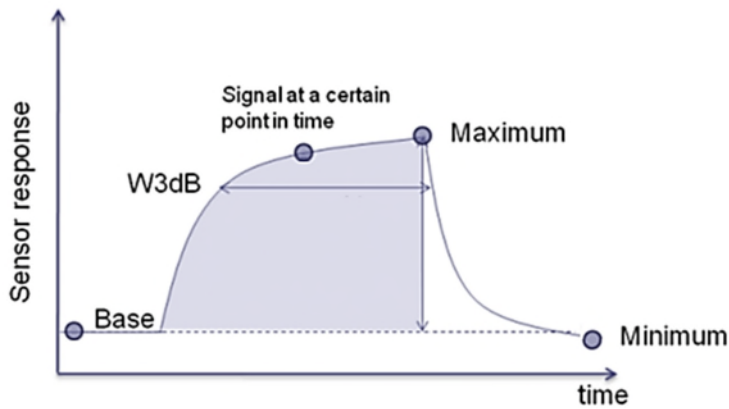


Fig. 4.2. Representation for the W3db feature extraction method. The sensor response (ordinate), versus time (abscissa), reaches its apex at the point labelled 'maximum' (exposure to odorant) before returning to the baseline resistance. W3db is the measurement between the value at 70% (3 dB) of the exposure to odorant and the same value for the recovery part of the curve (absence of odorant) (Mitrovics 2009).

AreaMax instead, was found to be the most suitable pre-processing technique for electrochemical gas sensors. AreaMax, represented in Fig. 4.3, is the measurement of the area for the response time (exposure to odorant) above the baseline from the first point to the point of maximum response (Mitrovics, 2009). This approach could be chosen since there was minimal recovery time for these type of sensors and their

higher selectivity to target chemical (when compared to metal oxide ones) was accurately represented by the area under the curve.

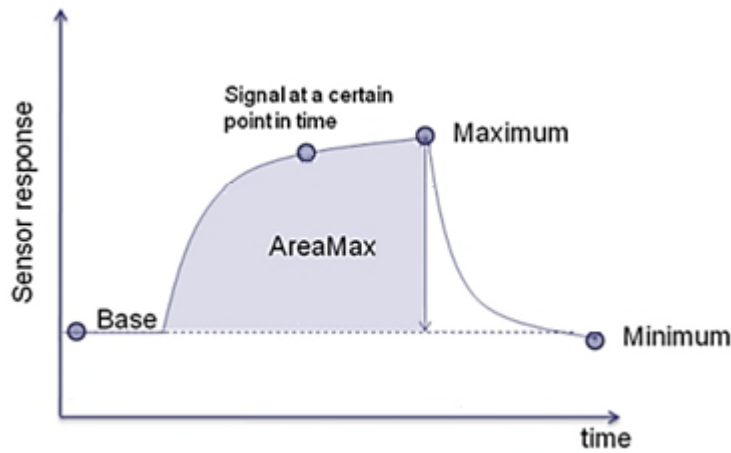


Fig. 4.3. Representation for the AreaMax feature extraction method. The sensor response (ordinate), versus time (abscissa), reaches its apex at the point labelled 'maximum' (exposure to odorant) before returning to the baseline resistance. AreaMax is the measurement of the area for the response time (exposure to odorant) above the baseline from the first point to the point of maximum response (Mitrovics 2009).

After feature extraction, the data set was processed with both unsupervised techniques for study of variance and classification for model construction and evaluation. For the exploratory analysis, two techniques were employed, PCA for dimensionality reduction and k-means for clustering (Pearson 1901; MacQueen 1967). To avoid over fitting of the classification model, the data was split into training and test sets, the first to build a predictive model, and the second to test its performance with 75% of the data allocated for model training and the remaining 25% for testing. This percentage allocation was justified by the size of the data set and the further use of k-folds for cross validation of the training set. To test the quality of different models, two approaches were considered: class probabilities and confusion matrices. Classification models generate both a class (discrete category) and a continuous prediction, which

usually is a probability indicating the likelihood for the specific class. In order to make a decision, usually the focus is on the discrete category (as in this experimental work), but the continuous prediction values for each class can be used for assessing the model's confidence about its prediction (Kuhn & Johnson 2013). Visualizing class probability is a method for assessing the results of a model. Such an example is shown in Fig. 4.9 and Fig. 4.10 where such probabilities are gauged by means of histograms. Confusion matrices instead are cross-tabulation of the observed and predicted classes for the data.

Sensitivity, a conditional metric employed in confusion matrices, is the rate at which the event of interest is predicted correctly for all samples in that event. This means that if the positive event of interest is a healthy control potato tuber, for example, this specific measure of 'accuracy' (i.e. sensitivity) is the ability of the model to accurately predict controls. This metric is particularly useful in practical deployment in potato stores, since it allows identification of healthy controls while disregarding all degrees of soft rot infections or of any other disease. The other conditional metric, which was considered less relevant as a measure of model reliability, is specificity, the rate (not to be confused with false positive rate) at which non-events samples are predicted as non-events. Different models with varying degrees of complexity were chosen in order to gauge the underlying data set. The diagram for the whole data analysis procedure is reported in Fig. 4.4.

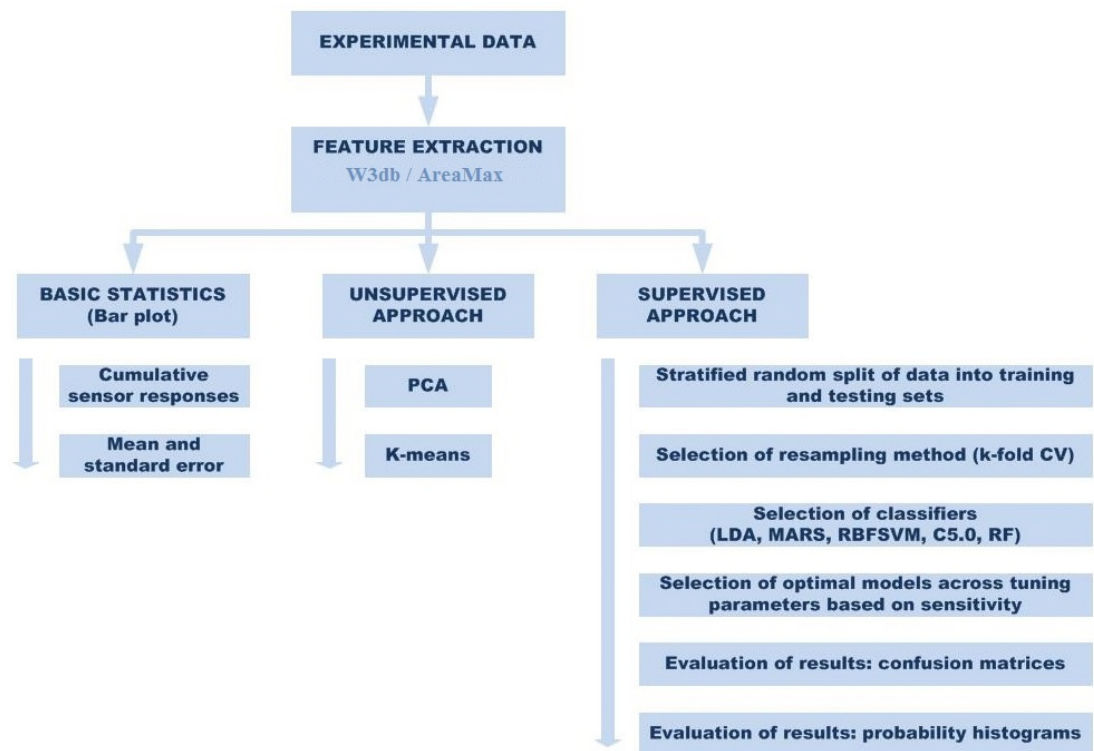


Fig. 4.4. Data analysis process: basic statistical analysis, unsupervised and supervised approaches.

4.3 Results

4.3.1 Metal oxide gas sensors response to ‘detection’ time point

Fig. 4.5 shows a bar plot with cumulative values for the extracted features from all sensors employed for sampling (with standard error over the sample class), for both time points, ‘detection’ and ‘early detection’.

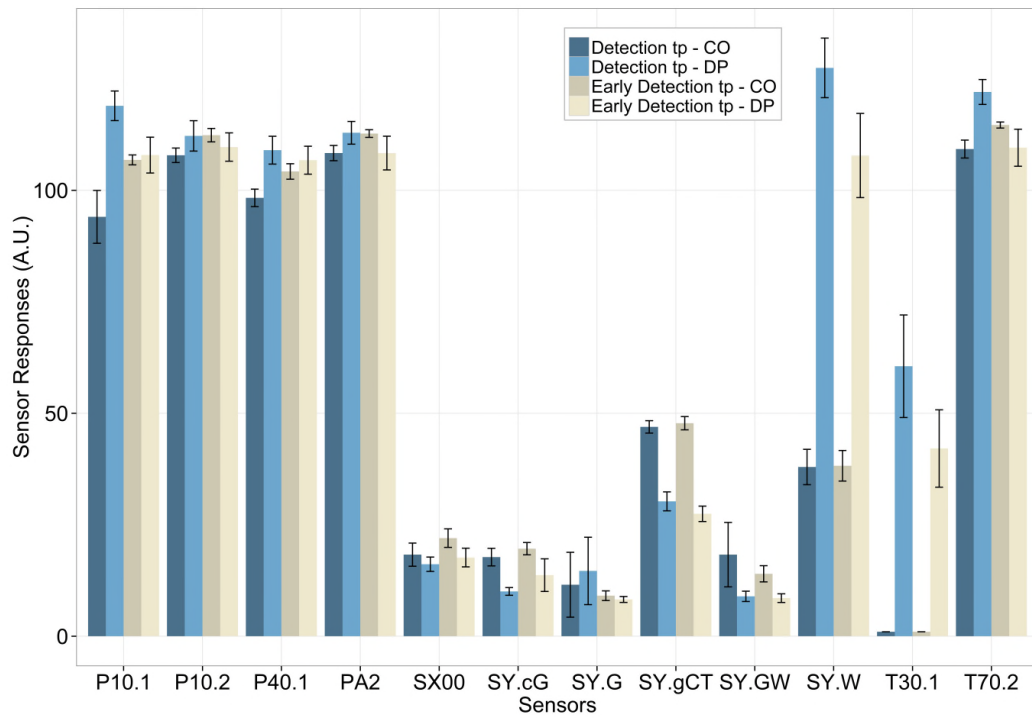


Fig. 4.5. Bar plot of raw data indicating differences in responses for all sensors at two time points (‘tp’). ‘CO’ indicates healthy controls and ‘DP’ to diseased potato tubers. The error bars represent standard errors of the mean values. The sensors nomenclature refers to Alphasmos FOX 200-4000 Manual Release 4.0.1.

Fig. 4.6 shows PCA scores and k-means clustering for the time point referred as ‘detection’ and indicates the features extracted for all the raw sensors data. Fig. 4.7 is the equivalent biplot for the first two principal components, which accounts for most of the predictor’s variance (79.8.2 %) in the data set. The biplot also indicates that most of the variance characteristic for the two groups can be attributed to a few MOX

sensors among those comprising the original array of the FOX3000 electronic nose, namely SY.W, T30.1 and SY.gcT. SY.W is reported to be responsive to hydrocarbons, while T30.1 to solvent, alcohol and polar compounds. The first sensor, SY.W, might be indicative of response to hydrocarbons pertaining to presence of disease, such as ethene, as indicated by Lui (Lui et al. 2005). Acetone vapour or ethanol, that the second sensor would be detecting, appear to be the only common polar solvents that were identified in past studies with GCMS (Kushalappa, Lui, Chen, & Lee, 2002; Lui et al., 2005; Varns & Glynn, 1979). The other sensor of interest, labelled as SY.gcT, is reported to be responsive to hydrocarbons in a similar fashion to SY.W, but is produced by a different manufacturer. In this latter case, it may be very possible that this response may be related to general organic decomposition, in a similar manner to landfill gas emissions. The final results for the subset of sensors, which have been selected as representative of a potential detection system for soft rot, are shown Fig. 4.8.

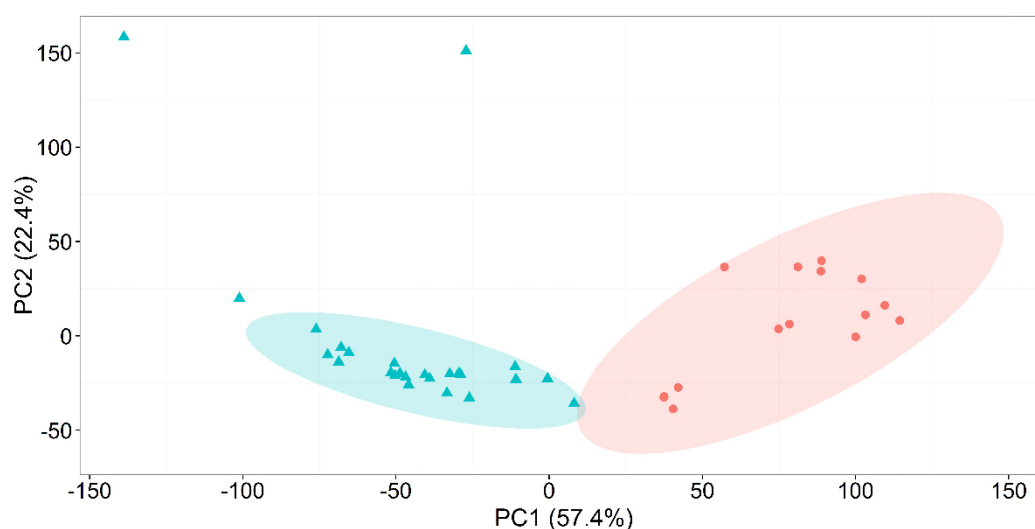


Fig. 4.6. PCA score and k-means plot with 95% confidence intervals based on CMOS technology measurements for all sensors at time point ‘detection’. Data points indicate healthy controls (cyan, triangles) and diseased potato tubers (red, circles).

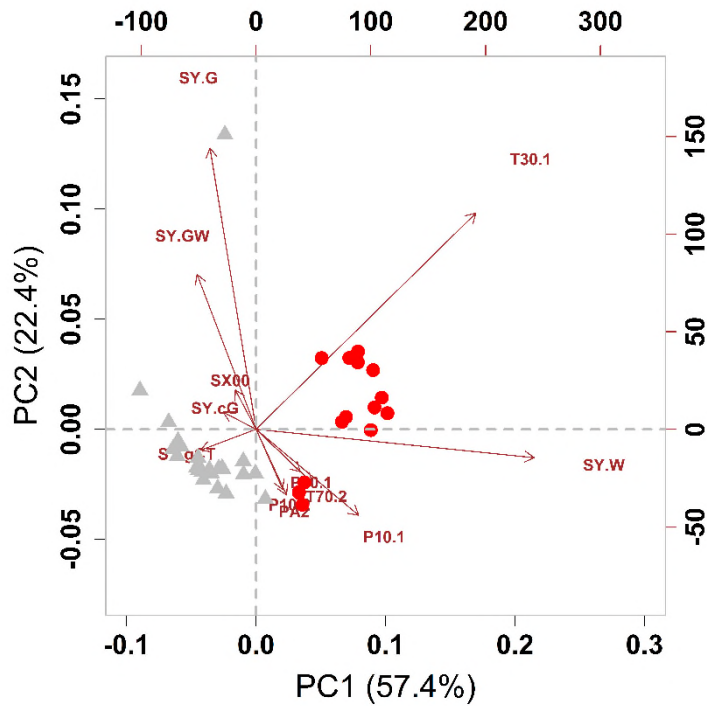


Fig. 4.7. Biplot for all sensors at time point 'detection'. Data points indicate healthy controls (grey, triangles) and diseased potato tubers (red, circles).

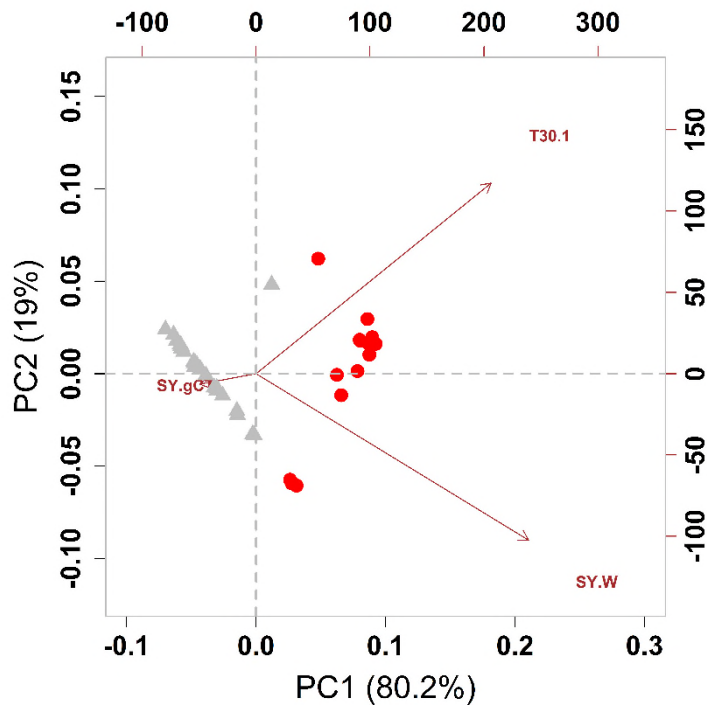


Fig. 4.8. Biplot for selected sensors (SY.W, T30.1, SY.gcT) at time point 'detection'. Data points are as indicated in Fig. 4.7.

For modelling, the data were split into 75% for training and 25% for testing (stratified random splits). Cross validation to estimate accuracy of all the models was carried out with a k fold CV (k-fold cross validation) of 10. In Table 4.4 are reported the values for sensitivity and selectivity metrics of the confusion matrix across all models and for the selected time point.

	C5	LDA	MARS	RBFSVM	RF
Sensitivity ('all sensors')	100%	100%	100%	100%	100%
Specificity ('all sensors')	100%	100%	100%	100%	100%
Sensitivity ('selected sensors')	100%	100%	100%	100%	100%
Specificity ('selected sensors')	100%	100%	100%	100%	100%

Table 4.4. Confusion matrices metrics for the selected time point 'detection'.

Fig. 4.9 and Fig. 4.10 show histograms of class probabilities for all sensors and the selected subset (SY.W, T30.1 and SY.gcT) respectively. In both cases, the outcome of class probabilities appear to show that all models perform well. In Fig. 4.9 there are only three histogram bins with very high probability of control ('CO') being control (left hand side of the graph) and vice versa very low chance of diseased tuners being controls (right hand side of the graph): this indicates that these models, namely C5, LDA and MARS are the most suited for the data set, always under the assumption of the similar starting conditions and pre-processing for all the models are selected. The other distribution, Random Forest (RF) skewed to the left (left column of the histogram) for control data and to the right for diseased potatoes is still a reasonably accurate model, as in the case of radial basis support vector machine. Fig. 4.10, for the selected sensors show very similar results, thus indicating that most models with minimal pre-processing can accurately models the underlying data set.

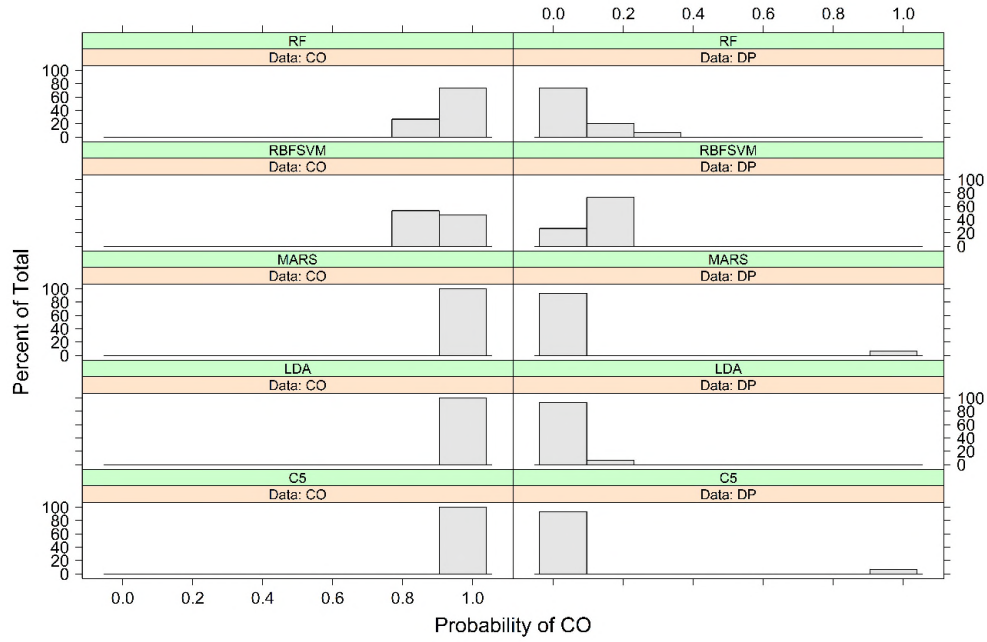


Fig. 4.9. Class probability histograms of different models for all sensors at ‘detection’ time point for healthy controls (‘CO’) and diseased potato tubers (‘DP’). The following models are represented: RBFSVM (Radial Basis Function Support Vector Machine), RF (Random Forest), MARS (Multivariate Adaptive Regression Splines), LDA (Linear Discriminant Analysis), C5 (C5.0 tree algorithm).

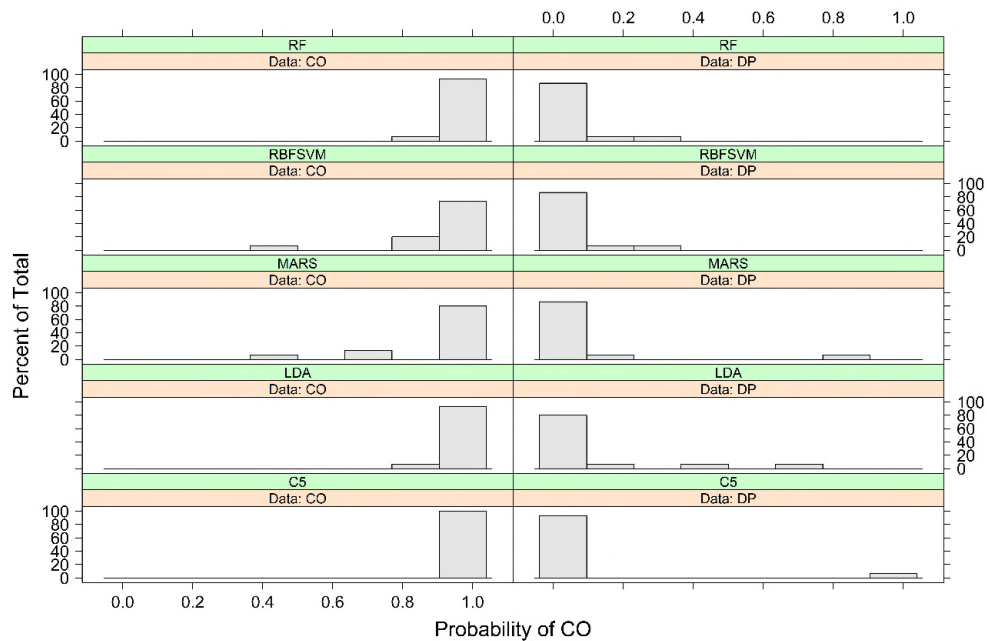


Fig. 4.10. Class probability histograms for selected sensors (SY.W, T30.1, and SY.gcT) at time point ‘detection’. Legend and notation are as indicated in Fig. 4.9.

4.3.2 Metal oxide gas sensors response to ‘early detection’ time point

A similar approach to the one described above was carried out for the second time point, ‘early detection’. The experimental outcome is shown in Fig. 4.11 and Fig. 4.12 for all data points. As found previously, a smaller set of sensors can be selected for this detection time point (Fig. 4.13). For ‘early detection’, discrimination between healthy controls and infected tubers was achieved with variance related to the chemical substances identified previously with the later ‘detection’ time point. Further data analysis was also done by means of the features extracted using fewer sensors (SY.W, T30.1 and SY.gcT). For both time points, again various models were selected and comparison carried out across different techniques using the same resampling approach (k-fold cross validation). All of the modelling techniques showed very high accuracy, sensitivity and selectivity, with the positive class being the control tubers.

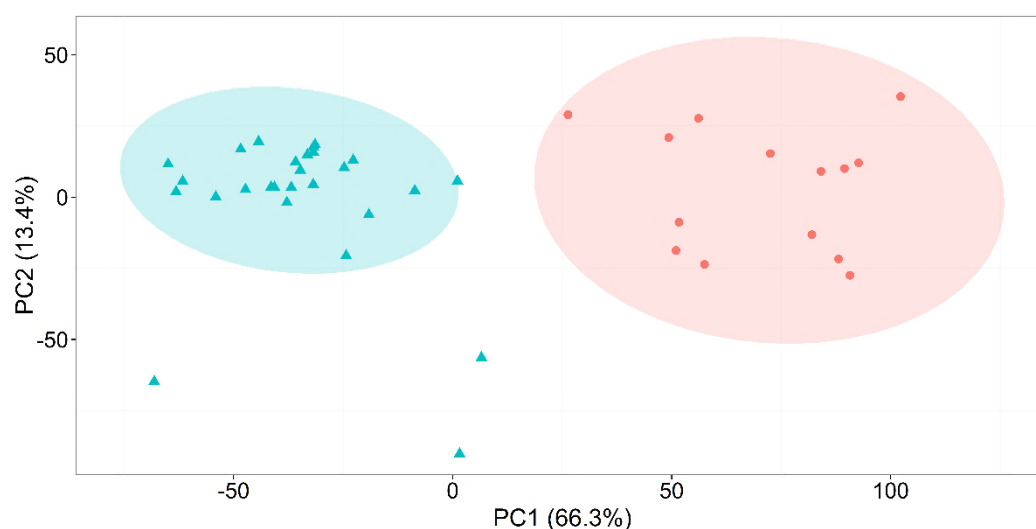


Fig. 4.11. PCA score and k-means plot with 95% confidence intervals based on CMOS technology measurements for all sensors at time point ‘early detection’. Data points indicate healthy controls (cyan, triangles) and diseased potato tubers (red, circles).

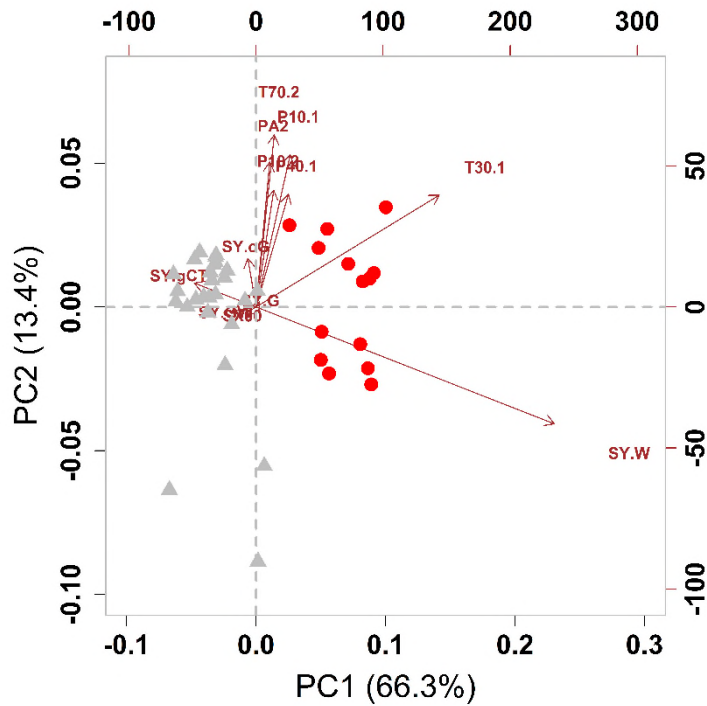


Fig. 4.12. Biplot for all sensors at time point 'early detection'. Data points indicate healthy controls (grey, triangles) and diseased potato tubers (red, circles).

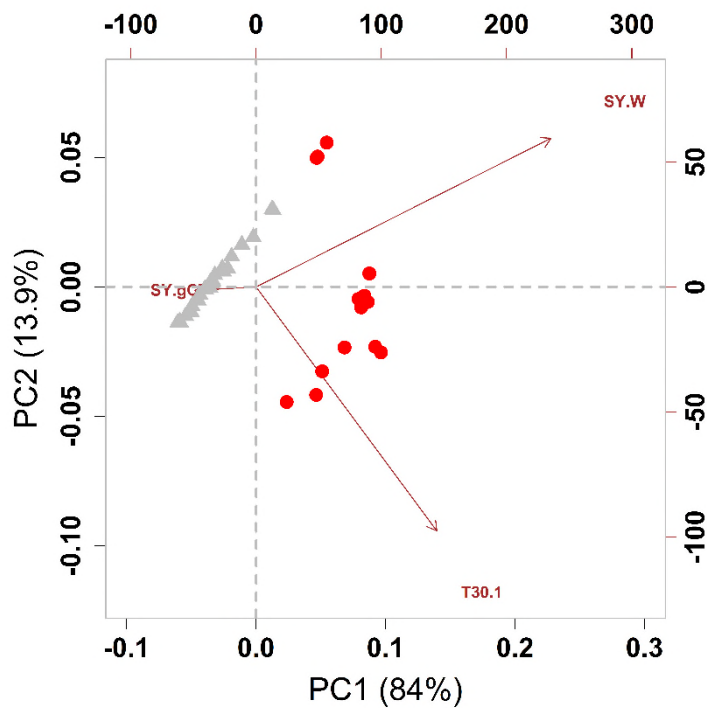


Fig. 4.13. Biplot for selected sensors (SY.W, T30.1, SY.gCT) at time point 'early detection'. Data points are as indicated in Fig. 4.12.

In Table 4.5 are reported the values for sensitivity and selectivity metrics of the confusion matrix across all models and for the selected time point.

	C5	LDA	MARS	RBFSVM	RF
Sensitivity ('all sensors')	100%	100%	100%	100%	100%
Specificity ('all sensors')	80%	80%	100%	100%	100%
Sensitivity ('selected sensors')	80%	100%	100%	100%	100%
Specificity ('selected sensors')	80%	80%	80%	80%	80%

Table 4.5. Confusion matrices metrics for the selected time point 'early detection'.

Fig. 4.14 and Fig. 4.15 illustrate the class probabilities for the second time point. However, unlike in the previous section covering 'detection', here the histograms for the model C5 and RF show a degraded performance while LDA, and radial basis function SVM appear to be the best suited as a models for this time point. An important consideration for both time points and both set of sensors is that all parameters have been kept within the same range across all models, which implies that a model performance could be improved by appropriate variable selection.

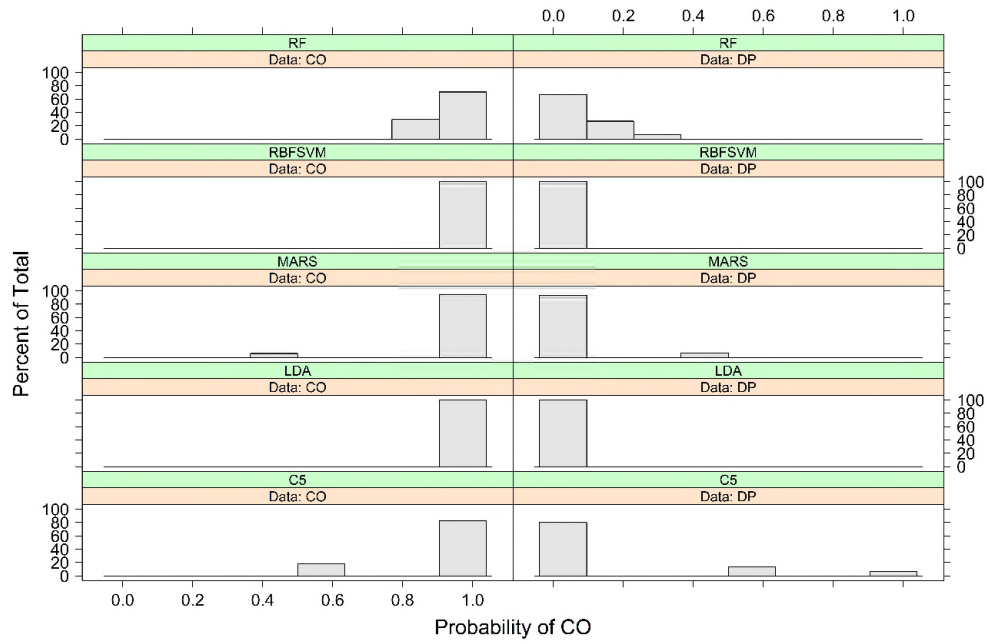


Fig. 4.14. Class probability histograms of different models for all sensors at ‘early detection’ time point for healthy controls (‘CO’) and diseased potato tubers (‘DP’). The following models are represented: RBF SVM (Radial Basis Function Support Vector Machine), RF (Random Forest), MARS (Multivariate Adaptive Regression Splines), LDA (Linear Discriminant Analysis), C5 (C5.0 tree algorithm).

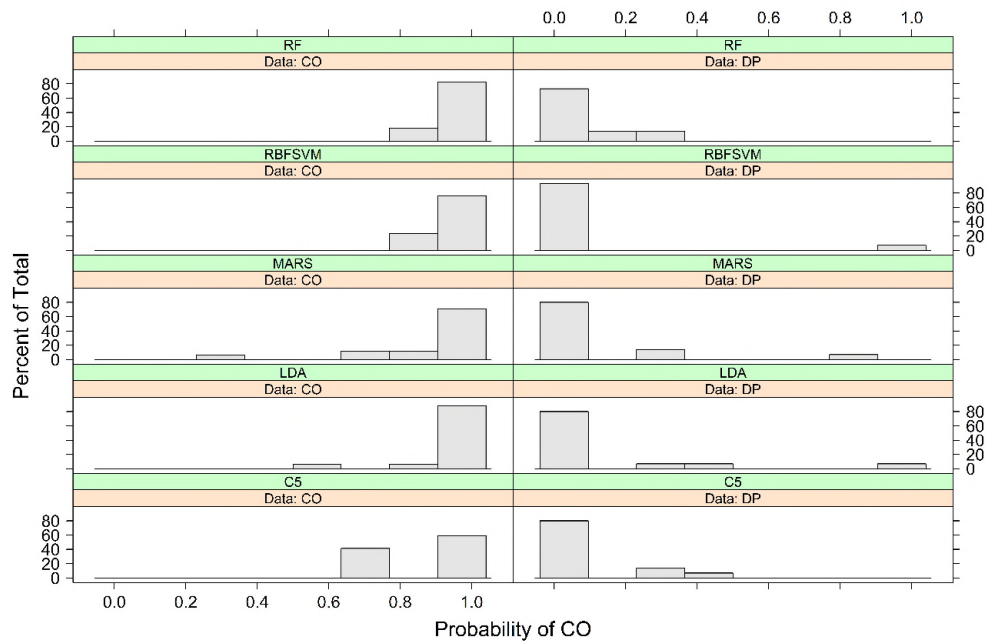


Fig. 4.15. Class probability histograms for selected sensors at time point ‘early detection’. Legend and notation are as indicated in Fig. 4.14.

4.3.3 Electrochemical/NDIR gas sensors response to ‘detection’ time point

As in previous section for metal oxide sensors, Fig. 4.16 shows a bar plot with cumulative values for the extracted features from all sensors and for both the time points ‘detection’ and ‘early detection’.

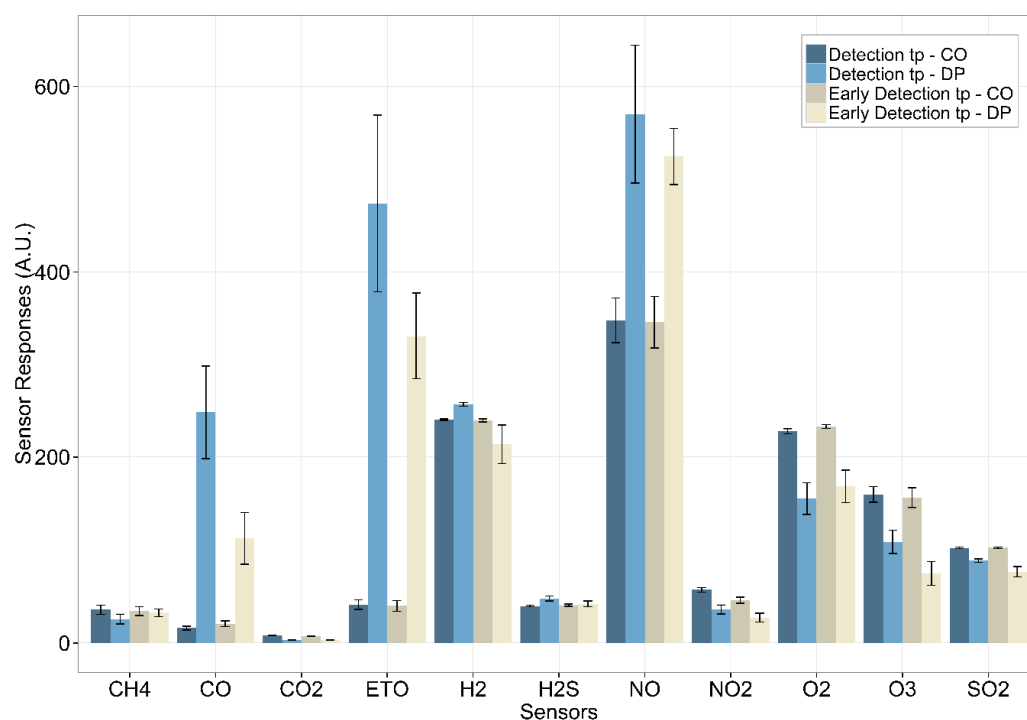


Fig. 4.16. Bar plot of raw data indicating differences in responses for all sensors at two time points (‘tp’). ‘CO’ indicates healthy controls and ‘DP’ to diseased potato tubers. The error bars represent standard errors of the mean values. The sensors nomenclature refers to the chemical compounds to which sensors are responsive.

Fig. 4.17 (PCA scores and k-means for time point ‘detection’) indicates the features extracted for all the raw sensors data while Fig. 4.18 is the equivalent biplot for the first two principal components, which accounts for most of the predictor’s variance in the data set, as in previous cases. The biplot indicates that most of the variance in the data set can be attributed to a three sensors, namely carbon monoxide (CO) ethylene oxide (ETO) and nitric oxide (NO). None of these chemicals were identified by other

researchers in past studies with the use of GCMS (Kushalappa, Lui, Chen, & Lee, 2002; Lui et al., 2005; Varns & Glynn, 1979). Of particular interest is the relative abundance of carbon monoxide in the presence of tubers infected with soft rot. The final results for the subset of sensors, which have been selected as representative of a potential detection system for soft rot, are shown in Fig. 4.19.

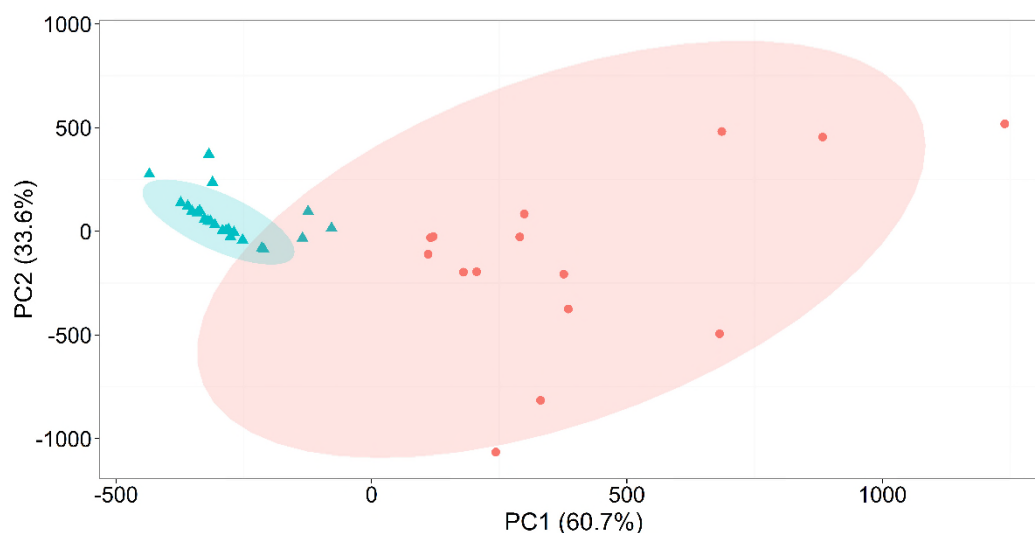


Fig. 4.17. PCA score and k-means plot with 95% confidence intervals based on electrochemical gas sensors technology measurements for all sensors at time point 'detection'. Data points indicate healthy controls (cyan, triangles) and diseased potato tubers (red, circles).

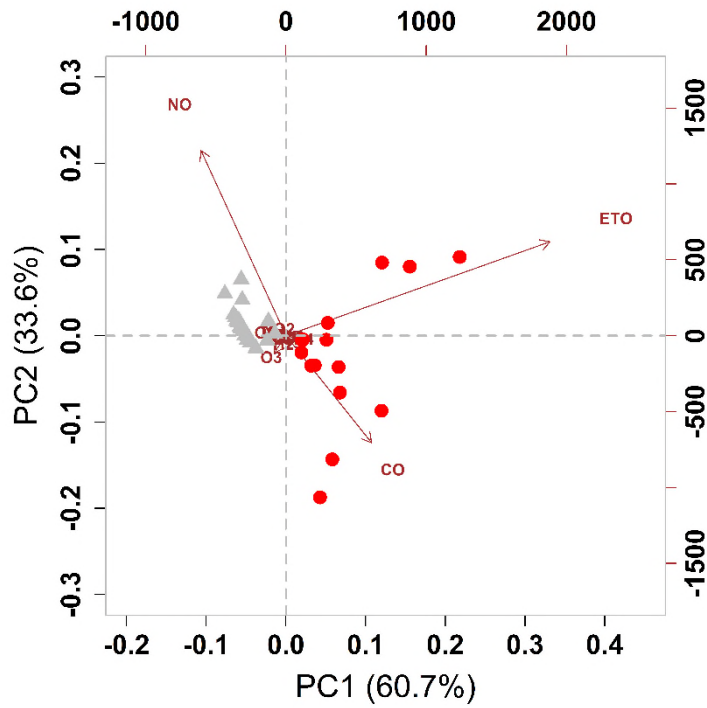


Fig. 4.18. Biplot for all sensors at time point 'detection'. Data points indicate healthy controls (grey, triangles) and diseased potato tubers (red, circles).

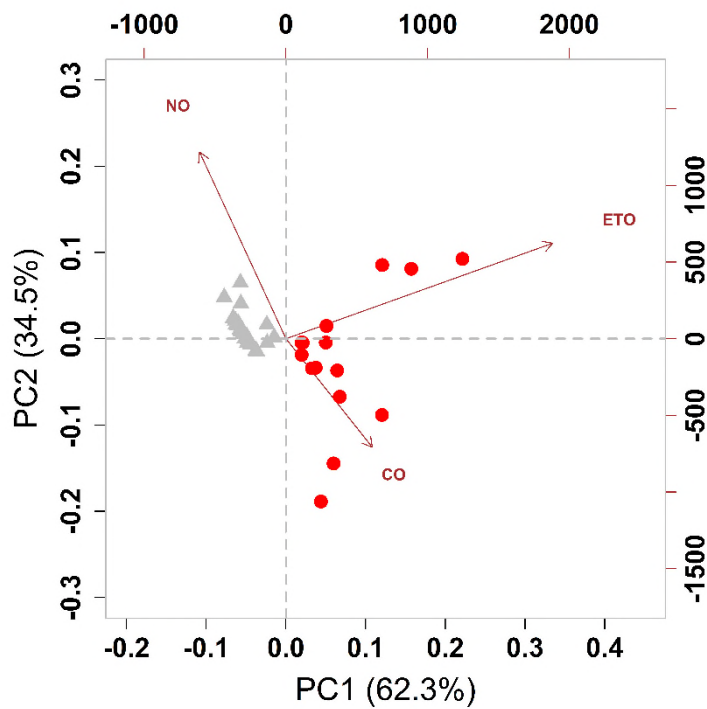


Fig. 4.19. Biplot for selected sensors (CO, ETO, NO) at time point 'detection'. Data points are as indicated in Fig. 4.18.

For modelling, the data was split into 75% for training and 25% for testing (stratified random splits) and cross validation was carried out with a k fold of 10 (as in the case of metal oxide sensors). In Table 4.6 are reported the calculated values for sensitivity and specificity of the confusion matrix across all models and for the selected time point.

	C5	LDA	MARS	RBFSVM	RF
Sensitivity ('all sensors')	100%	100%	100%	100%	100%
Specificity ('all sensors')	100%	100%	100%	100%	100%
Sensitivity ('selected sensors')	60%	100%	100%	100%	80%
Specificity ('selected sensors')	100%	80%	100%	100%	100%

Table 4.6. Confusion matrices metrics for the selected time point 'detection'.

Fig. 4.20 and Fig. 4.21 show histograms of class probabilities for all sensors and the selected subset (CO, ETO, NO) respectively. All histogram bins in Fig. 4.20 indicate very high probability of control ('CO') being control (left part of the graph) and very low probability of diseased tuners being controls (right part of the graph). This indicate this indicate that all techniques (similar starting conditions and pre-processing) can be employed as suitable models for the data set compromising the whole set of sensors. A lesser degree of model performance can be found in Fig. 4.21, for the selected sensors thus indicating that other sensors may contribute in minor part to disease identification.

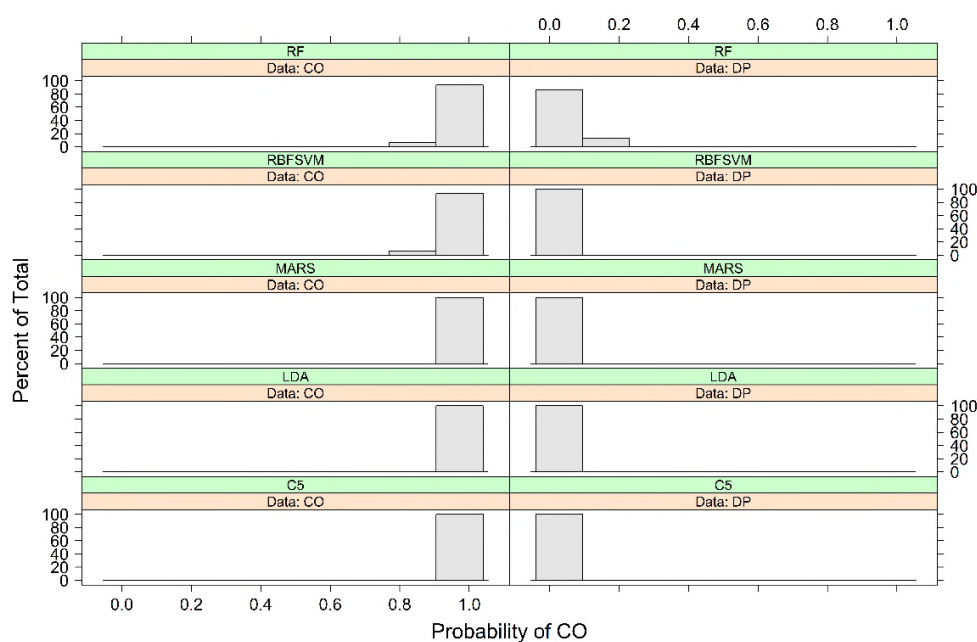


Fig. 4.20. Class probability histograms of different models for all sensors at ‘detection’ time point for healthy controls (‘CO’) and diseased potato tubers (‘DP’). The following models are represented: RBFSVM (Radial Basis Function Support Vector Machine), RF (Random Forest), MARS (Multivariate Adaptive Regression Splines), LDA (Linear Discriminant Analysis), C5 (C5.0 tree algorithm).

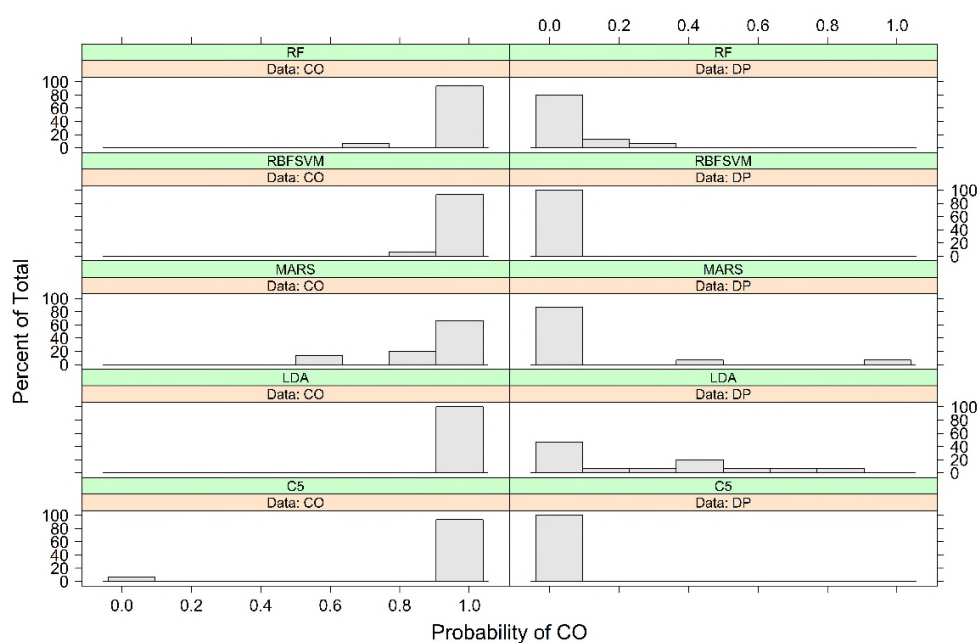


Fig. 4.21. Class probability histograms for selected sensors (CO, ETO, and NO) at time point ‘detection’. Legend and notation are as indicated in Fig. 4.20.

4.3.4 Electrochemical/NDIR gas sensors response to ‘early detection’ time point

The experimental outcome for the second time point, ‘early detection’ is shown Fig. 4.22 and Fig. 4.23 for the whole data set. As in the previous case, sensors were shortlisted and they are reported in Fig. 4.24. These sensors are carbon monoxide (CO), ethylene oxide (ETO) and nitric oxide (NO). For both ‘detection’ and ‘early detection’ these three sensors yield the same discrimination between healthy controls and infected tubers, albeit with a varying degree of variance related to the accumulation of chemical substances related to disease progression. For both time points, various models were also selected and comparison carried out across various models and by employing the same resampling approach (k-fold cross validation). All of the models showed very high accuracy, sensitivity and selectivity, with the control tubers being the positive class.

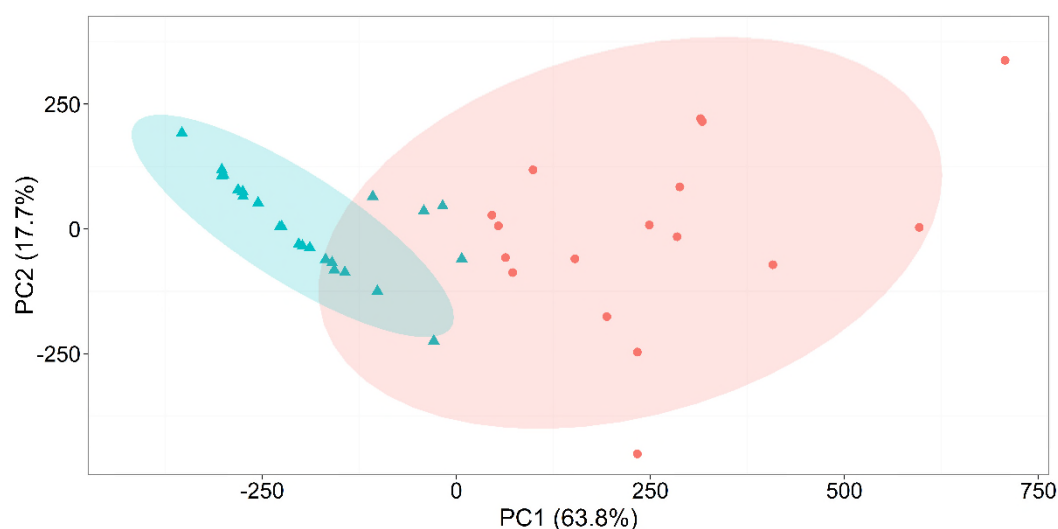


Fig. 4.22. PCA score and k-means plot with 95% confidence intervals based on electrochemical gas sensors technology measurements for all sensors at time point ‘early detection’. Data points indicate healthy controls (cyan, triangles) and diseased potato tubers (red, circles).

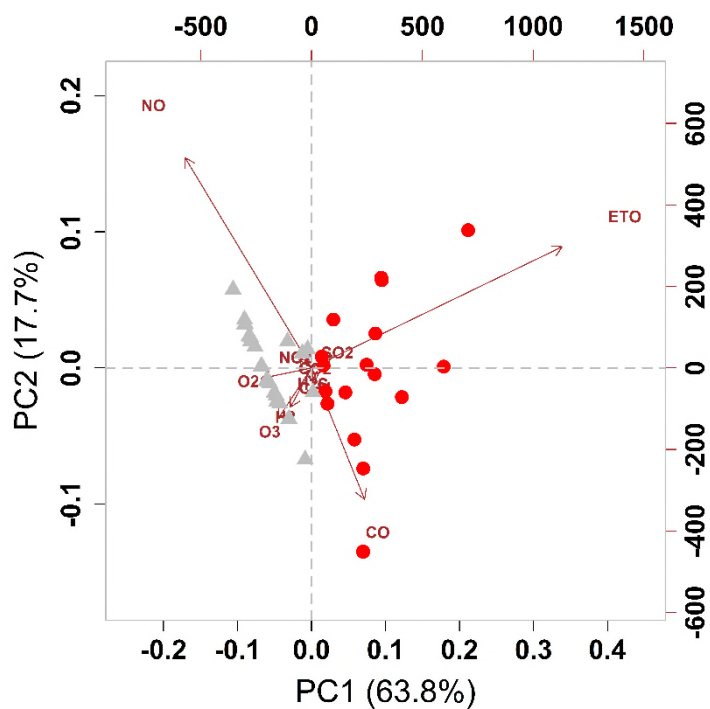


Fig. 4.23. Biplot for all sensors at time point 'early detection'. Data points indicate healthy controls (grey, triangles) and diseased potato tubers (red, circles).

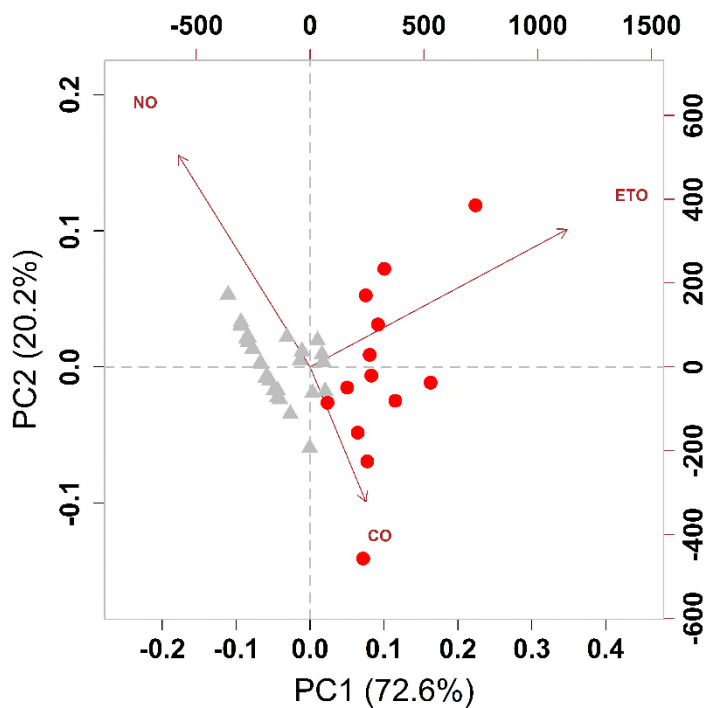


Fig. 4.24. Biplot for selected sensors (CO, ETO, NO) at time point 'early detection'. Data points are as indicated in Fig. 4.23.

In Table 4.7 are reported the calculated values for sensitivity and other metrics of the confusion matrix across all models and for the selected time point.

	C5	LDA	MARS	RBFSVM	RF
Sensitivity ('all sensors')	60%	100%	80%	80%	100%
Specificity ('all sensors')	100%	100%	100%	100%	100%
Sensitivity ('selected sensors')	60%	100%	80%	80%	80%
Specificity ('selected sensors')	100%	100%	100%	100%	100%

Table 4.7. Confusion matrices metrics for the selected time point 'early detection'.

Fig. 4.25 and Fig. 4.26 illustrate the class probabilities for 'early detection'.

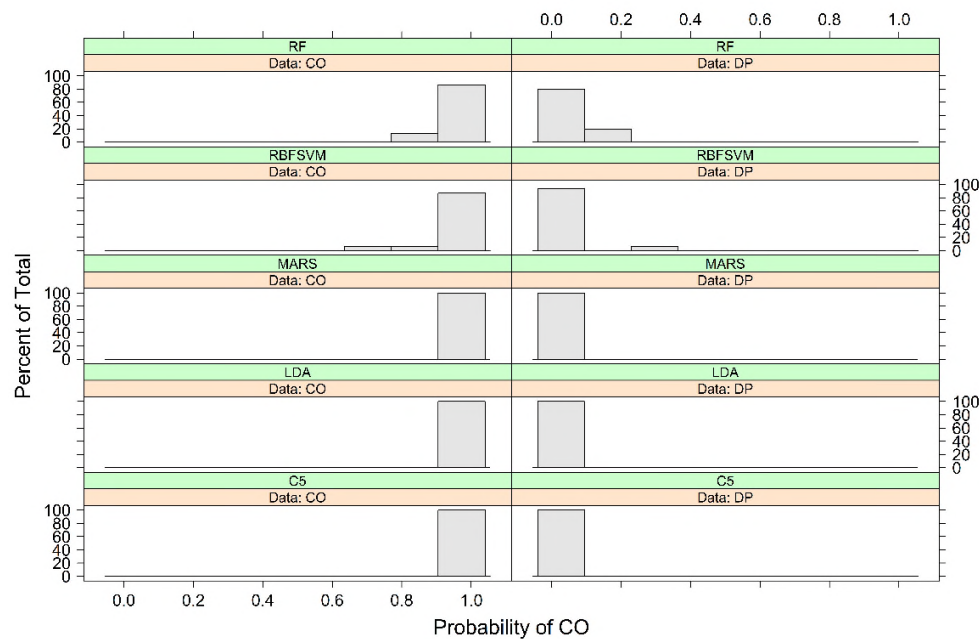


Fig. 4.25. Class probability histograms of different models for all sensors at 'early detection' time point for healthy controls ('CO') and diseased potato tubers ('DP'). The following models are represented: RBFSVM (Radial Basis Function Support Vector Machine), RF (Random Forest), MARS (Multivariate Adaptive Regression Splines), LDA (Linear Discriminant Analysis), C5 (C5.0 tree algorithm).

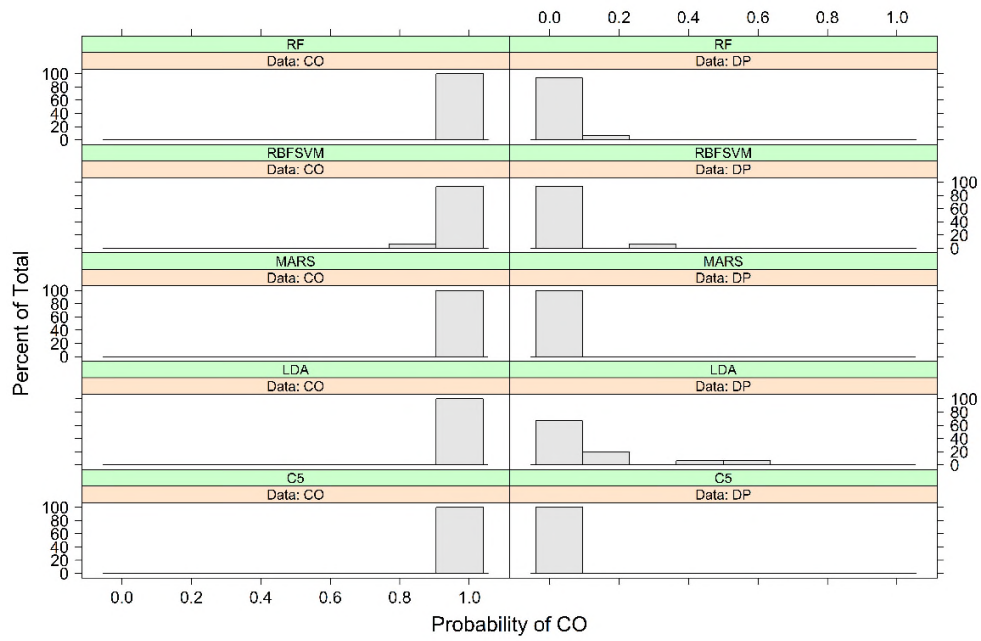


Fig. 4.26. Class Probability histograms for selected sensors at time point 'early detection'. Legend and notation are as indicated in Fig. 4.25.

4.4 Discussion

To date, no reliable non-destructive method exists for the early detection and monitoring of potato soft rot in stores. It has been determined that gas analysis may provide a potential solution by using a MOX based electronic nose as a viable practical approach to address this problem. In fact, results show that commercially available and cost-effective MOX (metal oxide) sensor technology is able to discriminate healthy controls from tubers infected with *P. carotovorum*, the most widespread pathogen affecting potatoes in storage. Detection of soft rot infection under selected laboratory conditions was achieved for samples at 5 and 2 days post inoculation, with similar results in both cases. In the former case, it was shown that the electronic nose is as good as current store practices for detecting soft rot symptoms. Furthermore, for the second time point it has been ascertained that, when no symptoms are identifiable by sensorial analysis (olfaction, tactile or visual inspection), the instrument results in good discrimination between healthy controls and infected tubers and is therefore valuable for early detection of soft rot disease.

In the past forty years, focus has been on the identification and quantification of chemical compounds as possible biomarkers of disease presence and progression. Results of the current experimental work appear to suggest that recognition of soft rot, or for any other potato disease that may result in similar tissue breakdown and decay, is likely to be related to sensors detecting degradation of organic material rather than specific compounds associated with the infection itself. This conclusion is drawn by the substances likely candidates, which may be generally associated with changes in organic tissue composition, in a manner similar to landfill gas emissions. Hence these sensors may be useful in the detection of a range of potato storage diseases that result

in release of such general biomarkers of infection but may not be able to specify either the pathogen causing the problem or the disease of interest. This anaerobic fermentation may be closely related to the main constituent of potato tubers (besides water) namely starch.

While the research on the chemical fingerprint, commenced by Varns and Glynn (Varns & Glynn, 1979), may well offer a valuable quantitative analytical perspective, it suffers from the difficult task of dealing with the large number of compounds involved and their variation with environmental conditions that a crop produces prior and after harvest (Dixon et al. 2002; Fiehn 2002; Wilson & Wisniewski 1989). A corollary of the above consideration is that a sensor (or more) should be able either to measure effectively an increase in either VOC or specific families of compounds.

This dichotomy has been partially addressed in the previous study with FAIMS and PID where data indicated that soft rot can be detected regardless of the possible chemical emissions involved. A similar approach has been followed by de Lacy Costello *et al.* (de Lacy Costello et al. 2000), who claimed that the best biomarker for determination of soft rot inception is a general increase in VOC (volatile organic compounds) in the headspace over infected potato tubers, rather than in any specific chemical compound, as also shown in the previous chapter.

However, the same authors claim that in their antecedent study (de Lacy Costello et al. 1996) ethanol was not found to be disease specific while ammonia accompanied progression of disease. As it has been shown in this piece of work, one of the sensor that appears responsive and disease specific is the one for ethanol/alcohols. However, no argument, investigation or experimental evidence was presented with regard to an increased need in sensitivity which would justify fabrication and deployment of

custom-made sensors. Nevertheless, at least at given simulated experimental conditions, the authors show that in general metal-oxide technology can be employed for detection of soft rot. Under this light, a commercially available metal oxide VOC sensors could be deployed in addition to the already selected subset.

However, further and thorough experimental results with commercial metal oxide sensors have shown that target compounds of chemical families could be potentially employed for soft rot monitoring either for different degree of VOC concentration (between controls and infected tubers) or as unique markers, as in the case of alcohols. Furthermore, this is the first time that commercial electrochemical gas sensors been employed for monitoring potato disease spread and specific compounds have been found to be associated to soft rot progression, in particular with regard to large quantities of carbon monoxide. The presence of carbon monoxide raises the issue not only of financial losses but also of health and safety in food storage for farmers.

The data analysis method presented here can be broadly classified into three parts: average estimation of sensors responses, unsupervised exploratory techniques to explore variance and models of the data set. Data pre-processing has been kept to a minimum for all models (only centring and scaling have been applied). More insight has been provided by considering both loadings and principal component scores in the same graph, by which distribution of variance could be gauged and a subset of the original sensor array could be easily selected.

A general approach for model selection has allowed to test the data set across a variety of models, by employing a set of similar standard conditions. To test the quality of different models, two approaches have been considered: class probabilities and confusion matrices. The predicted class generated by the classification comes in the

form of a discrete category and consequently the evaluation of class probabilities associated with the model is the first measure to gauge the model's confidence with regard to the predicted outcome. Furthermore, sensitivity, as a specific metric for evaluation of confusion matrix (cross-tabulation of the predicted and observed classes for the data set), allows for accurate control identification, thus making the system more robust and accounting for its inability to address other diseases. In conclusion, the predictive models also offer both more strength to previous analysis and a sound benchmark for evaluating under similar starting conditions different commercial sensors.

4.5 Conclusion

In this chapter it has been demonstrated that the two main commercial gas sensors technologies, namely metal oxide and electrochemical, can be successfully employed for pre symptomatic determination and monitoring of soft rot. The purpose of this work was to investigate an inexpensive, reliable and commercially viable alternative to FAIMS and PID sensors. Experimental results have shown that a few sensors could be deployed in a commercial potato store in the form of a network in order to monitor the facilities in a manner not possible with other approaches.

4.6 References

- Biondi, E., Blasioli, S., Galeone, A., Spinelli, F., Cellini, A., Lucchese, C., Braschi, I., 2014. Detection of potato brown rot and ring rot by electronic nose: from laboratory to real scale. *Talanta* 129, 422–30. doi:10.1016/j.talanta.2014.04.057
- de Lacy Costello, B.P.J., Evans, P., Ewen, R.J., Honeybourne, C.L., Ratcliffe, N.M., 1996. Novel composite organic/inorganic semiconductor sensors for the quantitative detection of target organic vapours. *J. Mater. Chem.* 6, 289. doi:10.1039/jm9960600289
- de Lacy Costello, B.P.J., Ewen, R.J., Gunson, H.E., Ratcliffe, N.M., Spencer-Phillips, P.T.N., 2000. The development of a sensor system for the early detection of soft rot in stored potato tubers. *Meas. Sci. Technol.* 11, 1685–1691. doi:10.1088/0957-0233/11/12/305
- Dixon, R.A., Achnine, L., Kota, P., Liu, C.-J., Reddy, M.S.S., Wang, L., 2002. The phenylpropanoid pathway and plant defence-a genomics perspective. *Mol. Plant Pathol.* 3, 371–90. doi:10.1046/j.1364-3703.2002.00131.x
- Fiehn, O., 2002. Metabolomics – the link between genotypes and phenotypes. *Plant Mol. Biol.* 48, 155–171. doi:10.1023/A:1013713905833
- Kuhn, M., Johnson, K., 2013. *Applied Predictive Modeling*, 2013th ed. Springer Science & Business Media.
- Kushalappa, A.C., Lui, L.H., Chen, C.R., Lee, B., 2002. Volatile Fingerprinting (SPME-GC-FID) to Detect and Discriminate Diseases of Potato Tubers. *Plant Dis.* 86, 131–137. doi:10.1094/PDIS.2002.86.2.131
- Lui, L.H., Vikram, A., Abu-Nada, Y., Kushalappa, A.C., Raghavan, G.S. V., Al-Mughrabi, K., 2005. Volatile metabolic profiling for discrimination of potato tubers inoculated with dry and soft rot pathogens. *Am. J. Potato Res.* 82, 1–8.

doi:10.1007/BF02894914

MacQueen, J., 1967. Some methods for classification and analysis of multivariate observations, in: Proceedings of the Fifth Berkeley Symposium on Mathematical Statistics and Probability, Volume 1: Statistics. The Regents of the University of California.

Mitrovics, J., 2009. MultiSensAnalyzer Version 0.99 Manual. Tübingen, Germany.

Pearson, K., 1901. LIII. On lines and planes of closest fit to systems of points in space. *Philos. Mag. Ser. 6* 2, 559–572. doi:10.1080/14786440109462720

Varns, J.L., Glynn, M.T., 1979. Detection of disease in stored potatoes by volatile monitoring. *Am. Potato J.* 56, 185–197. doi:10.1007/BF02853365

Wilson, C.L., Wisniewski, M.E., 1989. Biological Control of Postharvest Diseases of Fruits and Vegetables: An Emerging Technology*. *Annu. Rev. Phytopathol.* 27, 425–441. doi:10.1146/annurev.py.27.090189.002233

DATA LOGGER FOR ENVIRONMENTAL
ANALYSIS OF SOFT ROT VOCS

This page is intentionally left blank.

5 Data Logger for Environmental Analysis of Soft Rot VOCs

5.1 Introduction

In the previous chapters, it has been shown that a range of different gas detection technologies could be used for the detection of symptomatic (or even of pre-symptomatic) potato soft rot. Initial work with both FAIMS and the PID, proved to be simple and effective. Further work with discrete gas sensors formed into arrays (electronic noses) also yielded results that showed an accurate discrimination between controls and infected tubers. However, whilst the Lonestar FAIMS and Tiger PID instruments provided discriminative results based on either a specific fingerprint (FAIMS) or on overall volatile metabolites increase (PID), their cost point makes them more challenging to take forward into practical storage use. Fortunately, the electronic nose instruments uses an array of low-cost discrete sensors and the previous work yielded a shortlist of possible chemical families of interest (and relevant sensors). Furthermore, it is possible to use a discrete PID sensor and combine it with the other gas sensors shortlisted from the electronic noses study and then assemble this into a dedicated purpose-built system for storage monitoring.

Based upon these premises, a dedicated instrument was developed for use within both laboratory and storage facilities, using the specific sensors previously identified. This is the first time that this combination of sensors have been used together for the detection of potato infections. This chapter describes the design and construction of this instrument.

5.2 List of requirements

The first consideration in any engineering design is to draft a set of requirements and (functional) specifications. The requirements indicate a broad set of needed features whilst the specifications tend to be more detailed account of what is required (although a number of engineers use both terms interchangeably). A basic list of requirements (although with some details) is given below.

The instrument to be built will have the characteristics as indicated below:

- A power supply PCB (printed circuit board) to operate all other components within the instrument according to the following:
 - To be operated by 240V AC mains via a standard PC (personal computer) PSU (power supply unit) with a variable output voltage range, depending on cost and availability.
 - To be rated for a current draw across of the approximate requirement for the whole system (based on preliminary work, 5 A may be an indicative figure).
 - To be able to accommodate various output voltages ranges for the other parts of the system, according to need. These voltage ranges may be modified at a later date. Indicative initial voltages may be set at 12 (or 24) V for pneumatic components and 5 (or 3.3) V for digital integrated circuits.
 - A number of outlets for connection that exceeds the initial estimation of device parts to be supplied.

- Sensors and interfacing circuitry to collect data about VOCs under both laboratory and potato store environmental conditions according to the following:
 - Metal oxide gas sensors have to be employed and are as indicated in previous work (chapter 4). This will include alcohols, hydrocarbons, VOC. Other MOX sensors could also be added.
 - Electrochemical gas sensors have to be employed and are as indicated in previous work (chapter 4). This will include NO (nitric oxide), CO (carbon monoxide), ETO (ethylene oxide).
 - A PID sensor will also be employed to assess this technology for VOC determination in a real world environment as indicated in previous work (chapter 3).
 - A CO₂ gas sensor will be employed to monitor the respiratory cycle of tubers. This will have to be selective and robust to harsh environmental conditions.

- Air flow delivery part of the instrument will have to supply sample air in a reliable manner to the sensors chambers according to the following:
 - Valves will have to be controlling air for the estimated number of samples plus some redundancy.
 - Pump will need to be able to supply up to a 1L/min of air flow.
 - Valves and pumps will be controlled electronically from the microcontroller.

- A main board PCB to control the whole system according to the following:

- Core of the PCB will be based on an established and mature microprocessor rather than performance.
 - Additional components will be needed in order to accommodate real-time clock data to be associated as timestamps to sensor data and SD (secure digital) card for data storage and retrieval.
 - All signal processing, for which hardware is not strictly required, will be achieved whenever possible by firmware.
 - A user interface display of reasonable size (3.2”) for qualitative and prompt data logger diagnostics.
-
- All parts will be to be easy to source and to repair with limited costs and placed in a protected enclosure with ease of access as a prime criterion.

5.3 System architecture

In accordance with the list of requirements, the architecture for the data logger has been laid out and is indicated in the block diagram in Fig. 5.1. This architecture comprises the following system components:

- A power supply PCB (printed circuit board) as indicated in section 5.4.1.
- A PCB for MOX (Metal Oxide) sensors, EC (Electrochemical) sensors, PID (Photoionization Detection) and IR (infrared for CO₂) sensors, as outlined in section 5.4.2.
- An air flow delivery and PCB, as reported in section 5.4.3.
- A main control PCB and display as in section 5.4.4.

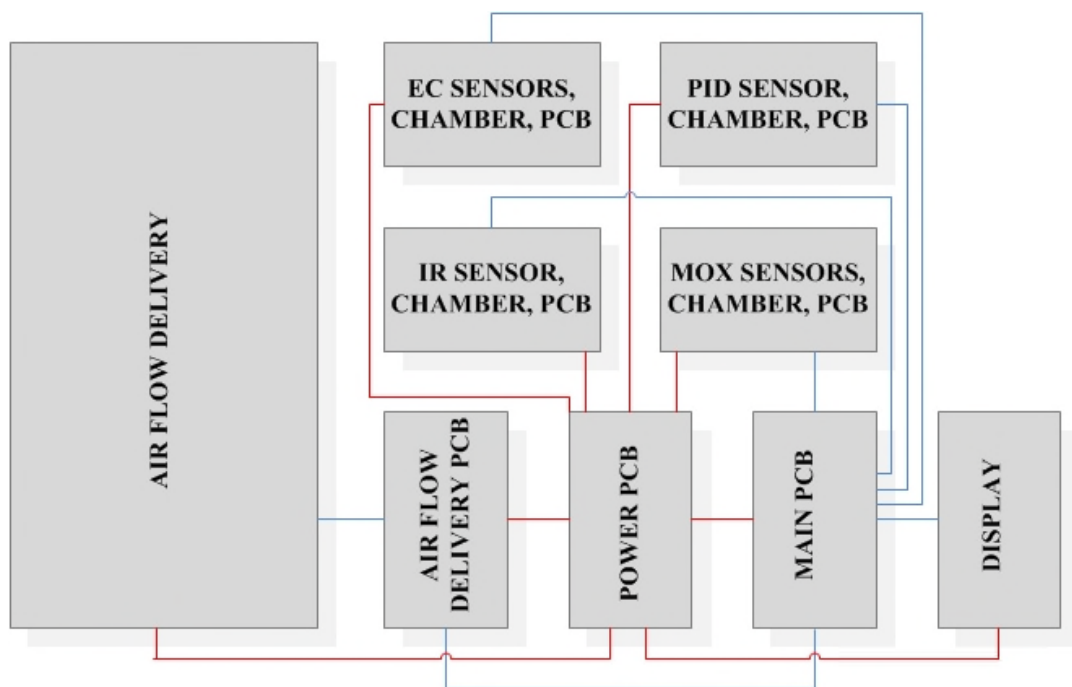


Fig. 5.1. Block diagram of system architecture. In red the power bus and in cyan the data bus respectively.

5.4 System components

5.4.1 Power supply

The power PCB (printed circuit board) unit is designed to be based on mains since this will allow to constant operation the instrument. Moreover, the instrument will also be able to accommodate increases in energy consumption through additional boards, sensors and other parts or components that may be needed in the course of experimental work. The unit is connected to an external DC (direct current) power supply that can tolerate an input voltage range of 9 to 18 V and it is rated at maximum current of 5 A (Multicomp Electronic Components Inc, 2012). Energy supply from the mains can be provided via two connectors, either directly wired to a bench power supply (for testing purposes) or to a portable power supply (for data logging application). In order to avoid or minimise improper function, disruption or permanently damage of the entire data logger related to supply, Traco Power THN 15 Series DC/DC (direct current to direct current) converters have been used. These offer output over-voltage, over-current, short-circuit protection and isolation between input and output (Traco Electronics AG, 2009). A PCB layout for the board is shown in Fig. 5.2. The PCB has a 4 slots for the THN 15 power modules. External passive components (filters) are as required by the European Union limits on radio disturbance characteristics for technology equipment (directive EN55022) and as suggested by the manufacturer (Traco Electronics AG, 2009). In the configuration chosen here, the power unit can provide constant accurate voltages for four 2-way header connectors at 12 V, four at 5 V (or 3.3 V) and two at 10 V. Each Traco TH15 at 12V can supply up to 1.3 A, while the 5 V version up to 3 A. The 10V supply feature is implemented via a common adjustable linear voltage regulator IC, the LM317, capable of supplying up to 1.5 A. Voltage regulators (such as the LM317) are generally inefficient if

compared to converters (such as the Traco THN15). The rationale for the LM317 is to accommodate a variable voltage source (via a potentiometer, as shown in the circuit in Fig. 5.3). In fact, variable voltage output was not available from the THN15 converters (the trim voltage option for these cannot provide the required voltage). Because of this inefficiency, the LM317, like all voltage regulators generates heat. The larger the difference between the input and output voltages, the more heat is produced and this has to be dissipated by a heatsink, also included in the design.

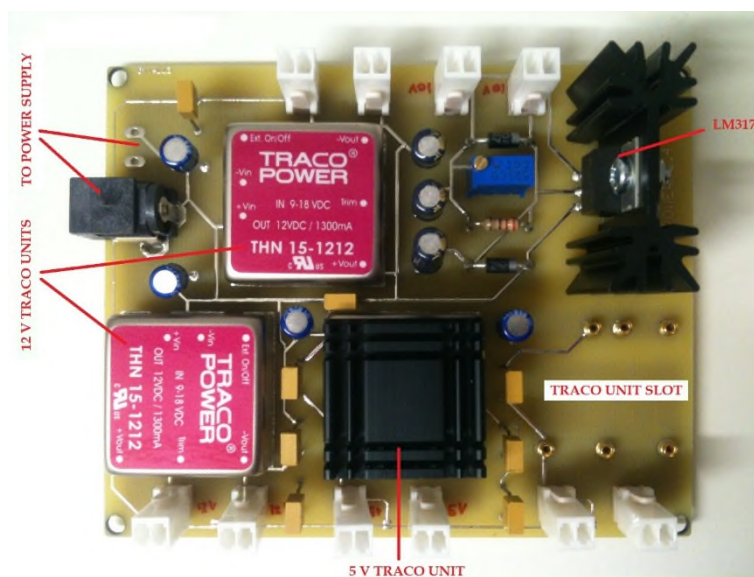


Fig. 5.2. Power supply unit PCB layout.

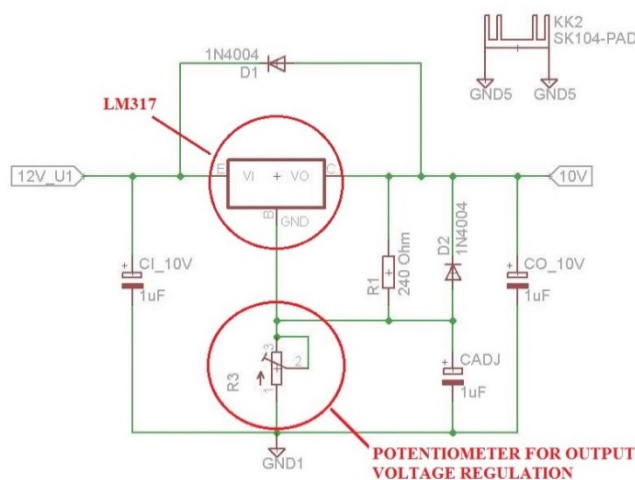


Fig. 5.3. LM317 support circuitry for desired voltage output, achieved by varying the 10 k potentiometer R3 (Texas Instruments Inc, 2014).

5.4.2 Sensors and data acquisition

5.4.2.1 Sensor selection

From the experimental work, a sensor shortlist for inclusion in a data logging unit for pre-symptomatic soft rot monitoring can be created. Among the array are metal-oxide sensors for detecting alcohols and hydrocarbons. The major worldwide supplier of MOX gas sensors is Figaro Engineering Inc., although other companies have commercialised this technology. Ready availability of parts has been the major factor while choosing this manufacturer. Moreover, no detailed information is provided by AlphaMOS with regard to the sensors present in the FOX3000 electronic nose. Figaro Engineering Inc. has also been in operation for decades pioneering the field (the founder of Figaro, Naoyoshi Taguchi designed the first of these type of sensors). The company manufactures sensors that can be matched to previous experimental studies, namely the TGS 2620 for alcohols, the TGS 2611 and TGS 2610 for hydrocarbons (Figaro Engineering Inc, 2014, 2013a, 2013b). TGS2620 is meant to replace T30.1 for alcohols and TGS 2611 for SY.W for hydrocarbons. TGS 2611 comes in two versions, one equipped with filter (TGS2611-E00) that is reported to eliminate the influence of interference gases and is highly selective to methane and one without filter, which can be employed for use in detection of hydrocarbons (Figaro Engineering Inc, 2013a). TGS 2610 covers the specific niche of industrial hydrocarbons LP (liquefied petroleum) gases, namely propane and butane (by use of a specific filter). This latter sensor will not be employed for this work due to its low specificity to the target chemical compounds. Furthermore, the supplier also manufactures sensors reported for general VOC detection, namely the TGS 2602 (Figaro Engineering Inc, 2015a).

In an early study, ammonia was also reported as associated to tubers infected with soft rot (de Lacy Costello et al., 1999). Hence this sensor has been included in the metal

oxide sensor array. However, these are from another well-established Japanese manufacturer, FIS Inc. The reason for selection of the FIS ammonia sensor SP-53B-00 (FIS Inc., 2007) is motivated by the power consumption, heating cycle and cost. In fact, the alternative Figaro Ammonia sensor TGS2444 has a 250 ms time interval for the heating cycle (thus requiring an additional control line, unlike the FIS sensor), and has a retail cost per unit of £ 60.23 (while the SP-53B-00 has a cost of £9.85).

With regard to the electrochemical gas sensors, three have been shortlisted from previous results obtained with the WOLF 4.1: these are NO (nitric oxide), ETO (ethylene oxide) and CO (carbon monoxide). All of these have been sourced at Alphasense Ltd (Alphasense Ltd, 2016a, 2016b, 2016c). Other manufacturers are present in the market that could have provided this type of technology, but this UK-based manufacturer was selected for availability of parts and to minimise servicing costs.

Alphasense manufactures the PID-AH with a dynamic range from 1 to 50 ppm and PID-A1 with a 100 ppb to 6,000 ppm (Alphasense Ltd, 2016d). PID-AH will be initially used with this work, and if needed it will be replaced with the wider range version.

In chapter 3, a CO₂ NDIR sensor yielded no results for discriminating infected tubers from controls. However, CO₂ could be an indicator of metabolic activity of potato tubers (as previously indicated in the study by Ouellette, in chapter 2). More, in previous work, dynamic headspace sampling was employed while in this work static headspace sampling, i.e. accumulation of volatiles, over time will be the main procedure. Hence, accumulation of CO₂ in the environment surrounding potato tubers may be associated to the increased respiratory rate due to presence of soft rot or, more

in general, to potato tuber tissue decomposition. The sensor chosen (Cirius 2) for inclusion in the data logger is manufactured by Clairair Ltd (Clairair Ltd, 2010). The manufacturer is highly specialised in providing a range of infrared detectors solutions and sourcing of product has been made for ease of acquisition and servicing.

A complete list for the above sensors is reported in listed in Table 5.1.

Sensed	Part Number	Manufacturer	Gas sensing type
Alcohols	TGS2620	Figaro Engineering Inc	MOX
Ammonia	SP-53B-00	FIS Inc	MOX
Carbon Monoxide	CO-A4	Alphasense Ltd	EC
Carbon Dioxide	Cirius 2	Clairair Ltd	NDIR
Ethylene Oxide	ETO-A1	Alphasense Ltd	EC
Hydrocarbons	TGS2611-C00	Figaro Engineering Inc	MOX
		Figaro Engineering Inc	MOX
Methane	TGS2611-E00	Figaro Engineering Inc	MOX
Nitric oxide	NO-A1	Alphasense Ltd	EC
Temperature/RH	SHT15	Sensirion AG	-
VOCs (non-specific)	TGS2602	Figaro Engineering Inc	MOX
VOCs (non-specific)	PID-AH	Alphasense Ltd	PID

Table 5.1. List of sensors in alphabetical order by sensed variable. MOX refers to metal oxide, EC to electrochemical and PID to Photoionization Detection.

5.4.2.2 Sensor interfacing

Metal oxide based gas sensors (Fig. 5.4) and a combined RH (relative humidity) and temperature sensor have been placed on the same PCB board. However the interfacing circuitry for the two types of sensors are different. The MOX are operated by two power loops (from supply to ground), one for the heater and the other for the sensing element. The electrical resistance of the sensing element R_s is dependent upon the amount of volatiles that come into contact with its substrate, thus generating a change

in voltage that can be harnessed through a potential divider. This can be achieved with a load resistor R_L in series with R_s (circuit schematic in Fig. 5.5). By rearranging the potential divider formula for the circuit, the value for the load resistance can be found. As stated also by the manufacturer, a value of circa 400 Ohms is the minimum value recommended. (Figaro Engineering Inc, 2005a, 2005b). Fig. 5.5 also shows output voltage across the load resistor versus gas concentration with various R_L values.

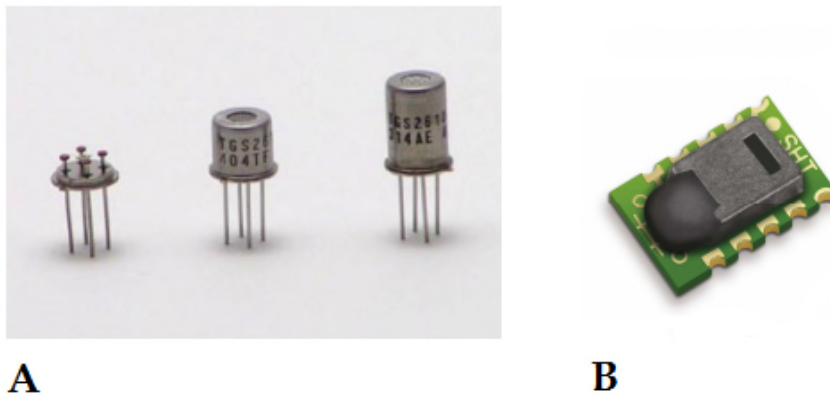


Fig. 5.4. From left to right in (A): uncapped sensing element for Figaro TGS2611 hydrocarbons (centre) and methane (the longer metal cap contains a filter material meant to be selective for the gas of interest), (Figaro Engineering Inc, 2013a). In (B), the temperature and relative humidity sensors SHT15 (Sensirion AG, 2011).

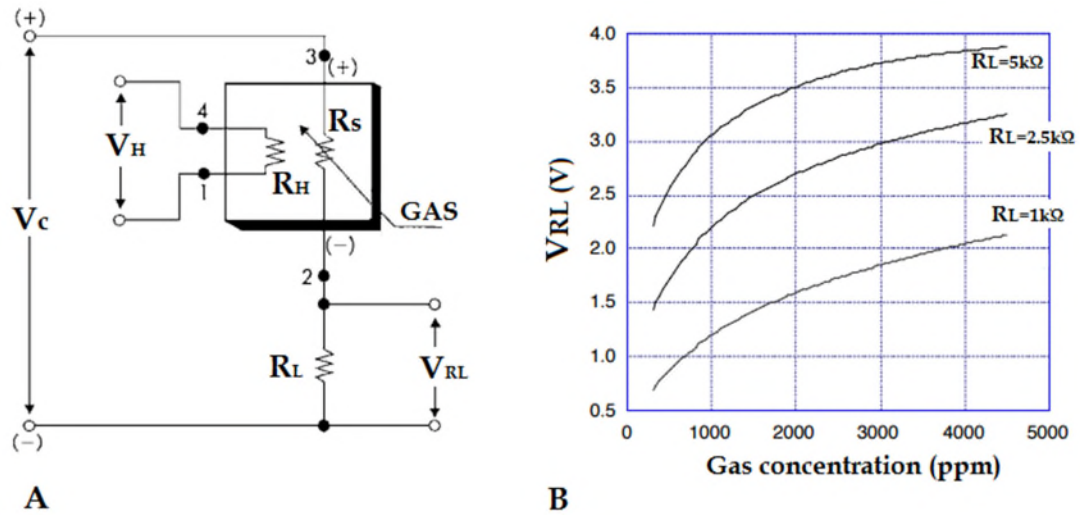


Fig. 5.5. Basic measuring circuit for a MOX sensor (A): V_C and V_H indicate the voltage applied to sensor element (R_S) and heater (R_H) respectively; R_L and V_{RL} indicate load resistance and voltage. Variation of output voltage for various values the load resistance (B), (Figaro Engineering Inc, 2005b).

The temperature and relativity humidity sensor selected for this application is the SHT15 from Sensirion AG. The component is the high end part of the SHT1x family and it has been found to be the most suitable for assembly on the MOX PCB board. Purpose of the sensor is to monitor environmental conditions inside the metal oxide sensors chamber. This is due to the dependency of these sensors on temperature and humidity, which for optimal performance have to be kept steady (Figaro Engineering Inc, 2015b, 2005b). Data from the part are collected via a digital 2-wire interface, one line for clock and the other for data. In Fig. 5.6 the PCB board is shown.

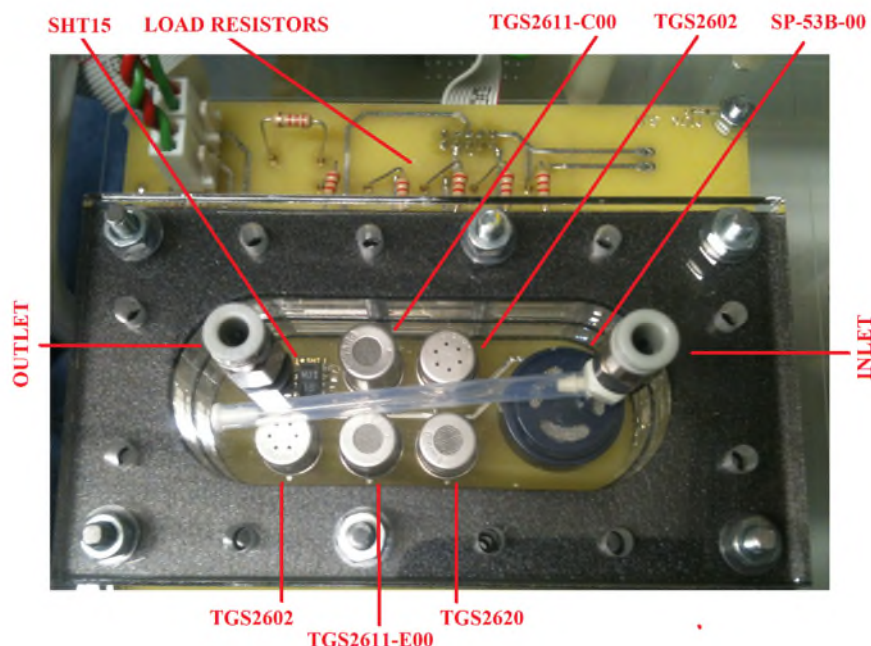


Fig. 5.6. Metal oxide gas sensors PCB and acrylic chamber (9 x 5 x 3 cm).

Results with the electrochemical sensors show that NO, CO, ETO (Fig. 5.7) may play an important role in symptomatic and pre-symptomatic detection of soft rot. However, this sensors require support circuitry, usually called the AFE (analogue frond end) interface. In this specific case, the main circuit needed for the application is also known as a potentiostat, or sensor bias circuit (an example is shown in Fig. 5.8). Such a concept can be elucidated more readily by the use by one of the target sensors. For example, when carbon monoxide is present at the chemical cell, hydrogen ions are generated and these migrate to the counter electrode (CE), thus leaving negative charge on the working electrode (WE). The current then flows from WE into the transimpedance amplifier, which converts current into a voltage (Texas Instruments Inc, 2013). A potentiostat circuit for gas analysis is also available from Alphasense Ltd (Fig. 5.7). This provides four slots, three for electrochemical gas sensors and one for the PID (Alphasense Ltd, 2016e).



Fig. 5.7. NO, CO, ETO, PID sensors and AFE board (Alphasense Ltd). Sensors (A), rear of AFE (B) and chamber (C).

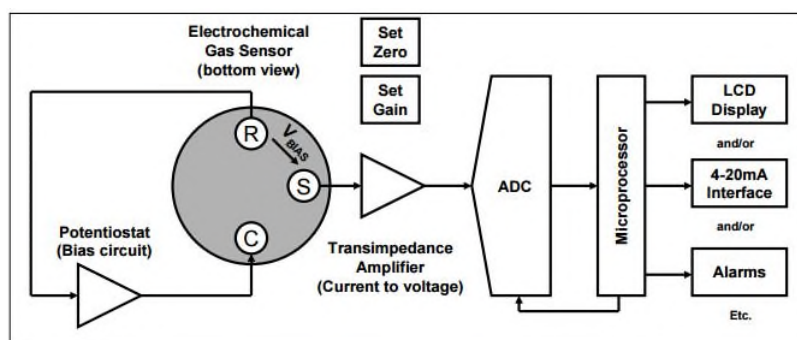


Fig. 5.8. Block diagram of AFE for electrochemical gas detectors with potentiostat circuit. C, R and S indicate counter, reference and sensing/working electrodes respectively (SGX Sensortech Ltd, 2015).

The CO₂ sensor Cirius 2 and comes equipped with an infrared transmitter board (Fig. 5.9). Cirius 2 is capable of a sensing range of up to 5000 ppm and is based on

nondispersive infrared technology. The component contains a source of infrared radiation, an infrared detector and an optical waveguide for gas diffusion (Clairair Ltd, 2010). The transmitter board contains a microprocessor and display for setting sensor parameters and a communications circuit. For signal output, the board uses either a RS232 interface protocol or a current source of 4-20mA output and for ease, the latter has been implemented. The voltage output for the microcontroller (by Ohm's law) via a (250 Ohm) load resistor (Clairair Ltd, 2015).

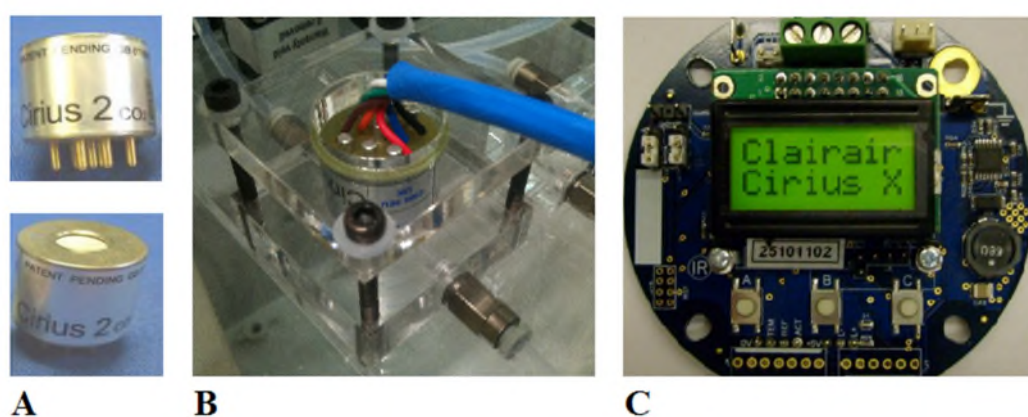


Fig. 5.10. NDIR CO₂ Cirius gas sensor (A), sensor in acrylic chamber (B) and Cirius X OEM 4-20mA Transmitter (C), (Clairair Ltd, 2015, 2010).

5.4.2.3 Oversampling

When sampling data with the logger instrument for subsequent analysis, these may not be readily of use hence the need further signal processing. However, at this stage of the project the likely experimental outcome is unknown and a further flexibility may be added into the design process by means of software-based approaches. This applies to signal resolution as well. The ATMEGA comes with a capability of up to 12-bits of resolution (depending on settings for internal voltage references) and further sampling resolution may be needed, depending on experimental outcome (Atmel Inc, 2014). Because of this, the decision has been made on having all signal processing (if and

when needed) in firmware. For this purpose a common technique to achieve ADC (analogue digital conversion) resolution is oversampling (Atmel Inc, 2005; Microchip Technology Inc., 2008; Silicon Labs Inc, 2013; STMicroelectronics Inc, 2013; Texas Instruments Inc, 2006). In short, the technique consists in increasing the amount of samples resulting in a higher representation of the input signal. For each bit of further desired resolution N , the original signal has to be sampled 4^N times. This will yield 4^N extra number of samples at the original resolution. After this operation, all these extra samples are summed and ‘averaged’ (decimated) by a factor of 2^N for each bit of additional resolution N . The resulting value is the representation of the signal at higher resolution. A C++ library for this purpose is available (courtesy of G. Staples). Tests for the library were first carried out with digital potentiometers and then in real-world setting, as indicated in Fig. 5.11.

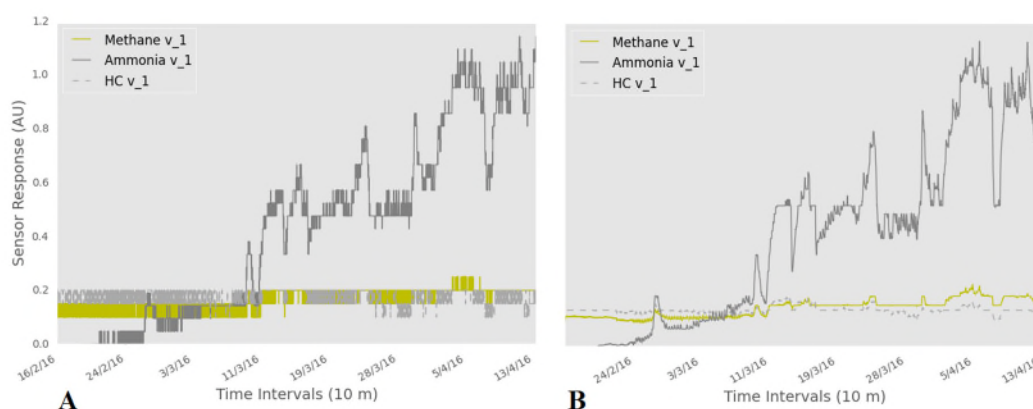


Fig. 5.11. Increase in resolution from 10-bit (A) to 16-bit (B) in experimental results.

5.4.3 Air flow delivery

5.4.3.1 Pneumatic components

The objective of the data logger is to sample air either from containers for laboratory work, or from the background environment in commercial potato stores. Two complete data logger units were assembled for either purpose. The unit employed for laboratory experiments was fitted with 5 valves for air management. This allowed a range of different sample types to be tested at the same time. Specifically: background environment analysis, unwounded controls, wounded controls and two for infected tubers. The other unit was deployed at the AHDB Sutton Bridge Crop Storage Research Centre instead and was fitted with 3 valves. This choice was motivated by the fact that the instrument had to be left in harsh environmental conditions without possibility of prompt action in case of malfunction. Hence, if mechanical failure occurred, the air flow could be promptly redirected to one of the other two valves.

For both units, sampled air is pumped through each valve in turn, then into each sensor chamber and pushed out of an exhaust. In the laboratory work, the exhaust is connected to a dedicated gas path line in order to minimise cross contamination of background air whilst sampling. To account for the inclusion of two main chambers, each fitted with either electrochemical or metal oxide gas sensors, the use of a dual path for air flow was chosen. This choice is motivated by two main constraints. The first one is to accommodate for different air flows caused by different sizes and dead volumes in each of the sensors chambers. The second issue comes from the desire to avoid undue sampling caused by alteration of air. In fact, on the AFE board the PID slot is located at the exhaust end in order to accommodate for ionization of air. Air, after entering the PID will be ionised, and consequently subsequent sampling by other sensors will be of ionised air (with ionised target molecules). Moreover, air molecules

will leave the metal oxide sensors chamber being heated and gone through a redox reaction (like in the case of electrochemical sensors) thus providing also a potentially depleted air sample. The smaller chamber, for the NDIR CO₂ sensor, is placed in series and the beginning of the electrochemical sensor chamber.

Air draft is electronically regulated by PWM (pulse width modulation) by firmware. In PWM a series of digital pulses is employed to control an analogue circuit. The length and frequency of these digital pulses determines the power delivered to the analogue circuit (National Instruments Inc, 2016). Pulse width modulation consists in modulating a square wave in order to encode an analogue signal value, in the specific case it allows speed control of the pump unit. The voltage is supplied to the pumps via a repeating series of on and off voltage pulses at the microcontroller logic level (5 V). The duty cycle is the ratio of the time these pulses are on or off. The power applied can be controlled by variation of the width of these on-off pulses thus altering the average voltage applied to the pump terminals. By changing this duty cycle, the speed of the pump can be controlled: the longer period the voltage pulses are in the on state, the faster the pump will operate and, vice versa, the shorter pulses the slower the pump. PWM allows then control of a pump with reduced power dissipation and ease of use.

However, the proportion of air to the two chambers is set by two manual valves in order to provide an equal initial flow of 300 mL/min (approximately 30 times less than the air volume of test containers). A diagram for the complete air path is shown in Fig. 5.12. Connection of various parts is provided the by PTFE (Polytetrafluoroethylene) tubing of 3.2 mm OD (outer diameter) and 1.64 mm ID (inner diameter). PTFE has been chosen due to its lubricity, chemical inertness and durability, as explained earlier in this work. Part of the tubing (for pumps inlets and outlets) is also constituted by

Tygon lab tubing of 10.2 mm OD and 3.2 mm ID. Selection of size and materials has been also based on availability of parts.

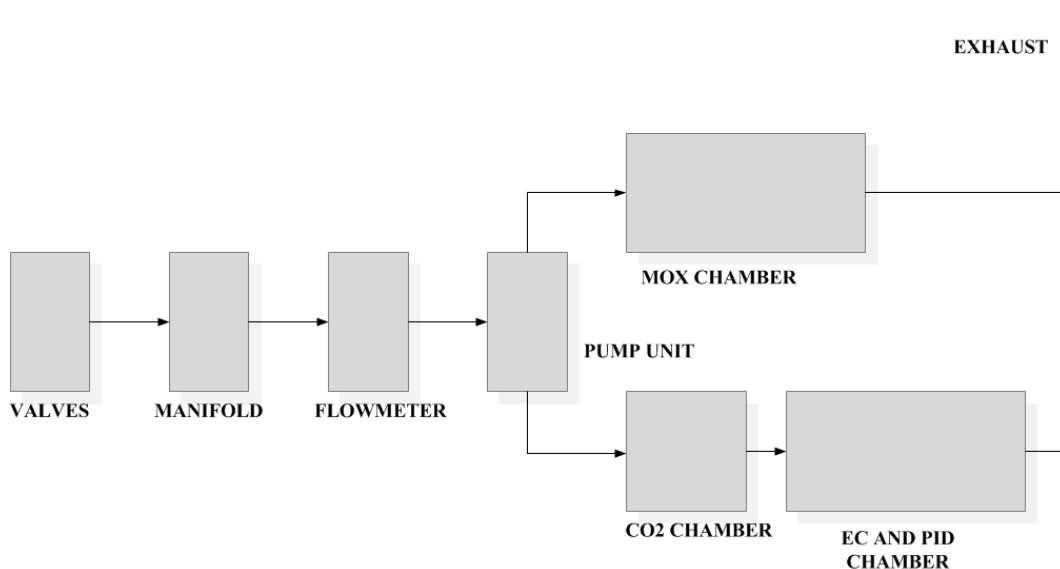


Fig. 5.12. Block diagram of air flow path.

All components (Fig. 5.13) were placed on custom-made acrylic plates, in order to simplify replacement and handling of parts. The valves selected were from Clippard Inc. - standard EV Series ETO-3-12 (Clippard Instrument Laboratory Inc., 2015). These are 3-way in-line mount electronic valves (normally closed): one inlet, one outlet and an exhaust to relieve possible pressure build-up. The components operate at 12 V (0.67 W power consumption). Other parameters reported by the manufacturer are pressure range of 28" Hg Vac to 105 psig and maximum air flow of 17 L/min at 7 bar, well within the specifications range for the pumps employed. These valves were also chosen as they are ultrasonically cleaned to remove both organic and inorganic contaminants such as particulate matter at the manufacturing stage (Clippard Instrument Laboratory Inc., 2015).

The air flow within the data logger is measured by an airflow sensor, namely the AWM43600 from Honeywell Inc. with a full range of 6 L/min (Honeywell Inc., 2016). The air flow sensor operates at 10 V with 75 mW of maximum power consumption and thus fits well within the limits of the gas sensing unit. From the datasheet, the specified required voltage is of 10 ± 0.05 V and thus it requires very high accuracy. This accuracy could not be provided by any of the aforementioned supply lines. To supply the flow sensor a common voltage precision reference integrated circuit was chosen, the REF102 from Texas Instruments Inc (Texas Instruments Inc, 2009). Two NMP015 KNF micro-diaphragm gas-sampling pumps were employed for air flow draw, one for each main chamber. The pumps (chosen for both reliability and availability) specifications is of free flow up to 1.4 L/min and a maximum pressure of 0.9 bar (Knf GmbH, 2016). Since these operate at a nominal voltage of 6V they have to be placed in series in order to accommodate the available supply lines (12V) from the both power unit and the control board. All parts described to date are shown in Fig. 5.13.

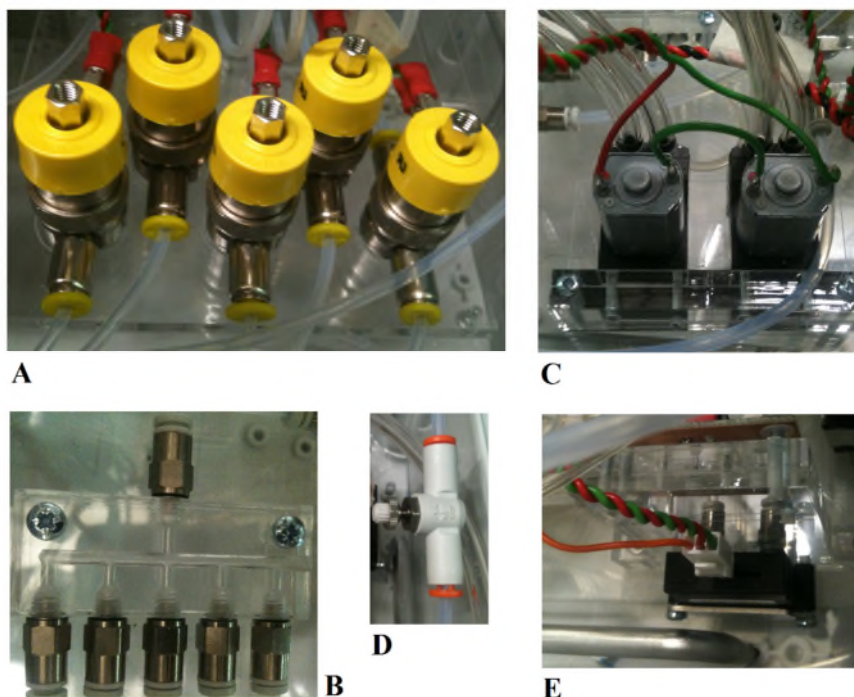


Fig. 5.13. Valves (A), manifold (B), pump unit (C), manual valve to change air flow (D) and flowmeter (E).

5.4.3.2 Electronic control

The control board (Fig. 5.14) uses logic MOSFETs (Metal Oxide Semiconductor Field Effect Transistor). These transistors can be used either as switches or for amplification. Here the MOSFET transistor is employed in a switching mode in order to open/close the valves and regulate the pump speed by means of PWM. The logic MOSFET allows gate control from a microcontroller and has a lower threshold voltage than normal MOSFETs. In this specific case the IRL540 (N-channel) is designed to be fully turned on from the logic level (5 V TTL) for the microcontroller deployment. The L indicates logic level for the popular MOSFET IRF series designed to be fully on at 10 V applied to the gate. In the control board PCB, in Fig. 5.14, the IRL540 is accompanied by other components that have protective functions. The 5.1 V Zener diode between the gate of the MOSFET and ground is meant to provide protection from excessive voltage:

the diode clamps the excessive voltage (at Zener level) and allows flow of current to ground. In addition, a diode (known as flyback or also freewheel diode) is connected across the pumps/valves positive and ground terminals in order to dissipate spikes of counter electromotive force caused by these inductive loads (since both pumps/valves have inductive parts) when each transistor is switched off: the current will then be directed away from the MOSFET . A further addition of a diode in series with a Zener diode (in parallel to the flyback components) allows faster switching (Croydom Inc, 2016). The arrangement described above is also known as a (Zener) clamping (or snubber) network. All the protective components are indicated in Fig. 5.15. In this work the configuration detailed so far is employed not only to switch on/off the valves for sample air supply, but also to regulate pump speed when appropriate: this is achieved through PWM, as detailed previously.

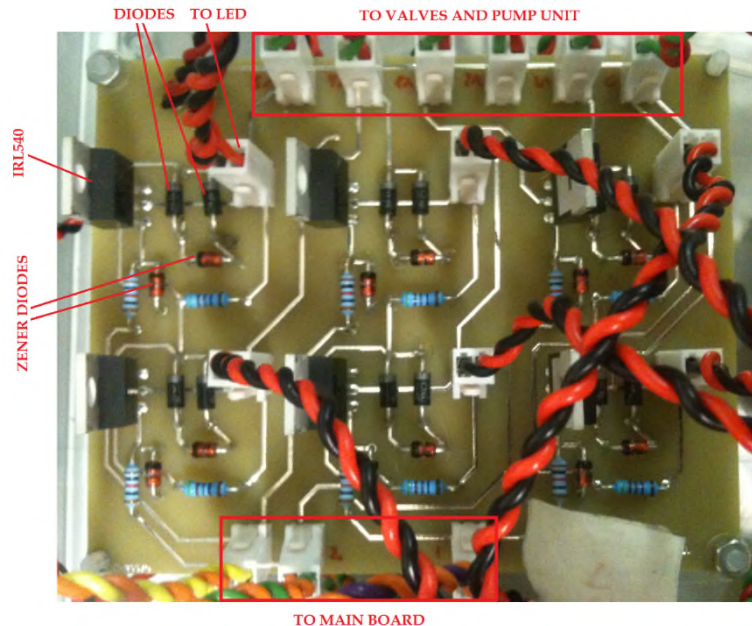


Fig. 5.14. Control PCB unit for data logging unit for 5 valves and pump pair unit.

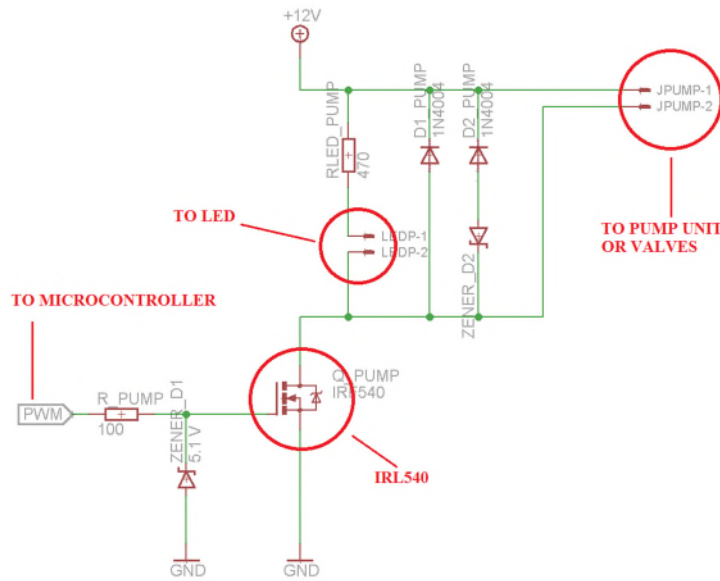


Fig. 5.15. Valves/pumps control and protection circuit components.

5.4.4 Main board and user interface

Management of the environmental data logging units requires a main control board. The integrated circuit chosen for this purpose is the ATMEGA 2560 microcontroller from Atmel (Atmel Inc, 2014). The reason for using this manufacturer is due to the availability of ready-made board prototypes, the possibility for ease of access to tested code libraries, the integrated development environment for firmware downloading and interfacing with the various boards and the number of features available for the chip. In the first case, a ready-made prototype, which can facilitate the assembly of the data logging system and its testing, is the Arduino MEGA 2560 (Arduino Srl, 2016a). Due to the nature of the project, the choice for this prototype board allows to free time and resources from costly development of the integrated circuitry needed to support such a microcontroller chip. In the past years, the fast development of this board and other similar units (all based on open source hardware) and the presence of a vast open community has led to the development of a large number of stable and reliable libraries that allow for code reuse. In a similar fashion the development environment, that

accompanies these prototype open source hardware parts, is easy to use and allows rapid integration of code libraries. The large number of pins available for the integrated circuit is also of particular interest for the number of sensors channels to monitor.

Other components included with the prototyping PCB are an RTC (real time clock) and a microSD (micro secure digital) card. The SD card is a memory card format developed by the SD Association for portable devices. The RTC is meant to provide date and time that can be associated to sensor data. For this purpose the DS3234 from Maxim Integrated has been shortlisted (Maxim Integrated Inc, 2015). Selection of this component has been made due to the presence an integrated temperature-compensated crystal oscillator and crystal, its use of the SPI (Serial Peripheral Interface) protocol to communicate with the microcontroller and availability of code (subsequently modified by the author into a library). SPI (3-wire) and I²C (2-wire) ports are the most common interface protocols for transmitting and receiving data between digital components. There are advantages and disadvantages for both, but SPI is preferred here for ease of implementation (no need for pull-up resistors) and noise immunity (Maxim Integrated Inc, 2016). Another important element is the storage of the data collected, which is implemented with a microSD card breakout board from Adafruit Industries Inc (Adafruit Industries Inc, 2016). The breakout also uses SPI for digital serial communication.

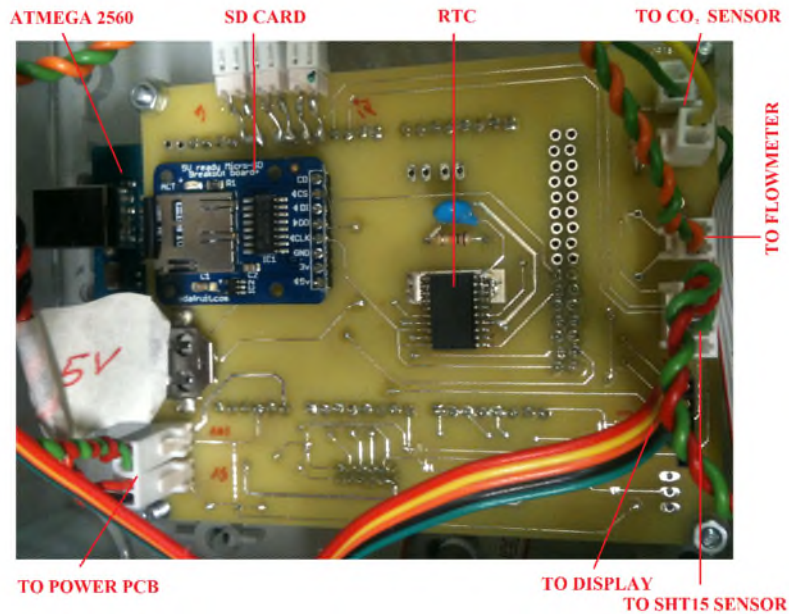


Fig. 5.16. System control PCB.

The graphical user interface is implemented by means of the display uLCD-32PTU, from 4D Systems and shown in Fig. 5.17 (4D Systems Pty Ltd, 2016). The display is a self-contained component that offers ease of coding and ready-made libraries for the Atmel processors. The communication protocol is based on the serial interface UART (universal asynchronous receiver transmitter).

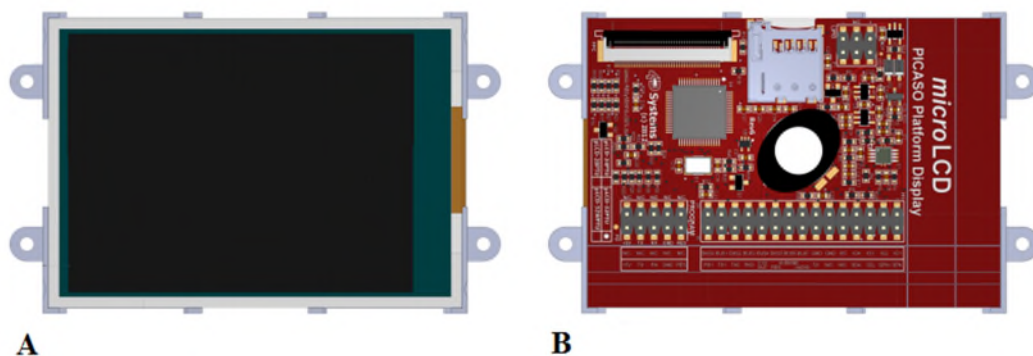


Fig. 5.17. Front of user interface display front (A) and rear (B), (4D Systems Pty Ltd, 2016).

5.4.5 Firmware

Firmware can be broadly defined as piece of low-level control software (stored in a non-volatile memory support) providing the microcontroller with the necessary set of instructions for operation, data handling and interaction with other electronic hardware components. The firmware downloaded onto the prototype board relies on a number of libraries and specific functions to achieve a data logging operation.

The main part of the source code is located in the ‘.ino’ file. The rest is contained in libraries that need to be included according to functionality. Once complied, the firmware is downloaded onto the microcontroller via the Arduino integrated development environment employed, that in the specific case is version 1.6.5 (Arduino Srl, 2016b). This main source file is based on two functions, namely `setup ()` and `loop ()`. The former is employed for all initialization steps while the latter contains code that runs continuously in a loop mode. Essentially, all software is written in the C++ programming language. All other additional source code libraries follow the language standard nomenclature with header and source files (with file extensions ‘.h’ and ‘.cpp’). Each part of the source code listed below refers to the C++ class type.

The ‘TRH class’ allows reading of temperature and relative humidity from the SHT15 IC via a 2-wire protocol, as indicated by the manufacturer (Sensirion AG, 2011). Methods are provided to collect temperature and humidity values from the chip, and to access the control register of the IC. The library is based on the software originally developed by Maurice Ribble (Ribble, 2015).

The ‘ADC class’ provides functionality between the microcontroller and sensors in order to improve resolution, as indicated earlier in this chapter. In the `setup ()` function

in the main file, the method provides the initialization of parameters for ADC speed and bits of resolution. The library has been originally developed by Gabriel Staples.

The 'SD class' allows for reading to and writing from SD cards and supports both FAT16 (File Allocation Table 16) and FAT32 file systems on the SD card standard (INTEGRAL MEMORY PLC, 2016; Microsoft Inc, 2016). The communication between microcontroller and SD card is achieved via the SPI protocol (Arduino Srl, 2016c; Maxim Integrated Inc, 2016). The library is provided with the integrated development environment employed (Arduino Srl, 2016d).

The 'RTC class' allows information flow to and from the real time clock DS3234 chip via the SPI protocol. The main function of the class (based on code developed by Richard Bronosky at Sparkfun Electronic Inc) is to read time and date from the IC. The class is employed for initialising, setting time/date and reading data from the control register of the IC. The code snippet for setting time and date consists in addressing the register as indicated in the datasheet (Maxim Integrated Inc, 2015). This operation is performed once, since an external coin cell battery allows the DS3234 to keep the specified time/date setting.

The 'Genie class' aims to ease information exchange between the microcontroller and the 4D Systems display uLCD-32PTU (Fig. 5.17) via UART (Universal Asynchronous Receiver Transmitter) serial communication (Texas Instruments Inc, 2010). The graphical user interface part of the display is designed with the ViSi-Genie environment from 4D Systems (4D Systems Pty Ltd, 2016).

Once the instrument is started, the code first checks and sets the system variables. This is followed by a set up operation to initialise serial communication and display, RTC (Real time Clock), ADC and SD (Secure) card. A continuous operation mode is then

commenced in order to loop through each valve for data collection (with collected data stored on SD card) at an interval of every 10 minutes, in the same fashion an industrial data logger would operate. The code deployed on the system is based on C++ and a basic flow chart describing software operation is shown in Fig. 5.18.

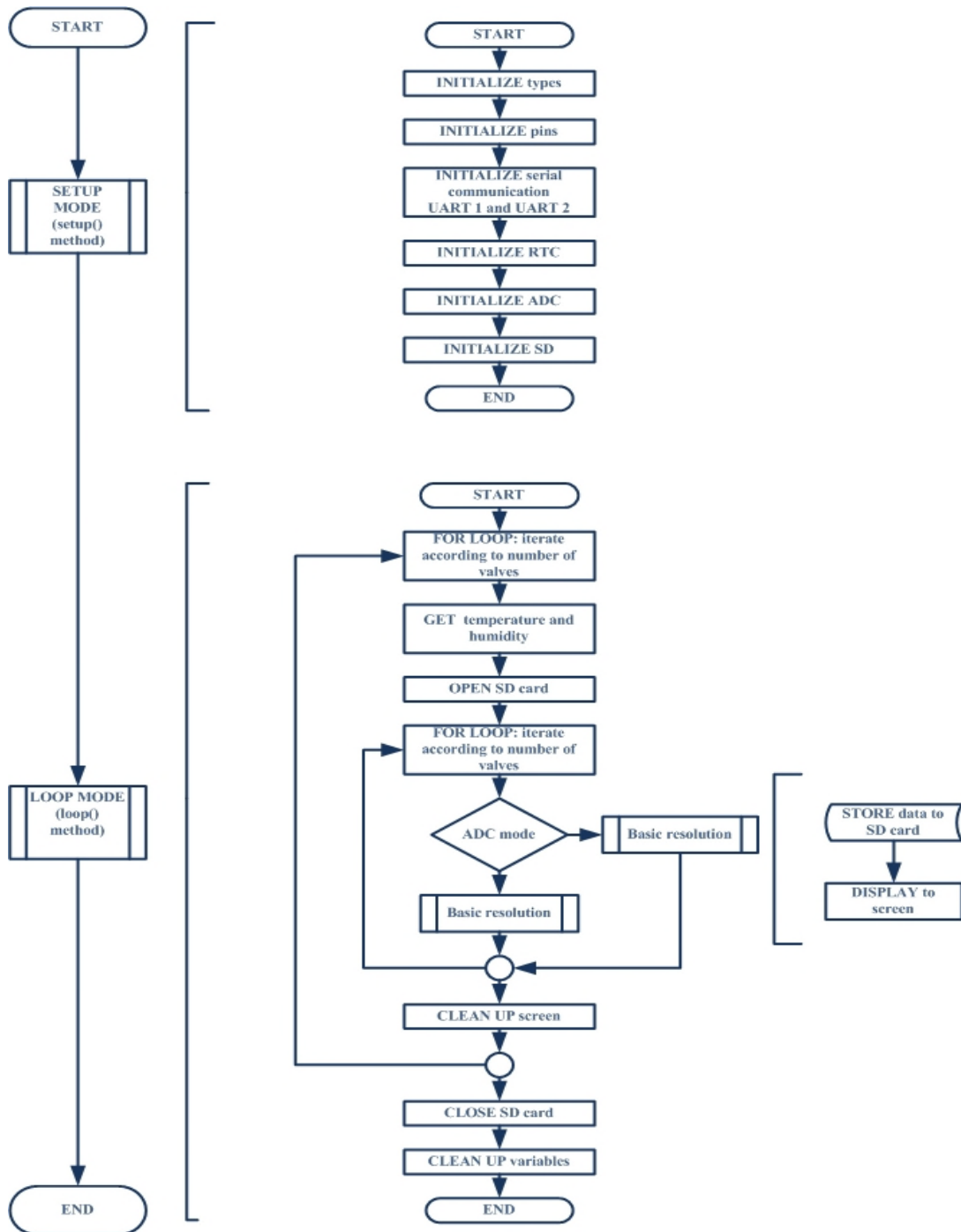


Fig. 5.18. Basic flowchart for firmware.

5.5 Assembled systems

Two data loggers been design, assembled and tested. The first unit was employed for laboratory work (Fig. 5.19 and Fig. 5.20), while the second was located in a potato storage facility at the AHDB Sutton Bridge Crop Storage Research Centre (Fig. 5.21). The experimental results are detailed in the next chapter. The instrument for laboratory experiments was fitted with 5 valves, a fan system (to prevent condensation) and a USB port for downloading firmware (Fig. 5.19). The instrument for store monitoring was sealed and comes equipped with three valves.

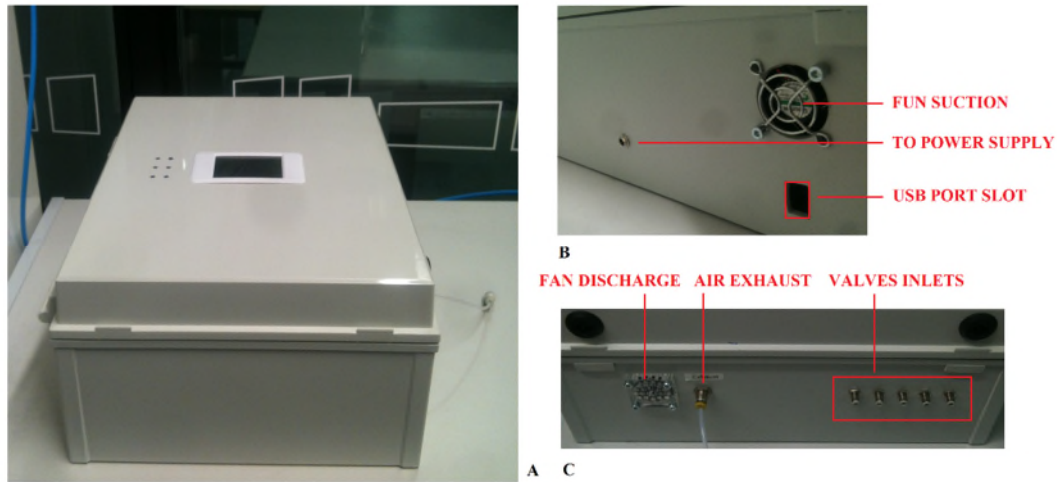


Fig. 5.19. Data logger for laboratory experiments (A). Side view: fan, power supply connector and slot for USB port in (B). Side view: fan discharge, air exhaust and air inlets in (C).

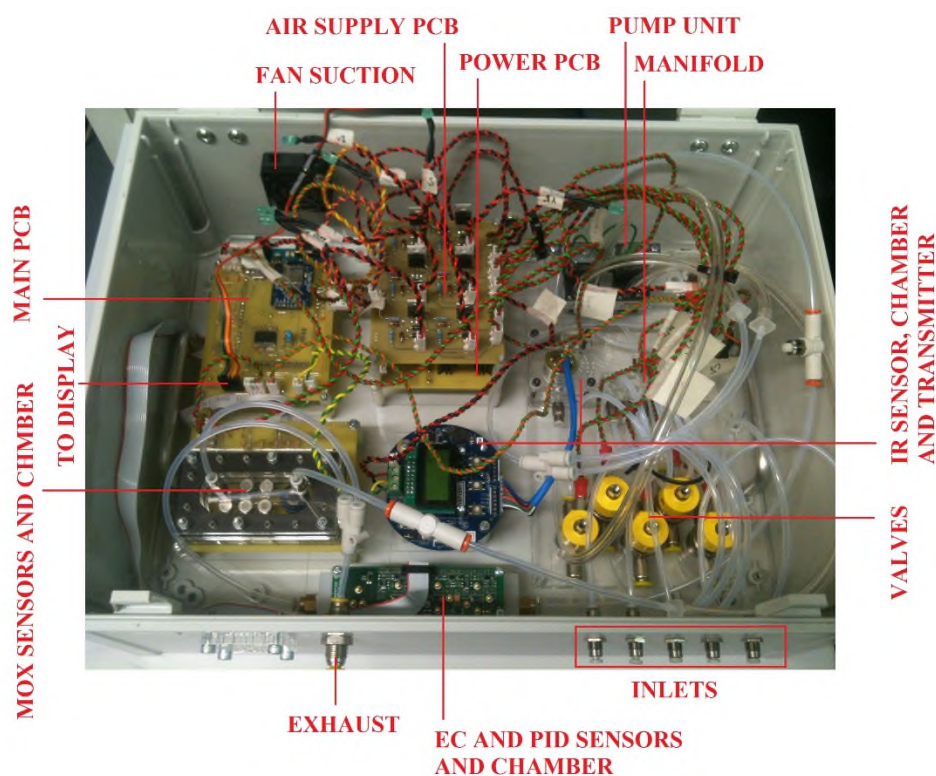


Fig. 5.20. Inside of data logger for laboratory experiments.

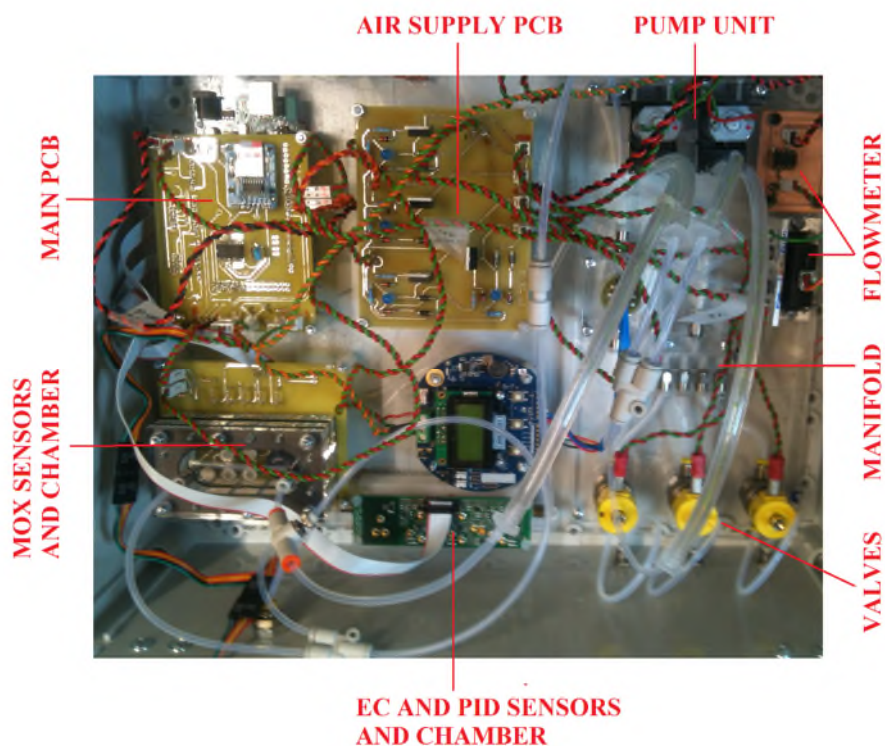


Fig. 5.21. Close-up of data logger deployed in stores at AHDB Sutton Bridge Crop Storage Research Centre.

5.6 Discussion

The design and development of an environmental data logger for soft rot detection has been presented. The main objective of the data logger is to carry out VOCs sampling for soft rot monitoring in a potato store. Laboratory tests (dilution work) allow assessment of device reliability and also insight into volatiles for a small scale store model. Unlike previous work presented here, this instrument is designed to provide a means to monitor volatiles and volatile changes in time. In fact, it is very likely that the overall trend of VOCs (or specific volatiles) over time will be key in early detection of soft rot. This will allow assessment of the potential of VOC profiling for soft identification (and potentially for other potato storage diseases). The unit does not aim to be exhaustive in all its components and its assembly. In fact, improvements and modifications have been carried out throughout the experimental work. In the next chapters the results obtained with the instrument will be described.

5.7 Conclusion

In this chapter it has been indicated the rationale, features, design process and construction of an inexpensive but reliable bespoke system for gas analysis of soft rot. Two units of the ad-hoc instrument have been developed for use in either laboratory or storage facilities. The device is initially described in terms of requirements and system architecture and later in terms of hardware, electronic and software components. It has been fitted with sensors previously shortlisted in this thesis as likely candidates for further work in soft rot detection.

5.8 References

- 4D Systems Pty Ltd, 2016. uLCD-32PTU, 3.2" TFT Intelligent Display [WWW Document]. URL http://www.4dsystems.com.au/product/uLCD_32PTU/
- Adafruit Industries Inc, 2016. MicroSD card + breakout board. USA.
- Alphasense Ltd, 2016a. NO-A1 Nitric Oxide Sensor. UK.
- Alphasense Ltd, 2016b. ETO-A1 Ethylene Oxide Sensor O-A1 Ethylene Oxide Sensor. UK.
- Alphasense Ltd, 2016c. CO-A4 Carbon Mono CO-A4 Carbon Monoxide Sensor xide Sensor. UK.
- Alphasense Ltd, 2016d. PID-A1 Photo Ionisation Detector. UK.
- Alphasense Ltd, 2016e. Analogue Front End (AFE) Alphasense A4 Air Quality Gas Sensor Alphasense A4 Air Quality Gas Sensors. UK.
- Arduino Srl, 2016a. Arduino MEGA 2560 & Genuino MEGA 2560 [WWW Document]. URL <https://www.arduino.cc/en/Main/ArduinoBoardMega2560>
- Arduino Srl, 2016b. Download the Arduino Software [WWW Document]. URL <https://www.arduino.cc/en/Main/Software>
- Arduino Srl, 2016c. SPI library [WWW Document]. URL <https://www.arduino.cc/en/Reference/SPI>
- Arduino Srl, 2016d. SD Library [WWW Document]. URL <https://www.arduino.cc/en/Reference/SD>
- Atmel Inc, 2014. Atmel ATmega640/V-1280/V-1281/V-2560/V-2561/V. USA.
- Atmel Inc, 2005. AVR121: Enhancing ADC resolution by oversampling. USA.
- Clairair Ltd, 2015. Cirius X OEM 4-20mA Transmitter. UK.
- Clairair Ltd, 2010. Cirius 2 Miniature Infrared Gas Sensor for Carbon Dioxide. UK.
- Clippard Instrument Laboratory Inc., 2015. Miniature Pneumatic Products &

Solutions. USA.

Croydom Inc, 2016. Coil Suppression & DC Output Solid State Relays. USA.

de Lacy Costello, B.P.J., Evans, P., Ewen, R.J., Gunson, H.E., Ratcliffe, N.M.,

Spencer-Phillips, P.T.N., 1999. Identification of volatiles generated by potato tubers (*Solanum tuberosum* CV: Maris Piper) infected by *Erwinia carotovora*, *Bacillus polymyxa* and *Arthrobacter* sp. Plant Pathol. 48, 345–351.

doi:10.1046/j.1365-3059.1999.00357.x

Figaro Engineering Inc, 2015a. TGS 2602 - for the detection of Air Contaminants. Japan.

Figaro Engineering Inc, 2015b. Technical Information for Volatile Organic Compound (VOC) Sensors.

Figaro Engineering Inc, 2014. TGS 2620 - for the detection of Solvent Vapors. Japan.

Figaro Engineering Inc, 2013a. TGS 2611 - for the detection of Methane. Japan.

Figaro Engineering Inc, 2013b. TGS 2610 - for the detection of LP Gas. Japan.

Figaro Engineering Inc, 2005a. Technical Information for Methane Gas Sensors. Japan.

Figaro Engineering Inc, 2005b. Technical Information on Usage of TGS Sensors for Toxic and Explosive Gas Leak Detectors. Japan.

FIS Inc., 2007. FIS GAS SENSOR SP-53B for Ammonia Detection (Low concentration). Japan.

Honeywell Inc., 2016. Honeywell Sensing & Control - AWM40000 Series [WWW Document]. URL <http://sensing.honeywell.com/products/Airflow-Sensors/AWM40000/Ne/3025/N/3467>.

INTEGRAL MEMORY PLC, 2016. CARDS - What is the difference between

SDHC and SD cards? [WWW Document]. URL

<http://www.integralmemory.com/faq/cards-what-difference-between-sdhc-and-sd-cards> (accessed 1.1.16).

Knf GmbH, 2016. MICRO PUMPS [WWW Document]. URL

<http://www.knf.com/products/oem-pumps/product/products/diaphragm-gas-pumps/micro-pumps/>

Maxim Integrated Inc, 2016. SPI/I²C Bus Lines Control Multiple Peripherals [WWW Document]. URL <https://www.maximintegrated.com/en/app-notes/index.mvp/id/4024>.

Maxim Integrated Inc, 2015. DS3234 Extremely Accurate SPI Bus RTC with Integrated Crystal and SRAM. USA.

Microchip Technology Inc., 2008. Achieving Higher ADC Resolution Using Oversampling. USA.

Microsoft Inc, 2016. File Systems [WWW Document]. URL

<https://technet.microsoft.com/en-us/library/cc938437.aspx> (accessed 1.1.16).

Multicomp Electronic Components Inc, 2012. External Power Supply. USA.

National Instruments Inc, 2016. Pulse Width Modulation (PWM) Using NI-DAQmx and LabVIEW [WWW Document]. URL <http://www.ni.com/tutorial/2991/en/> (accessed 1.1.16).

Ribble, M., 2015. sensirion SHT15 humidity/temperature sensor [WWW Document]. URL

<http://wiring.org.co/learning/basics/humiditytemperaturesht15.html>

Sensirion AG, 2011. Datasheet SHT1x (SHT10, SHT11, SHT15) Humidity and Temperature Sensor IC. Switzerland.

SGX Sensortech Ltd, 2015. Electrochemical Sensors Application Note 2 - Design of

Electronics for Electrochemical Gas Sensors. UK.

Silicon Labs Inc, 2013. Improving ADC resolution by oversampling and averaging.
USA.

STMicroelectronics Inc, 2013. Improving STM32F1x and STM32L1x ADC
resolution by oversampling. USA.

Texas Instruments Inc, 2014. LM317 3-Terminal Adjustable Regulator. USA.

Texas Instruments Inc, 2013. AN-1798 Designing with Electro-Chemical Sensors.
USA.

Texas Instruments Inc, 2010. Universal Asynchronous Receiver/Transmitter
(UART).

Texas Instruments Inc, 2009. REF102 10V Precision Voltage Reference. USA.

Texas Instruments Inc, 2006. Oversampling the ADC12 for Higher Resolution.
USA.

Traco Electronics AG, 2009. THN 15 Series Application Note. Switzerland.

EXPERIMENTAL WORK WITH THE VOC DATA LOGGER

This page is intentionally left blank.

6 Experimental work with VOC data logger

6.1 Introduction

In previous chapters, it was shown that FAIMS, PID, metal oxide and electrochemical sensors had potential for both symptomatic and pre-symptomatic detection of soft rot. This led to the possibility that volatile monitoring of the disease could be feasible also in real-world conditions. In fact, commercial potato stores are environmentally controlled, with air forced through the crop. Hence, disease monitoring in store could potentially be achieved through the use of gas analysis by employing sensors or sensor systems which are financially viable for the agricultural industry. This led to the development, manufacture and test of a prototype gas analysis system, as reported in the previous chapter.

Of the other equipment used in this study, the FAIMS sensor was excluded on the basis of financial considerations, as its cost point was not appropriate for monitoring storage facilities. Moreover, the technology could not be easily and effectively implemented into a data logging system for the purpose of academic research. However photoionization, metal oxides and electrochemical detectors could be readily assembled into a unit that was financially viable. Hence, the environmental analysis instrument allowed both prompt verification of research indicated in earlier chapters and further study in order to assess pre-symptomatic identification and monitoring of soft rot disease in storage.

The work presented here reports on the experimental protocols carried out and their outcomes in order to assess the potential of the sensors previously shortlisted. Two different types of studies were completed. The first one under laboratory conditions

aimed at an evaluation of a ‘scaled-down’ store model with various representative sample types of the different states in which tubers could be found. This also allowed testing and optimisation all parameters for later use in store. The second setting involved work at the AHDB Crop storage Research Centre and aimed to assess the potential of the unit for soft rot monitoring in real potato store conditions.

6.2 Materials and methods

6.2.1 Experimental laboratory work at Warwick

6.2.1.1 Sample preparation

The protocol for sample preparation, handling and inoculation is the one suggested by Dr Glyn Harper (AHDB Potato Council, Sutton Bridge Crop Storage Research) with the use of *P. carotovorum* isolate SBEU_08. The procedure is outlined below but further details can be found in the chapter on FAIMS and PID work (3.2.2 Experimental sampling protocol):

- Rehydration of tubers by soaking them in water for about 1 hour prior to inoculation.
- Inoculation with *P. carotovorum* isolate SBEU_08 for infected tubers. No wounding for one of the control tubers. Wounding with a pipette tip at the stolon of the other tuber in order to assess potato wounding volatile profile.
- For the first set of experiments, potatoes were stored in sealed plastic boxes at 25 ± 1 °C in an incubator to allow rapid disease progression and suspended on a mesh over water (400 mL), to maintain high humidity. For the second set of experiments the tubers were stored in 9 L plastic containers on acrylic base

suspended over 400 mL of water with an and (Fig. 6.1). The tubers were stored in this condition for circa 4 hours prior to sampling.

- All tubers used were deemed healthy by sensorial inspection at the start of each experiment but control.

6.2.1.2 Sampling protocol

For sampling, tubers were placed into a 9 L plastic container (Addis Housewares Ltd, 2016) as indicated in Fig. 6.1 with a gas path inlet and outlet added via 1/8" push-fits (SMC Pneumatics Ltd, 2016). Overall, 4 containers were used for the various sample types: unwounded control, wounded control and one infected potato for each the other two containers. Background was also monitored. Hence 5 types of samples (and 4 containers) were analysed. Purpose of the first one was to assess varying background conditions due to other concurrent experiments in the laboratory. Unwounded and wounded controls were meant to assess the possible difference in volatile profiles for controls. The two containers, each with an infected tuber, were to address variability in soft rot progression among diseased tubers. Sampling was carried out for each individual container at a flow rate of 330 mL/min and the mixture of air and emissions from the sample type fed to data logger unit (chapter 5) for analysis. Inoculation dosage was twice the amount of used in previous work (20µL) in order to create a situation of 'overmatch' to other potential diseases present in the other tubers or in the inoculated samples.

After previous preliminary work had established the optimal protocol for sampling, two types of experiments were carried out. In the first set, the tubers were stored in the incubator for a period of 24 hours and then, after 4 hours, moved into the 9 L containers

prior to sampling. In the second set they were stored inside the sealed 9 L containers for 4 hours before sampling. Sampling was then carried for a number of days (circa one week) in order to allow disease progression. Duration for the sampling period was chosen according to disease progression and other factors influencing disease spread (such as potato greening and sprouting). Data for each sample type were collected at an interval of 10 min, as of common practice in industrial data loggers. After the experimental procedure was completed, containers were thoroughly cleaned, sterilized and baked into an oven at 50 °C for few hours in order to remove leftover odours from experiments.

Layout of the experimental set up is shown in Fig. 6.1 and available sensors for the unit are reported in chapter 5.

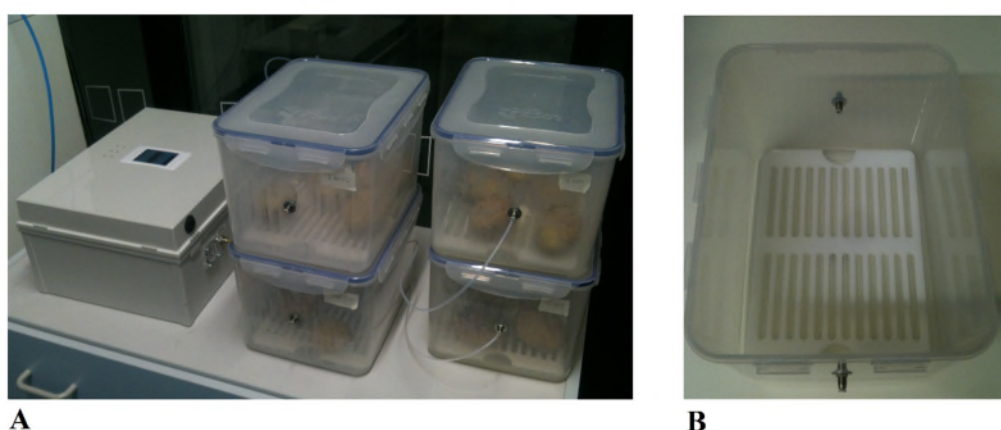


Fig. 6.1. Laboratory setup. In (A) the data logging unit connected to the 4 containers via PTFE tubing. In (B) the inside of each container with acrylic mesh for suspension of samples over the water bath for humidification.

6.2.2 Experimental storage facility work at SBCSR

6.2.2.1 Sample preparation

The protocol for sample preparation, handling and inoculation has been carried out by Dr Glyn Harper and Graeme Stroud at SBCSR. Inoculum per tuber was of 25 μ L with

3 wounds per tuber. The procedure was outlined in the previous section and in past chapters, but in this specific case after inoculation with *P. carotovorum* (isolate SBEU_0) potatoes were stored in 30 L sealed plastic boxes at 15 ± 0.5 °C and at 95% RH in a store room for 4 days (Fig. 6.2) to allow for rapid disease development.

6.2.2.2 Sampling protocol

The four 1 ton wooden crates controls were placed inside a store room of circa 56 m³ that was slowly brought to 95% RH and 15 ± 1 °C (Fig. 6.1, Fig. 6.2). The store room is located in Sutton Bridge (Lincolnshire, UK) at the AHDB Crop Storage Research Centre (SBCSR). Prior to being located in the room the controls were treated with SmartBlock® for sprout suppression (AMVAC Chemical Corporation Inc, 2016). The controls were kept under these environmental conditions for 7 days. For sampling of soft rot, infected tubers were then placed into 4 plastic containers (Fig. 6.3, B and D) in two rows to allow for better air circulation. About 40 kg of potatoes were infected. The duration of experiment with diseased tubers lasted for 21 days and sampling was carried out with intervals of 10 minutes.



Fig. 6.2. Potato storage rooms (A) at Sutton Bridge Crop Storage Research Centre. In (B) the storage room employed for experiments with four 1 t potato crates.



A



C



B



D

Fig. 6.3. Inside the test room as shown in Fig. 6.2. Air circulation system (A); infected tubers on the left-hand side, four 1t potato crates on the right-hand side in (B), (D) and data logger in (C).

6.3 Results

6.3.1 Laboratory work with completed time course

This part of the study was carried out in order to evaluate and test both the data logger and a suitable protocol for laboratory work. Moreover, this research provided insights into later work at the experimental storage facility in Sutton Bridge. The results are reported in Fig. 6.4 to Fig. 6.14. In these diagrams, as in others that follow, the legends indicate the different valves (and associated containers) and the compound of interest. B_v1 refers to the background environment in the laboratory, CO_v2 to the control tubers, CS_v3 to control tubers with one stabbed sample at the stolon, D_v4 and Dv_5 for controls with one diseased tuber placed in each container. Two containers with infected tubers were employed in order to assess if and what variation could be found in progression of soft rot over time.

The results for electrochemical gas sensor NO (nitric oxide) and for ETO (ethylene oxide) indicate that no discrimination among types of samples (background, unwounded control, wounded control and two infected) could be identified (Fig. 6.4 and Fig. 6.5).

In Fig. 6.6 the CO (carbon monoxide) graph shows a very marked response for one of the two infected tubers. CO was identified as one marker in chapter 4 and consequently selected for the array of sensors in the data logger. In the same chapter, it was shown that carbon monoxide was subject to a certain degree of variance depending on the sample. At this stage it was not clear if soft rot infection was present in the other tuber since results for the same experiment indicated that the two potatoes were affected from a common condition that could be related (directly or not) to soft rot (Fig. 6.7 to Fig. 6.13). More, at this stage doubts remained with regard to the fact that this outcome could be dependent on cross-sensitivity of the sensor to other volatiles.

Fig. 6.8 and Fig. 6.9 show the response of the Figaro TGS2602 (general VOC detection), labelled as VOC1 and VOC2. It may be worth noting that two sensors were employed here in order to assess both the performance of air flow in the custom-built chamber (the two components were placed at opposite sides of the MOX chamber) and evaluate robustness of overall volatiles profile with metal oxides sensors (time course showing an overall VOCs increase was considered an important disease identifier). Both (as also in subsequent experiments) yielded strikingly similar results. Likewise, the PID chart in Fig. 6.7 suggests a trend in shape and slope, similar to VOC1 and VOC2. It appeared that all the three detectors of volatile metabolites were operational and able to perform adequately. However, as in the case with CO, doubts remained about the fact that this appeared to be the response associated to only one of the tubers.

Moreover, a steady plateau in the graph reached by the carbon monoxide sensor in Fig. 6.6 (while a constant increase in PID trend over time in Fig. 6.7) could suggest the presence of different chemicals involved in these responses. However, a further note can be added with regard to the ionization potential, which for carbon monoxide is 14.01 eV while the PID lamp employed features a ionization potential of 10.6 eV (Baseline-MOCON Inc, 2007; NIST National Institute of Standards and Technology, 2016a). The other alternative explanation would be the by-product of chemical interaction of the volatiles contained in this enclosed environment.

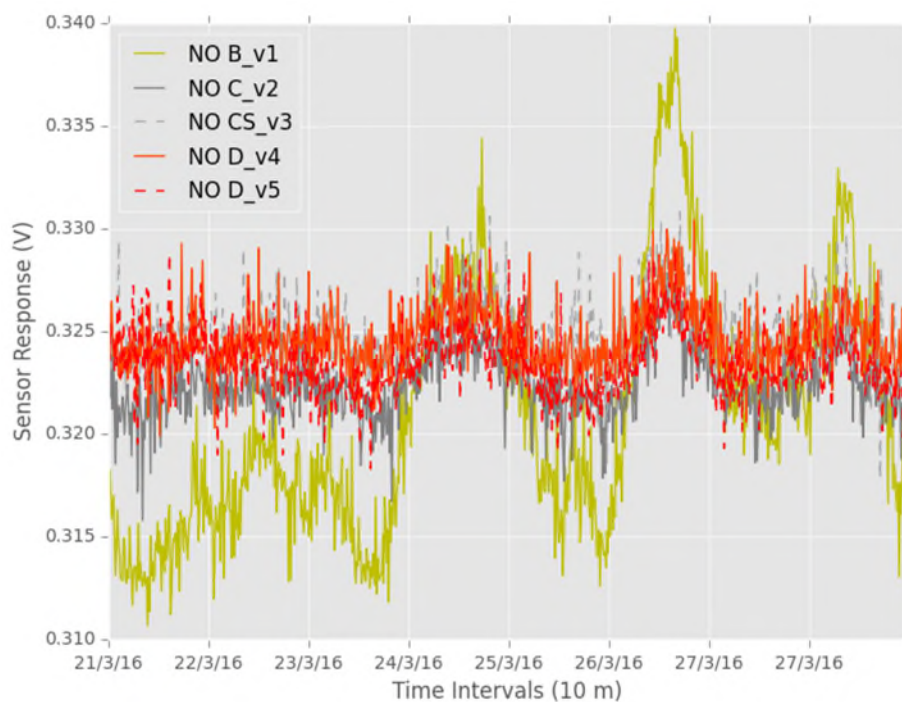


Fig. 6.4. Electrochemical gas sensor response for NO (nitric oxide).

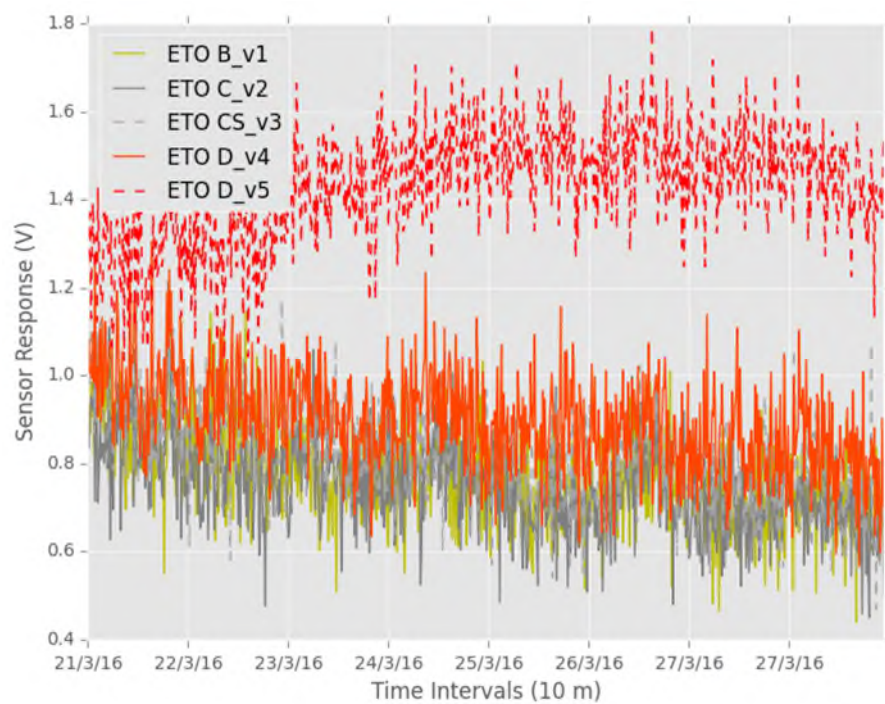


Fig. 6.5. Electrochemical gas sensor response for ETO (ethylene oxide).

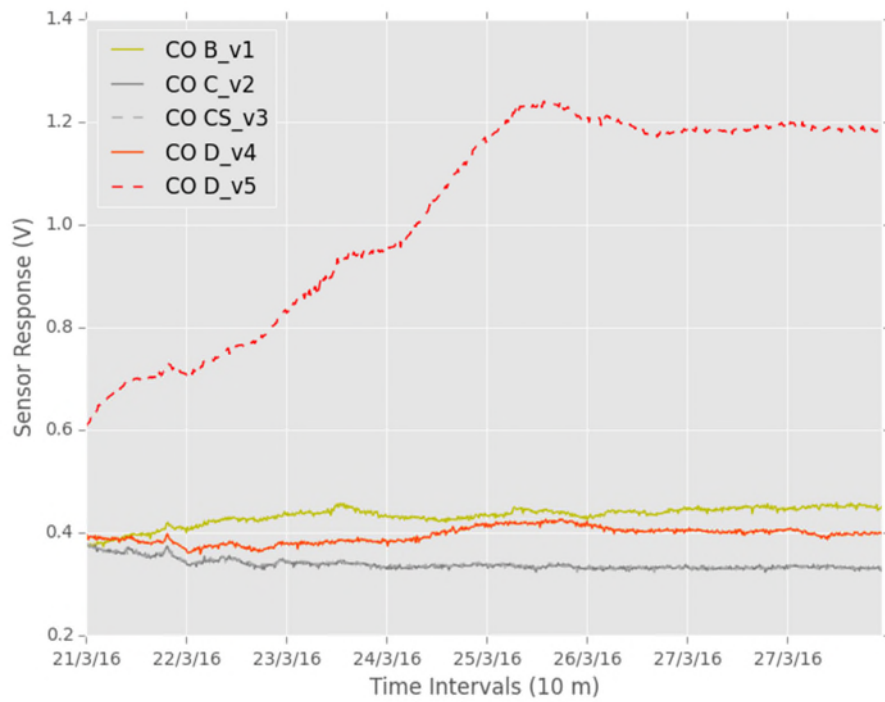


Fig. 6.6. Electrochemical gas sensor response for carbon monoxide.

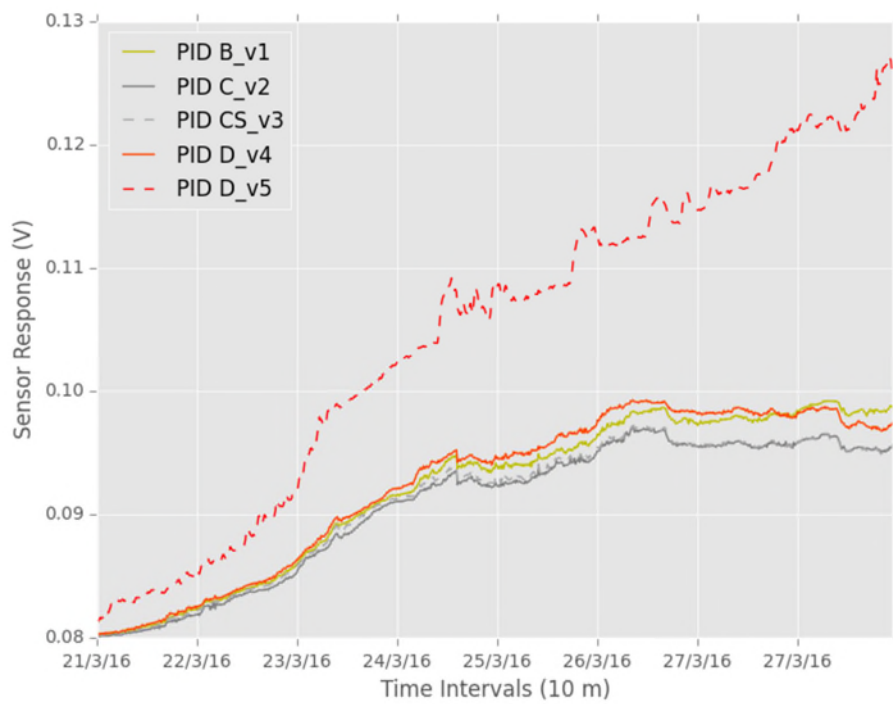


Fig. 6.7. PID gas sensor.

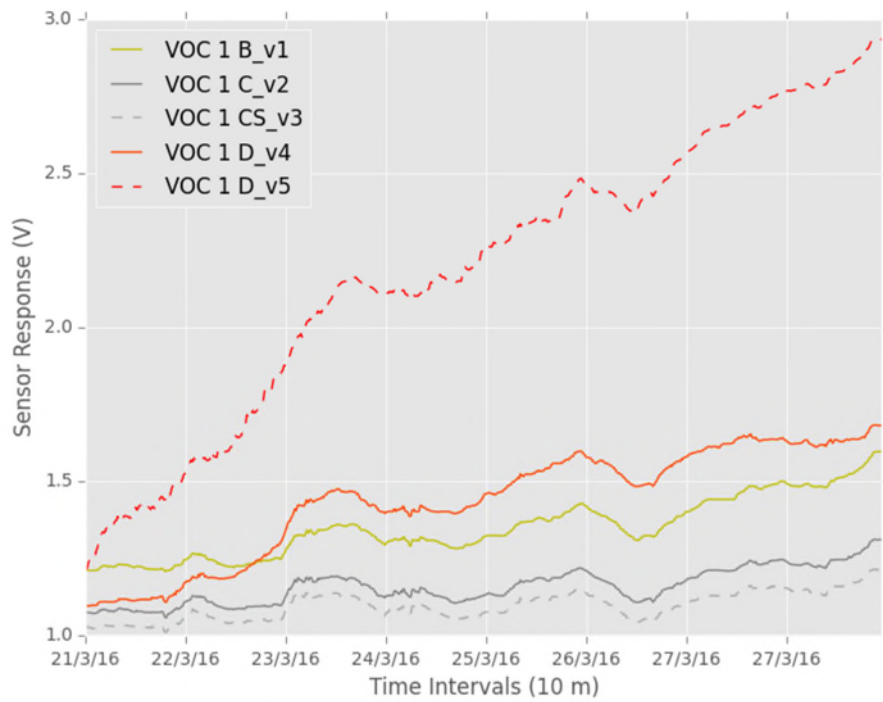


Fig. 6.8. MOX VOC (volatile organic compounds) sensor results.

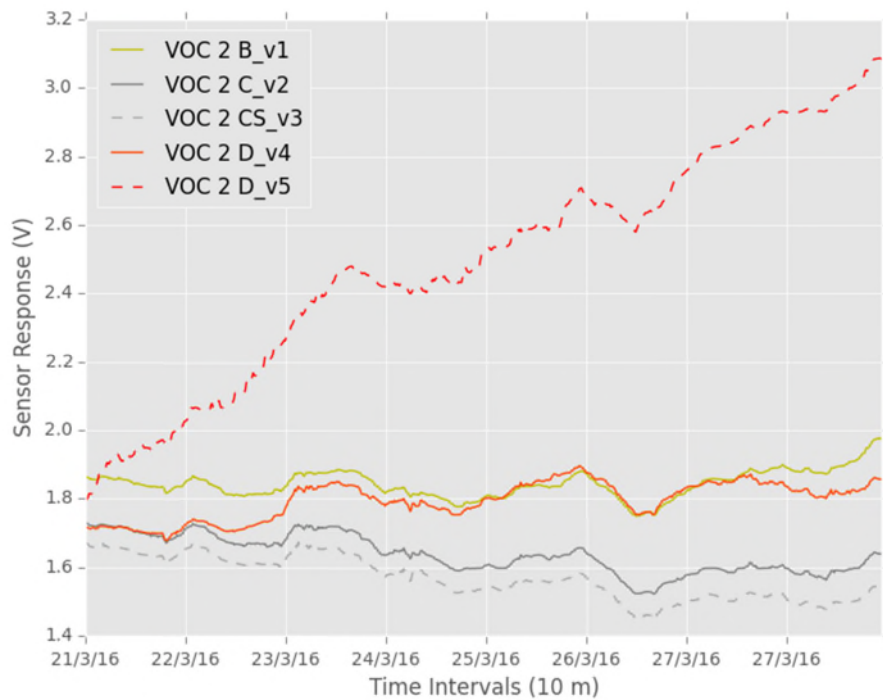


Fig. 6.9. MOX VOC sensor results.

In Fig. 6.10, Fig. 6.11, Fig. 6.12 and Fig. 6.13 are the time series responses for sensors selected to detect alcohols, ammonia, methane and hydrocarbons respectively. All results appear to point to a very similar outcome. One observation is that the responses

for methane and hydrocarbons is virtually identical (Fig. 6.12 and Fig. 6.13). This could imply that a common chemical to both gas sensors is likely to be methane, or a similar lightweight hydrocarbon. It is also possible that ethene may be indicative of disease spread, as shown in past research (Lui et al., 2005). Another interpretation is that the filter to remove some interference may not to be as effective as indicated by the manufacturer. This would also explain the lack of cross-sensitivity to alcohols that, according to the manufacturer, would be present in the response for the hydrocarbon version (without filter) of the sensor (Figaro Engineering Inc, 2013).

Furthermore, as shown in Fig. 6.6 and also from the graphs on volatiles, only one of the two infected tubers seemed to be affected by disease. However, from Fig. 6.10 to Fig. 6.13 both of the tubers, even if to different degrees, appeared to share a common condition. The question that remains unanswered is if this is because of tissue decomposition due to other bacteria strains or soft rot disease progression. This may well require further future work by means of bacteria identification and quantification techniques such as qPCR (quantitative polymerase chain reaction) and is beyond the scope of this work.

Fig. 6.14 shows the results for CO₂ to the different sample types. In this case it appears that the two initially infected tubers share a common profile with a smaller difference if compared to both controls (stabbed or unwounded).

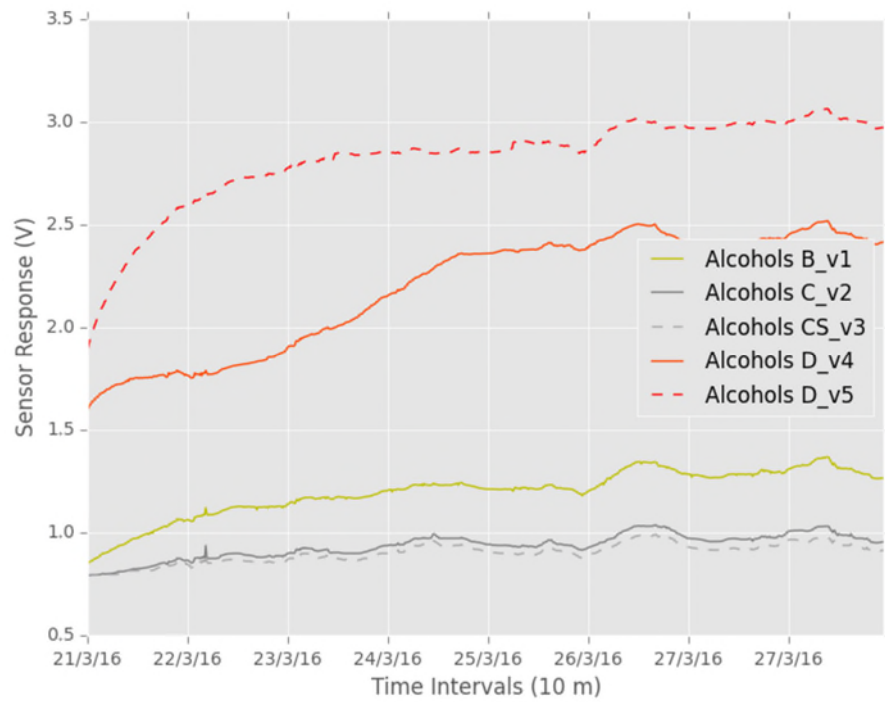


Fig. 6.10. Metal oxide gas sensor response for alcohols.

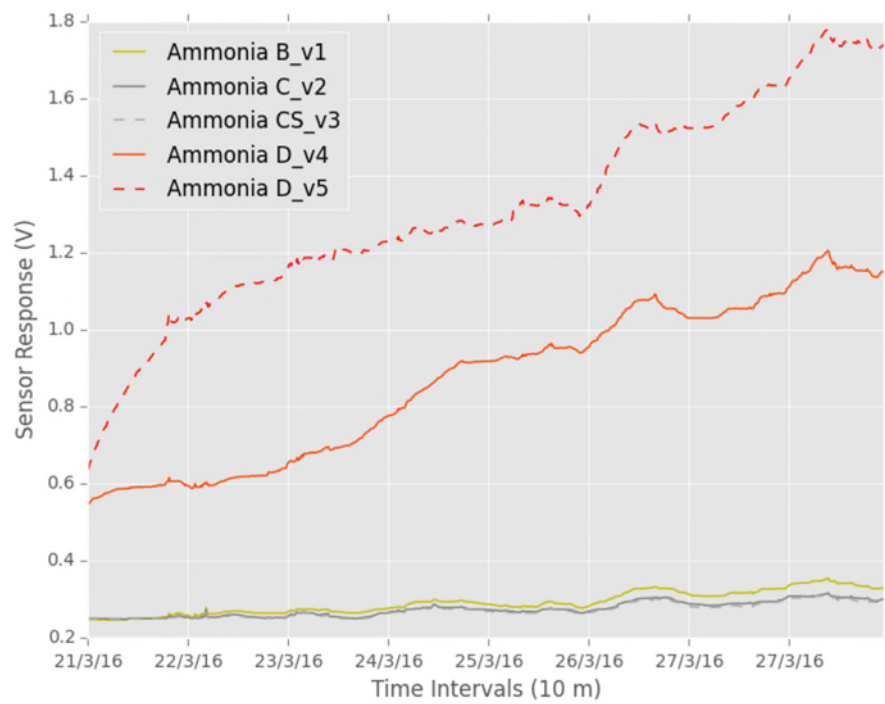


Fig. 6.11. MOX sensor response for ammonia.

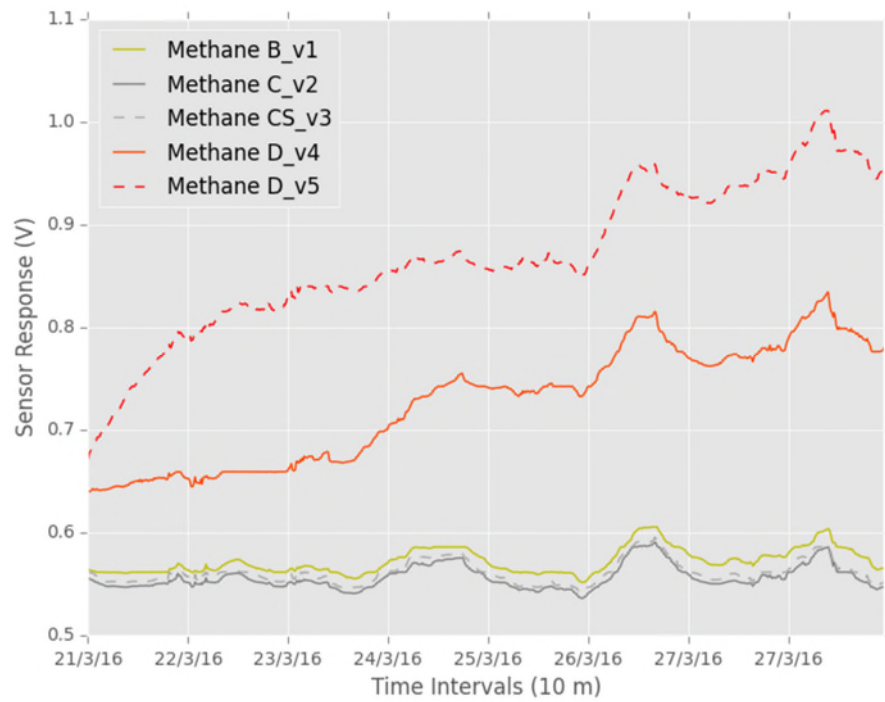


Fig. 6.12. MOX sensor response for methane.

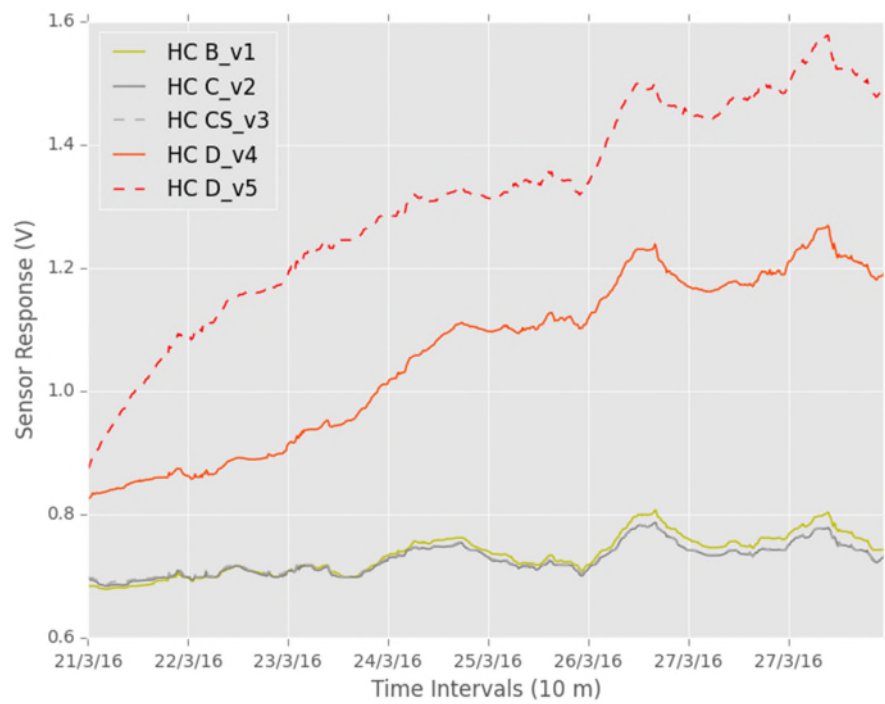


Fig. 6.13. MOX sensor response for hydrocarbons.

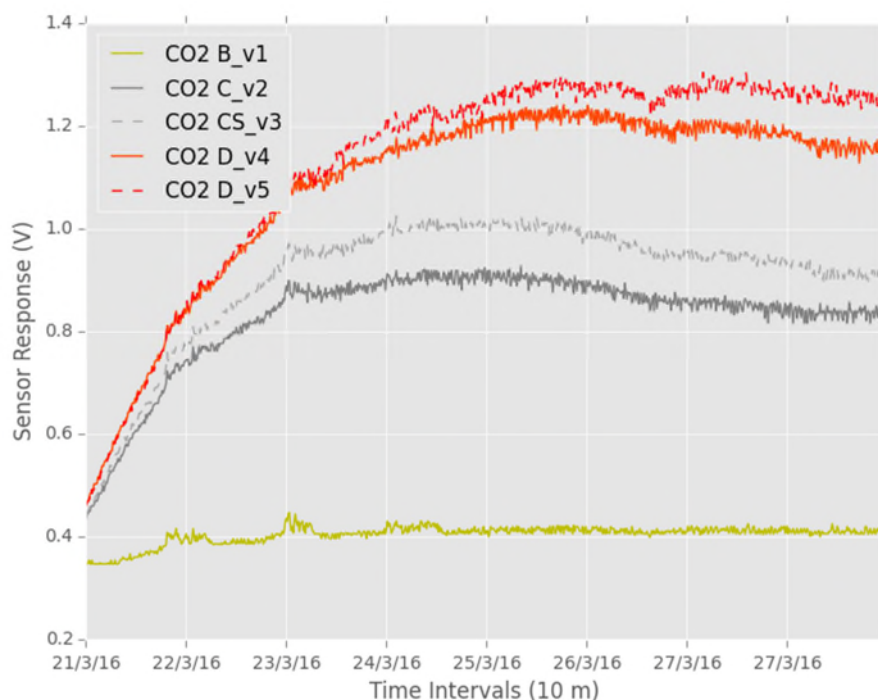


Fig. 6.14. Response for NDIR CO₂ sensor.

6.3.2 Laboratory work to evaluate early time course

The purpose of the previous section was to show signal responses for all the sensors and among all samples types (background, unwounded control, wounded control and two infected) over a comprehensive time frame. A secondary objective was to minimise other factors (background noise, greening, sprouting, temperature and humidity) that could affect sampling of potato tubers. Here instead, the aim is to illustrate further early inception of disease spread and experimental variations.

After reviewing the previous results, a modified methodology (as indicated in 6.2 Materials and methods) was used to slow down disease progression in order to address volatiles changes at an early stage. Fig. 6.15 to Fig. 6.19 show the results for this type of experiment. Fig. 6.15 indicates the outcome for the carbon monoxide sensor. As in the previous case, variability was present in the same experimental set. However, here the amount of the chemical detected over time almost reached a saturation level within

a relatively short time frame. This shows that a considerable degree of variability among samples could be expected either for a broad spectrum of volatiles or for specific chemical compounds (this was also reported in previous chapters). At the end of the sampling procedure, tubers were cut in half and photographed to gather indication of the degree of infection but only blackening of tissue around the inoculation wound could be found to be associated to CO increase (Fig. 6.20).

Fig. 6.16 and Fig 6.17 shows the results for the PID and one of the VOC sensors respectively (the other having a very similar profile). In this case, the VOC and PID responses diverged from one another and for one of the infected samples. This could be indicative of cross-sensitivity by the VOC sensor to large quantities of carbon monoxide. In fact, due to the high ionization potential of carbon monoxide and the lower IP of the lamp used, it is unlikely that detection of the chemical could be achieved by the PID unit. Another possibility considered was the chemical interaction among different volatiles.

Fig. 6.18 and Fig. 6.19 show the data points for sensors reported by the manufacturers as responsive to alcohols, ammonia and hydrocarbons respectively (as indicated in the previous chapter). At this early stage these did not seem to offer much difference. However, as seen in Fig. 6.10 for alcohols, this reached a plateau while the others kept trending up. The PID again offered a deeper understanding of possible VOCs involved. In fact, methane has an ionization potential IP of 12.98 eV (NIST National Institute of Standards and Technology, 2016b) and similarly other hydrocarbons have IP well above the PID UV lamp of 10.6 eV (Baseline-MOCON Inc, 2007; NIST National Institute of Standards and Technology, 2016c). However, ethene has a ionization potential of 10.52 eV (NIST National Institute of Standards and Technology, 2016d). Similarly ethanol (or some other alcohols in general) and

ammonia have IP below the lamp threshold, possibly indicating these are compounds likely involved into the process of disease spread (Baseline-MOCON Inc, 2007; NIST National Institute of Standards and Technology, 2016c).

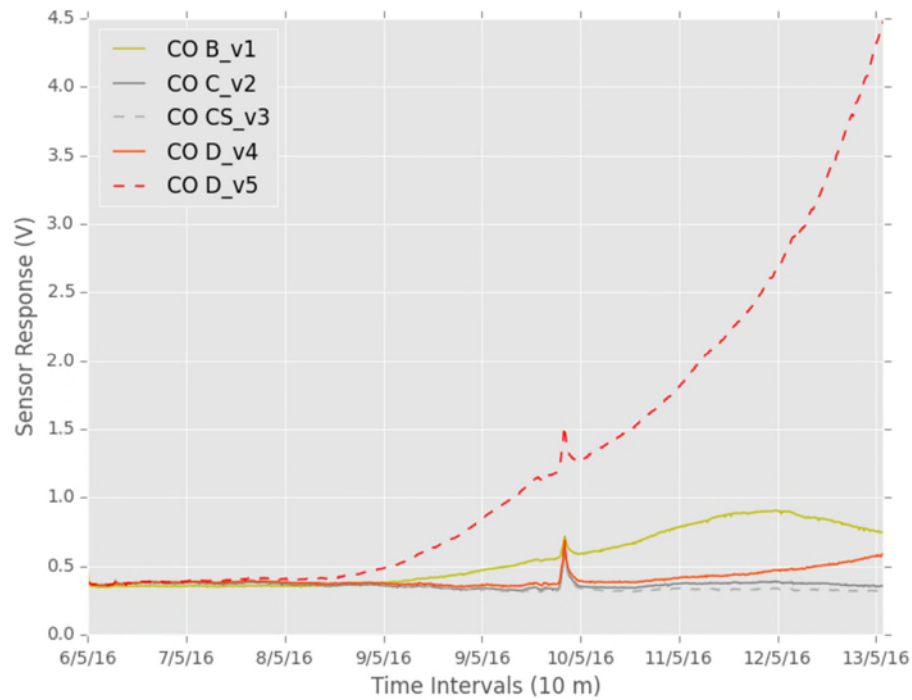


Fig. 6.15. Carbon monoxide sensor response.

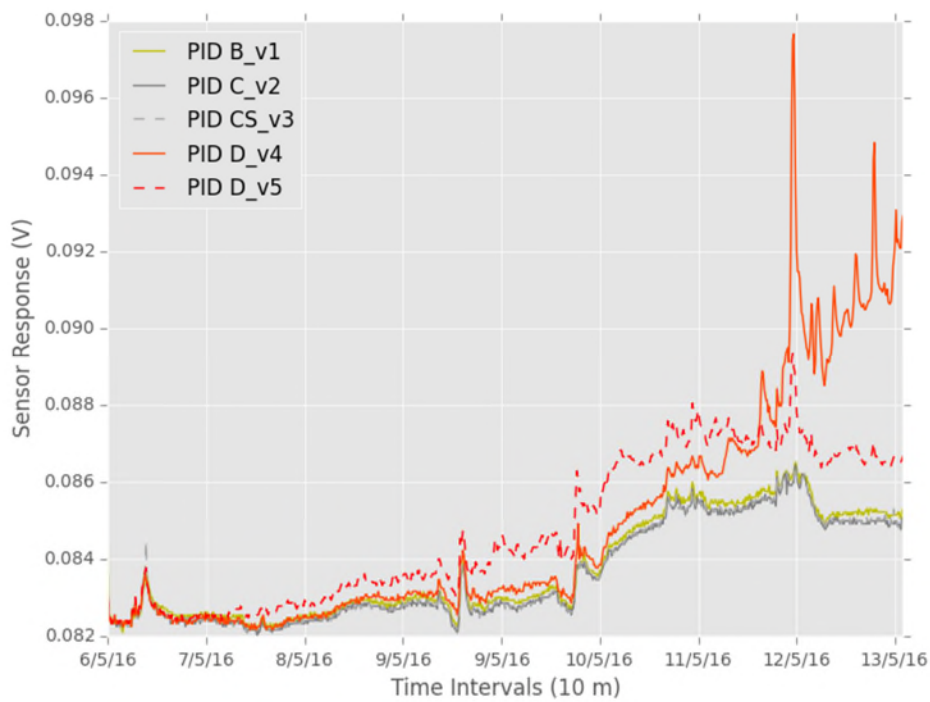


Fig. 6.16. PID sensor response.

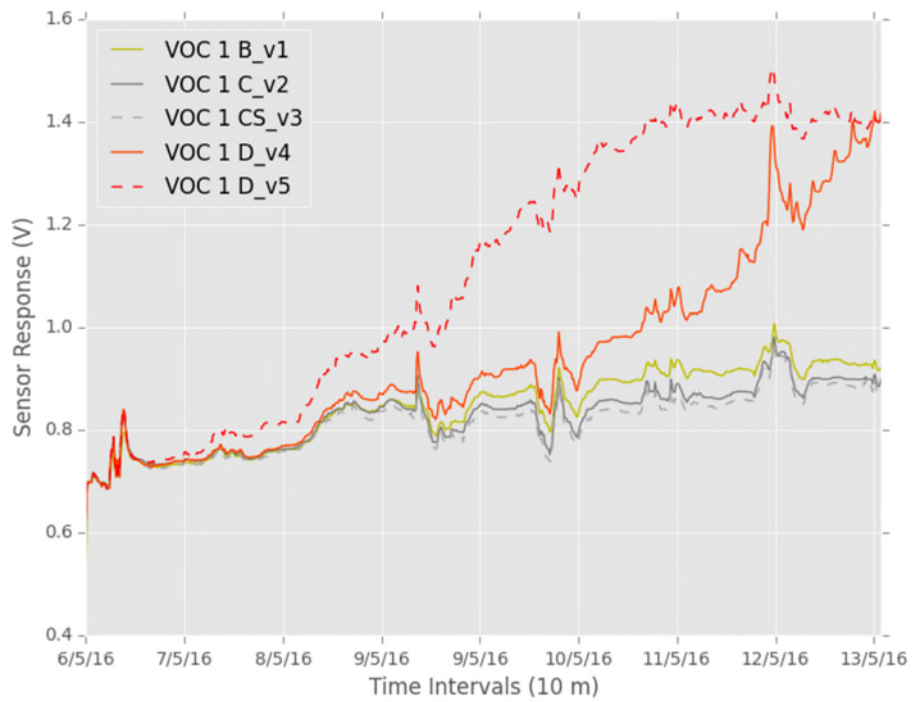


Fig. 6.17. Metal oxide VOC sensor response.

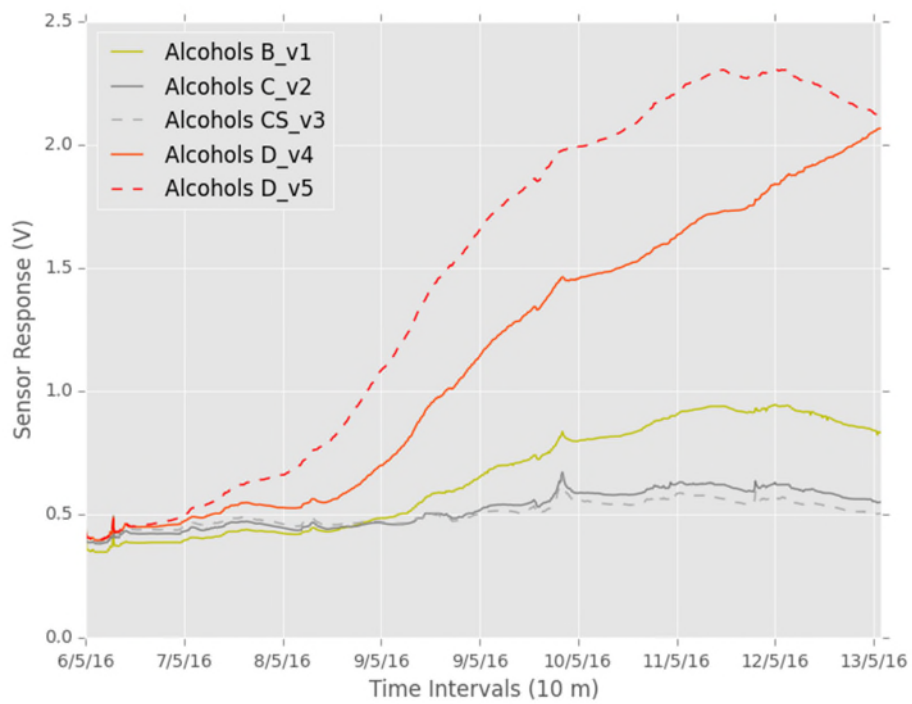


Fig. 6.18. Metal oxide alcohools sensor response.

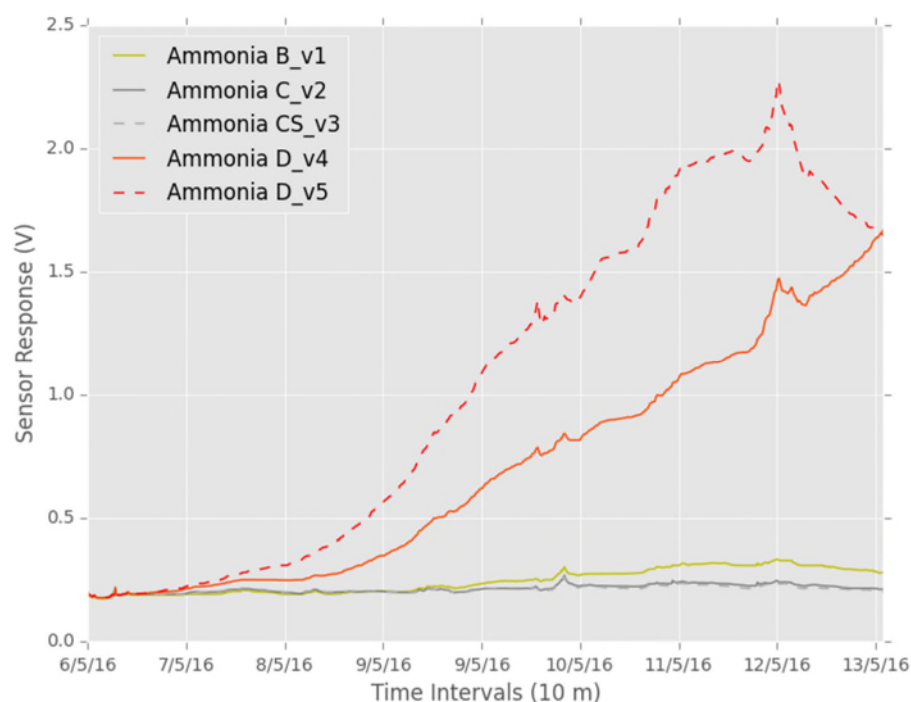


Fig. 6.19. Metal oxide ammonia sensor response.

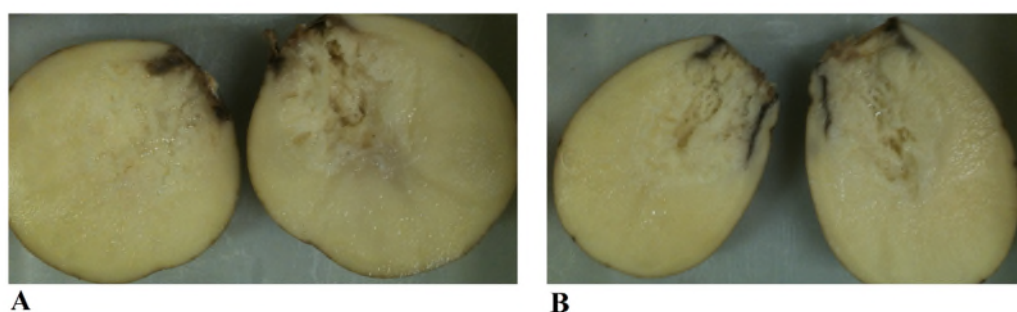


Fig. 6.20. The two infected tubers employed for this work. The first associated to V4 while the second to V5 (with large quantities of carbon monoxide).

6.3.3 Experimental work at the SBCSR potato store facility

The purpose of the work presented here was to test both the potential of the data logger and the possibility of soft rot detection and monitoring in a real-world storage facility (held the AHDB Sutton Bridge Crop Storage Research Centre).

In Fig. 6.21 to Fig. 6.25, is shown the outcome for experimental work in the storage facility (the orange line indicates when the infected batch was placed inside the room

together with the four ton crates). Fig. 6.21 shows that the electrochemical gas sensors for NO and ETO yielded no response to infected tubers, as reported for previous work in laboratory conditions. However, in Fig. 6.22 the carbon monoxide sensor was of a relatively significant abundance as a disease marker, although in far smaller quantity when compared to tests with electronic noses (as reported in previous work with the electronic nose and later with the data logger). Although substantial variety was reported for CO in tests with individual samples, an averaged result among samples in store was expected to be more indicative of disease progression. As explained in the materials and methods section inoculation was carried out 4 days before placing the infected tubers in the storage room.

Results for PID and the metal oxide VOC sensors are reported in Fig. 6.23. As in the previous case, these yielded no useful outcome for soft rot disease detection. At this stage it could be only a speculative consideration that the lack of either carbon monoxide or volatile detection was due to the lack of sensitivity of the detectors employed. Hence an increase in the numbers of tubers in infected batch (the current amount of diseased tubers is of 1% of the whole batch) may provide enough signal for detection using these sensors.

In Fig. 6.24 and Fig. 6.25 show the graphs for the remaining metal oxide components. These all performed within expectation, but for alcohols the TGS2620 outperformed all others. In all cases initial detection was achieved after four days from inoculation with *Pectobacterium*.

Results for the CO₂ sensor were not reported due to the failure of the control board during experimental work.

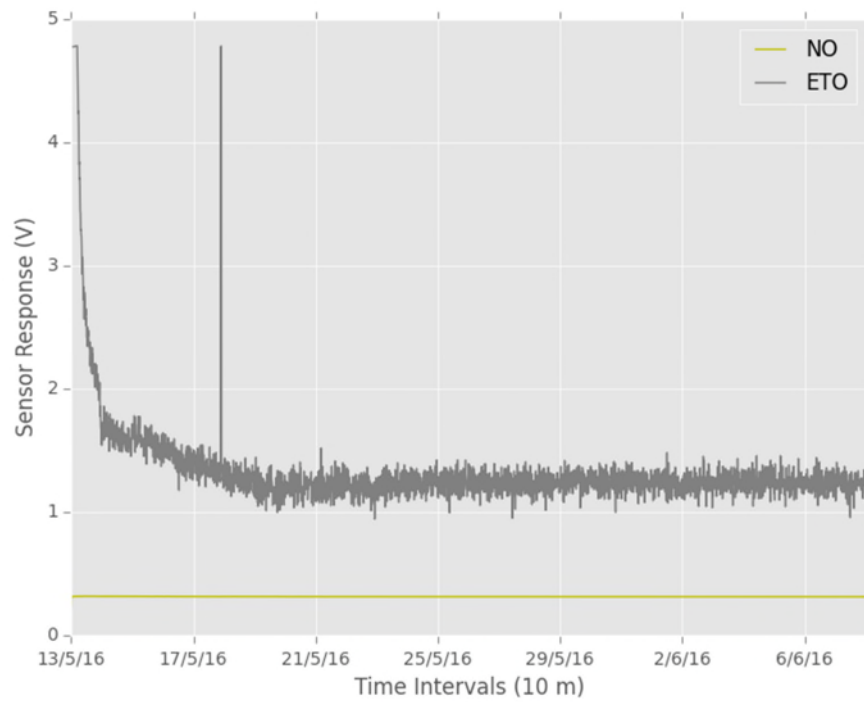


Fig. 6.21. Electrochemical gas sensors: NO, ETO.

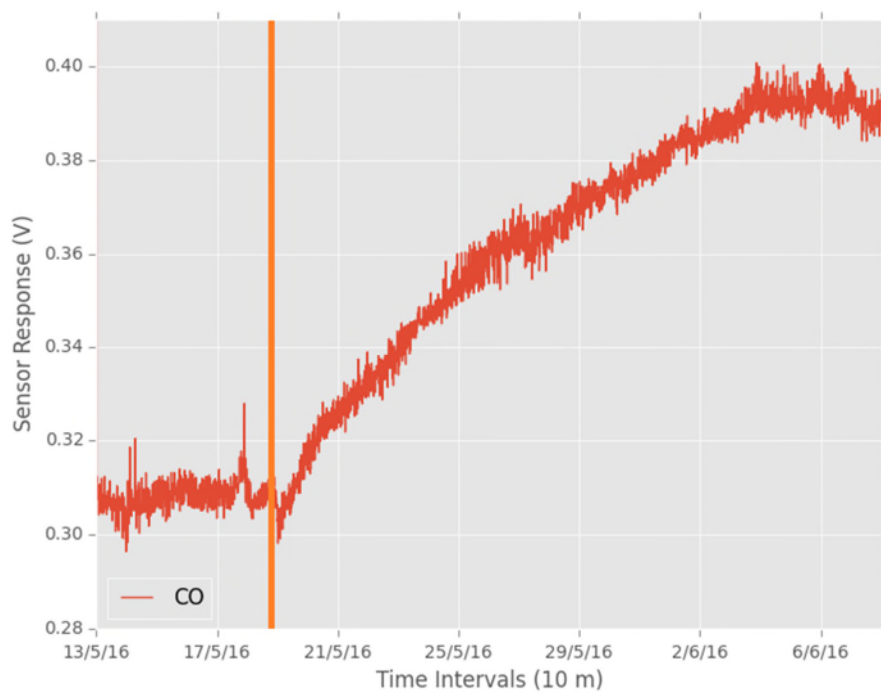


Fig. 6.22. Electrochemical gas sensor: carbon monoxide. The orange line indicates when infected tubers were placed into the storage facility.

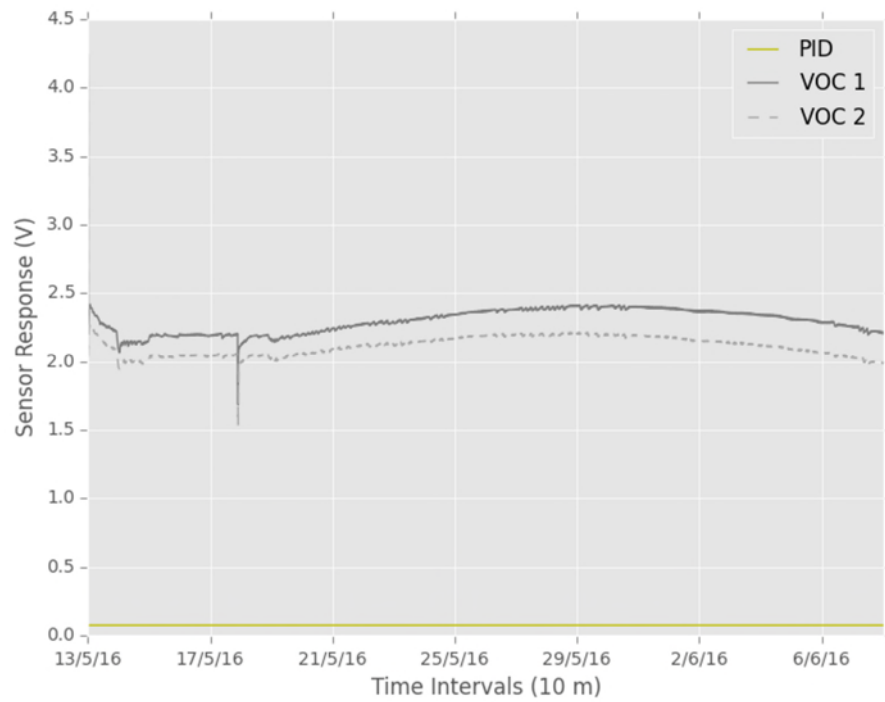


Fig. 6.23. Photoionization detection and metal oxide VOCs sensors.

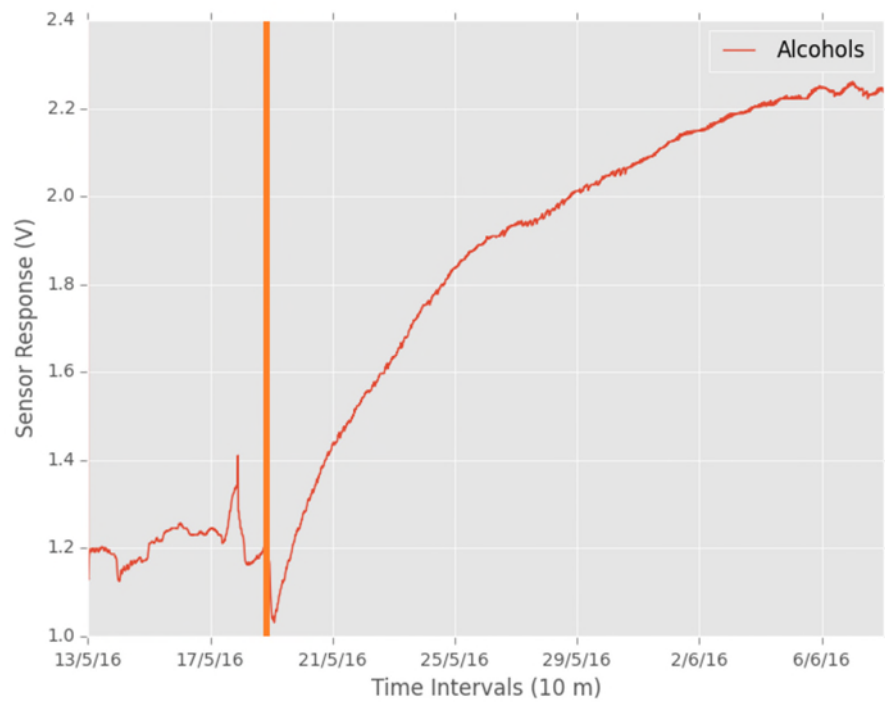


Fig. 6.24. Metal oxide gas sensor for alcohols. The orange line indicates when infected tubers were placed into the storage facility.

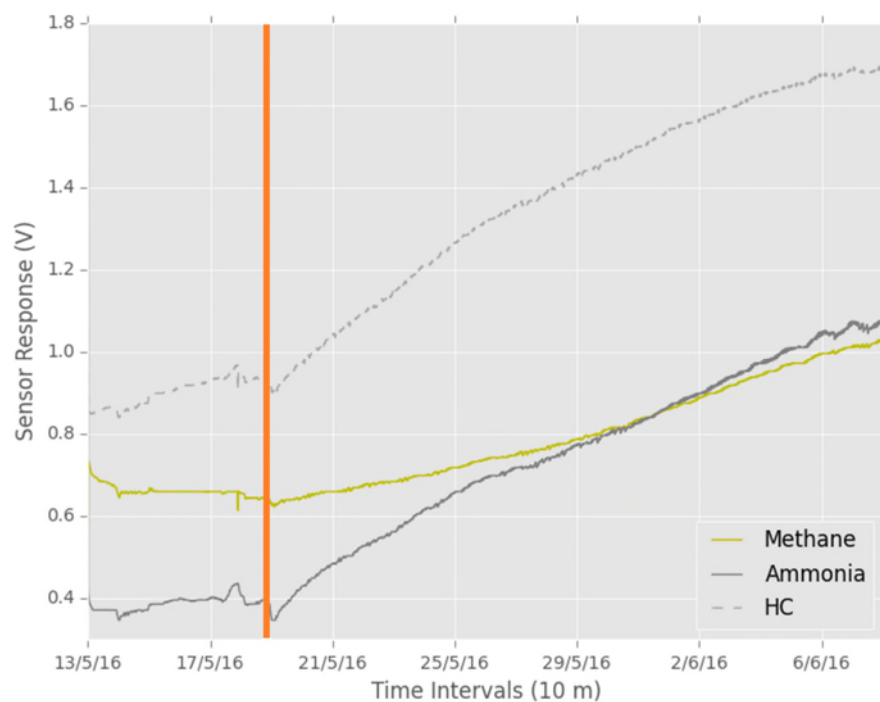


Fig. 6.25. MOX sensors for methane, hydrocarbons and ammonia.



Fig. 6.26. Tubers infected with soft rot after 21 days inside the storage room (A); control tubers with visible signs of sprouting after 28 days since the start of the experiment (B).

6.4 Discussion

In earlier chapters two time points were chosen to evaluate various gas sensing technologies for soft rot disease monitoring. The rationale for this approach was meant to address two core objectives of the research. The first one was to evaluate what sensors and/or technologies could be benchmarked against sensorial analysis employed by experts in the field for symptomatic assessment of soft rot. The other time point was meant to identify pre-symptomatic inception of disease by using gas sensing technologies when the tactile, olfaction or visual inspection would otherwise fail.

The purpose of research reported in this chapter was to assess the progression of soft rot over time in both simulated and real storage conditions. The laboratory work had the aim both to test the data logger (with the previously shortlisted sensors) and to gather insight into disease progression in a store scale-model. This could be accomplished since different types of samples (background, unwounded control, wounded control and two infected potato tubers) were tested under the same laboratory set-up. More, the protocol not only allowed the study all sample types but also to evaluate the concurrent effects of environmental variables on sensors responses. It may be argued that in a real store condition variability encountered would average out and an overall response (whether VOC-specific or not) instead would suffice for symptomatic or pre-symptomatic determination of soft rot. This is true, however the methodology, besides a per se contribution to knowledge in the field, offered the possibility to assess concurrent VOC profiles for controls and disease tubers. Hence, the laboratory data could be qualitatively benchmarked against the ones obtained in a commercial potato store. In fact, this was of particular importance since work at the

Sutton Bridge Crop Storage Research Centre storage facility could only be completed with regard to soft rot disease progression over time (due to financial and logistics restrictions).

NO and ETO sensors were not able to successfully discriminate controls and diseased samples neither in laboratory conditions nor as possible detectors to be employed in store. The other electrochemical gas sensor shortlisted in the work with electronic noses, i.e. carbon monoxide, discriminated controls and infection thus providing to be suitable for deployment in commercial stores. However, doubts remain about the low intensity of the CO sensor response in real store conditions. In fact, there is reasonable possibility that the outcome may be associated to cross-sensitivity to alcohols (or other compounds or family of chemicals). However, this would raise a question for the lack of carbon monoxide in real stores. It may be possible that the reason for lack of detection is due to the fact that CO is a heavy molecule and therefore, usually sinks to the ground. If the unit were raised in the air, it would be harder to monitor CO.

General VOC profiling, regardless of the technology, did not yield to expectations and appeared not to be suitable for further study or deployment. However, the PID could be of use in future laboratory research. A deeper understanding of the volatiles involved in the process could be gathered by the use of different ionization potentials for various chemicals with different IP in the lamps employed. In fact, the lack of response for the PID could suggest that specific VOCs (with IP greater than 10.6 eV) build-up over time might be the cause of emissions and could be employed for possible diagnostics.

All metal oxide sensors responded well both in laboratory conditions and in potato stores. It appeared from laboratory work that concurrency of different chemicals could

be involved in the metabolic process of decomposition and consequently in VOC profiling. However, cross-sensitivity of the various sensors to the same chemical family could not be ruled out. In particular, it should be noted the constant high level of response to alcohols. Indeed it may be the case that this could be associated with the presence of starch in the tubers. Starch comprises up to 80% dry weight of potato tubers and its (anaerobic) decomposition into simple sugars may be the main culprit for the emission of the specific volatiles (Jaspreet and Lovedeep, 2016). Moreover, it should be noted that environmental conditions influence growth, metabolic processes and, consequently, starch decomposition (G. Lisinska and Leszczynski, 1989).

6.5 Conclusion

In this chapter it has been shown that the custom-built research instrument and the sensors array employed can be successfully employed for pre-symptomatic determination and monitoring of soft rot in a commercial potato store.

In particular, some of the sensors previously shortlisted (ETO, NO) appeared not to be of use for soft rot monitoring either in laboratory experiments or in store. Others (metal oxides) among the sensors previously selected showed to be possible candidates for practical implementation in store. Doubts remain about the electrochemical carbon monoxide sensor and its possible cross-sensitivity to alcohols. However the detector could be employed as a low power alternative to the more power-intensive metal oxides sensors.

As a final consideration it may be worth noting that while soft rot has been thoroughly investigated, this has not been the case for other potato tubers diseases. In fact, it is possible that these other infections may be detected (because of tuber tissue decomposition) in a similar fashion to the one that was reported in this work. However, if this speculative hypothesis were to be true it would need to be verified experimentally in future work.

6.6 References

- Addis Housewares Ltd, 2016. Rectangular Containers [WWW Document]. URL <http://www.addis.co.uk/kitchen-and-food-storage/food-containers/clip-close/rectangular-containers.html> (accessed 11.20.15).
- AMVAC Chemical Corporation Inc, 2016. SMARTBLOCK® Plant Growth Regulator [WWW Document]. URL <http://www.amvac-chemical.com/Product-Details/pid/218> (accessed 7.10.16).
- Baseline-MOCON Inc, 2007. piD-TECH® plus Photoionization Sensor User's Manual. USA.
- Figaro Engineering Inc, 2013. TGS 2611 - for the detection of Methane. Japan.
- G. Lisinska, Leszczynski, W., 1989. Potato Science and Technology. Elsevier Science Publishers Ltd, Poland.
- Jaspreet, S., Lovedeep, K., 2016. Advances in Potato Chemistry and Technology, 2nd ed. Elsevier Inc, UK.
- Lui, L.H., Vikram, A., Abu-Nada, Y., Kushalappa, A.C., Raghavan, G.S. V., Al-Mughrabi, K., 2005. Volatile metabolic profiling for discrimination of potato tubers inoculated with dry and soft rot pathogens. *Am. J. Potato Res.* 82, 1–8. doi:10.1007/BF02894914
- NIST National Institute of Standards and Technology, 2016a. Carbon monoxide [WWW Document]. URL <http://webbook.nist.gov/cgi/cbook.cgi?ID=C630080&Mask=20> (accessed 8.10.16).
- NIST National Institute of Standards and Technology, 2016b. Methane [WWW Document]. URL <http://webbook.nist.gov/cgi/cbook.cgi?ID=C74828&Mask=20> (accessed

8.10.16).

NIST National Institute of Standards and Technology, 2016c. NIST Chemistry WebBook [WWW Document]. URL <http://webbook.nist.gov/chemistry/> (accessed 8.10.16).

NIST National Institute of Standards and Technology, 2016d. Ethylene [WWW Document]. URL <http://webbook.nist.gov/cgi/cbook.cgi?ID=C74851&Mask=20> (accessed 8.10.16).

SMC Pneumatics Ltd, 2016. Industrial Automation Product Catalogue. UK.

CONCLUSIONS AND FUTURE WORK

This page is intentionally left blank.

7 Conclusions and Future Work

Food waste is a considerable problem and a worldwide issue. In the UK, the potato tuber is a staple crop and produce can be lost for a number of reasons, with post-harvest storage being a major contributor (with an estimated loss of circa 5% of the entire crop each year). In the UK the potato tuber yield has considerably increased over the years due to improvements in farming practices, with most of the produce losses resulting from post-harvest long-term storage (Market Intelligence 2015-2016, UK Agriculture and Horticulture Development Board). In these stores, most of the crop waste is caused by the disease known as ‘soft rot’. The aim of this research was pre-symptomatic diagnostics and monitoring by means of gas analysis techniques of potato soft rot for deployment in commercial stores.

The objectives of the research are listed below:

- 1) To research and report on previous work for detection by gas analysis of potato soft rot or other relevant studies.
- 2) To shortlist other available gas analysis technologies, not previously reported, that could be employed for monitoring of the aforementioned disease.
- 3) To evaluate such techniques for both symptomatic and pre-symptomatic progression of soft under laboratory conditions.
- 4) To shortlist a technology/sensor, as suitable set of technologies/sensors, among the ones tested with potential for ease of deployment in store and at low cost (subject to objective 3) above).
- 5) To design, manufacture and test a purpose-built research instrument comprising the aforementioned technologies (subject to objectives 3) and 4) above).

- 6) To deploy the instrument for monitoring of soft rot under laboratory and commercial store conditions (subject to objectives 3) and 4) above).

These goals are discussed in more detail below.

7.1 Conclusions

The first part of the work reported on the literature with regard to studies on volatile profiling of soft rot that spanned over a period of decades. The results showed no common consensus on chemicals or approaches. In part of the studies, the outcome appeared to suggest potential volatile metabolites markers related to disease inception and progression. However, other researchers suggested that overall volatile metabolites profile over time (in contrast to specific metabolites markers) had to be considered as the main discriminating factor in disease monitoring. Regardless of these contrasting views, experimental work for disease spread was always carried out by means of gas chromatography (GC) or gas chromatograph mass spectrometry (GC-MS). GC and GC-MS are well-established technologies and are used for VOC analysis due to a combination of high accuracy, selectivity, resolution and being the ‘gold standard’. However, there are considerable drawbacks, including high costs of purchase and maintenance, the large number of variables involved for selection of parts prior to work, laborious manual processing of samples and complex data sets. These factors make this approach costly, impractical, time consuming and prone to errors. Therefore, GC and GC-MS are less suitable for continuous monitoring of soft rot spread in controlled laboratory conditions, and even more inadequate to be applied in the challenging environmental conditions found in commercial potato stores. Moreover, store managers would require a simple, practical and cost-effective solution. This part of the work aims to address objective 1) above.

However, there are a range of other technologies that could be deployed for potato storage monitoring. These appeared to offer new possibilities for determination and monitoring of soft rot (or more in general potato diseases). The original hypothesis was that these techniques could be employed to achieve early detection and management of the aforementioned disease in a more practical and cost effective manner than GC/GC-MS. It should be mentioned that these technologies are well established approaches in the other fields, whether in research or industry, and have been so over many years. The novelty in the current research resides in the application of these well-established technologies for detection of potato disease. Moreover, overall increase in metabolites over time might provide a simpler approach to specific volatiles identification. Hence, when the hypothesis was originally formulated, a priori knowledge of chemicals involved in soft rot spread was deemed not necessary, nor sought after, but was not excluded as a possibility. This part of the work aims to address objective 2) above.

In this work, the hypothesis for gas analysis monitoring of disease spread was initially investigated with FAIMS (Field Asymmetric Ion Mobility Spectrometry). Work with FAIMS technology was carried out with the Lonestar (Owlstone Nanotech Ltd, UK). This approach allowed determination of a broad range of volatiles without prior knowledge of the substances involved in disease presence. At this early stage of work, the need to accurately assess the technology emerged and a suitable experimental protocol for laboratory work was developed. The first objective of the protocol aimed to evaluate if the technology could successfully discriminate between controls and diseased tubers and how this could be benchmarked against sensorial analysis (tactile, olfaction or visual inspection), the common practice for identification of potato soft

rot in store. The second objective aimed to evaluate if pre-symptomatic identification could be achieved when sensorial analysis proved ineffective.

The experimental outcome proved that early diagnostics via dynamic headspace sampling with FAIMS could be achieved both at symptomatic and pre-symptomatic stages. Further work with PID (Photoionization Detection) technology was carried out with the Tiger instrument (Ion Science Ltd, UK). The results from the PID sensor substantiated and strengthened the original hypothesis that it was possible to employ gas analysis sensors for potato tubers disease monitoring at selected time points. Furthermore, both the Lonestar FAIMS and Tiger PID, as applied in this research, offered a considerable more practical and reliable engineering approach when compared to the more established techniques of GC/GC-MS, tools of previous experimental research. In fact, FAIMS has the advantages of having high sensitivity and of being deployable in this type of environment. In addition, the PID has the ability to operate in a more reliable manner, with a wide detection range, can be battery powered/handheld and at lower cost in the environmental conditions of commercial potato stores. Therefore, the PID was shortlisted as a financially viable technical solution when compared to FAIMS for possible store deployment. Moreover, both technologies are more sensitive, reliable, cost effective and easier to implement in commercial stores than GC/GC-MS.

Finally, the PID also proved to be valuable in monitoring disease progression over time. In fact, work with FAIMS suggested the very fingerprint associated to disease inception was constant over time for diseased tubers (but with overall increase in volatile metabolites concentration). Instead there was a marked overall increase in VOC over time when detected by the Tiger instrument (as shown in chapter 3, in Fig.

3.13 and Fig. 3.14). In short, it can be concluded that the early part of the research proved that gas analysis could be applied for both detection and early detection of soft rot under selected laboratory conditions. This is also the first time that both FAIMS and PID technologies have been employed to detect potato soft rot disease spread. This part of the work aims to address objective 3) above.

Following these studies, further work was carried out with other main discrete commercial gas sensors technologies (metal oxide, electrochemical, infrared), usually used for industrial safety and environmental monitoring. The underlying motivation for choosing these techniques was to undertake a complete review of these different gas sensing technologies when applied to the detection of soft rot. In addition, if successful, how well did they work and if there were any drawbacks or trade-offs involved. This experimental work further validated and supported the hypothesis that a range of different gas sensing technologies could be employed, at least in a controlled environment, for potato disease detection. This latter part of the research followed the same experimental method adopted and outlined in earlier chapters for both pre-symptomatic and symptomatic soft rot disease monitoring. However, unlike the early part of the work with FAIMS and PID, the larger number of sensors allowed some possibility to address selectivity to specific chemicals or chemical groups (as also suggested in past research) by means of readily available commercial detectors.

Results from the 12 metal oxides sensors of the FOX3000 electronic nose (AlphaMOS Ltd, France) indicated that only three MOX sensors were needed for discrimination of diseased tubers. These were reported by the manufacturer to be responsive to hydrocarbons and to alcohols. A summary of the results is indicated in chapter 4 in Fig. 4.5.

The results with the WOLF 4.1 (University of Warwick, UK) also showed that another three detectors were likely candidates for soft rot monitoring with electrochemical gas detectors. These were reported by the manufacturer as responsive to carbon monoxide, ethylene oxide and nitric oxide. A summary of results for this type of experimental work is reported in Fig. 4.16 (chapter 4). This part of the work shows that different technologies could be employed for the task at hand. This is also the first time that arrays of metal oxides, electrochemical and infrared gas sensors have been employed for detection of potato soft rot. This part of the work aims to address objective 3), as indicated above.

The main outcome of the work detailed so far aimed at a proof-of-concept study for the detection and the early detection of soft rot. In the next stage of the research, the objective was to investigate the potential of these sensors in commercial stores. This required the design, construction and testing of an ad-hoc research instrument comprising the previously shortlisted technologies. The instrument was conceived as a research tool to evaluate possible practical implementation in store. However, while most of the sensors could be featured in the newly development system, FAIMS was left out due to its high-cost for a final solution and the difficulty in integrating the system into a store environment. This part of the work aimed to address objective 4) and 5), as indicated above.

In last set of results, it was shown that the custom-built research instrument and the sensors array employed within it could successfully be used for the pre-symptomatic determination and monitoring of soft rot in a commercial potato store. However, not all sensors shortlisted from previous laboratory experiments performed adequately. In fact, all metal oxide sensors yielded discriminative outcome when diseased tubers

were located into the research/commercial store room. The representative outcome for these experiments is reported in Fig. 6.24 and Fig. 6.25 (chapter 6). This was not the case for the PID and electrochemical sensors, and the reasons behind this require further investigation. It could be speculated that the sensitivity of electrochemical and the PID was not sufficient to detect soft rot biomarkers in the diluted environment of a store. The outcome of this part of the project and, more in general for the whole research, shows that the gas analysis approach can be easily deployed for soft rot disease monitoring in potatoes stores and using arrays of low cost sensors. This part of the work aims to address objective 6), as indicated above.

All the considerations listed above can be briefly summarised as follows:

- Early work evaluated a wide range of technologies in laboratory environment and have proved to be effective for both detection and early detection of soft rot.
- The hypothesis that gas sensors can be employed has been proven in principle.
- These gas sensors technologies can be implemented easily and cheaply in a purpose-built instrument for deployment in potato stores.
- Results in the latest type of commercial stores show that the selected sensors can effectively warn of and monitor early soft rot inception.
- The hypothesis that other technologies beyond GC and GC-MS can be employed for potato disease monitoring has been proved in practice with store deployment.

7.2 Future Work

This research has shown that gas sensors can be employed for the detection and monitoring of soft rot. In particular, the experimental outcome proves that gas analysis can detect volatiles associated to soft rot under the controlled environmental conditions. These conditions can be found in real stores. However, in practice, ventilation, temperature and humidity can be modified depending on commercial use of the produce, store management practices and external environmental conditions. Variation of these conditions and effect on sensor response would probably be the most important aspect to be addressed in future work.

Moreover, the set-up used for experiments at the AHDB Crop Research Centre was implemented in a new type of store room that is now being tested for commercial deployment. However, the most common unit in the UK is still the ‘box store’. A box store consists of hundreds of stacked 1-ton wooden crates in a large shed. Several of these buildings (also with different dimensions) can be found on the same site. Because of the larger dimension of these facilities, further work will be needed to investigate the effects of dilution on volatile emissions detected by the bespoke environmental analyser. It is also likely that a number of these units may be needed and deployed across each facility. Likewise, ‘bulk stores’ can still be found across the country for storage management. The difference between these two types of facilities resides in the fact that potatoes are stacked in bulk on the floor of large sheds. More, ventilation is achieved via ducts that provide the air circulation needed for tuber health. Further work could address the identification of the most effective number, distribution and parameters settings for the purpose-built gas sensor units.

A further element of study would be a complete and detailed data collection on background in all types of stores. In fact, it is a common practice for store managers to vary environmental parameters in order to address tuber health. However, variation in ventilation, temperature and humidity may alter sensor responses. In addition, the different types of stores should be monitored over a longer period of time, or for entire storage seasons. On the other hand, it may not be possible, or advisable, for store managers to monitor soft rot loss in less contained and controlled such box or bulk stores.

Another issue that should be considered, is that there are many other diseases affecting potato tubers. Among these, and in the United Kingdom, silver scurf, black dot, skin spot, dry rot, and gangrene are considered a post-harvest storage problem, although soft rot is by far the major culprit for losses in stores. The different degree of concurrency of these different diseases and their volatile emissions may also be investigated.

At this stage of the work, the origin of the detected volatiles has not been determined, but can be speculated. Research on this could be an objective, or even the main aim, on the underlying biochemical processes involved in tuber decomposition. However, as a final commercial solution, knowing the exact chemicals is not as critical. In this research, it has been speculated that volatiles are originated from either an anaerobic or aerobic process of potato tissue decomposition. A future study could also focus on verification and quantification of this hypothesis.

Maris piper, the potato variety used in this work, is the most widespread tuber in the UK, but other varieties are also present and are of commercial interest to store managers and farmers alike. Further research may investigate the response of the gas analysis unit to volatiles from different potato varieties infected with soft rot (or any other storage disease).

Finally, experimental investigation could also focus on a detailed study of factors affecting some of the sensors. In fact, all electrochemical and PID gas sensors proved reliable in a laboratory setting. However, under the given controlled conditions they appeared to yield not results in the presence of diseased tubers. It could be speculated that a lack of sensitivity might be an issue, or rather that the environmental setting may be prohibiting to the proper functioning of the technology, or simply that the dynamics of disease spread changes considerably under these conditions and these gases/volatiles could not be detected.

This page is intentionally left blank.